THE PLACING OF LINE SURGE ARRESTERS AND FUSES ON 11 AND 22 KV LINES TO PROTECT EQUIPMENT AGAINST LIGHTNING

Thesis presented in partial fulfilment of the degree
M.Eng. at the University of Stellenbosch
March 2001

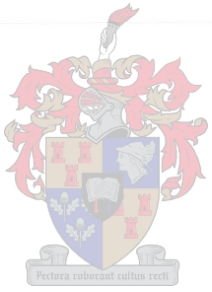

Student:
WJ Dirkse van Schalkwyk

Study leader
Dr. JP Holtzhausen

Stellenbosch University http://scholar.sun.ac.za

Declaration

I, the undersigned, hereby declare that the work contained in the thesis is my own original work, unless otherwise stated and has not previously, in its entirety or in part, been submitted at any other university for a degree.

WJ DIRKSE VAN SCHALKWYK

February 2001

Stellenbosch University http://scholar.sun.ac.za

Summary

Unshielded distribution lines has a poor performance during lightning activity. Lightning initiates flashovers between the phases and earth and causes line breakers to trip several times during a lightning storm. In addition equipment like fuses, surge arresters and transformers are damaged by lightning and cause in some cases long power interruptions to customers.

The application of line surge arresters on distribution lines is a solution that is implemented worldwide to limit the lightning related problems. This thesis investigated using line surge arresters in conjunction with bushing-mount fuses to decrease nuisance fusing and transformer damage during lightning activity.

Two new pieces of equipment (dropout surge arresters and transformer bushingmount fuses) were developed and strategically placed on 4 different distribution lines. Equipment failures decreased by 90 % while financially the project had an excellent return on investment.

Opsomming

Distribusie lyne sonder skermdrade presteer swak gedurende weerlig aktiwiteit. Weerlig veroorsaak oorvonking tussen fases en aard geleiers wat lei tot breker klinke. Transformators, sekerings, stuwingsafleiers en ander toerusting word ook deur weerlig beskadig en veroorsaak in sommige gevalle lang toevoer onderbrekings.

Installering van lyn stuwingsafleiers op distribusielyne is 'n metode wat wêreldwyd gebruik word om oorvonking en weerligskade te beperk. Hierdie tesis ondersoek die installering van lyn stuwingsafleiers en deurvoerder gemonteerde sekerings om transformator skade en onnodige blaas van sekerings te beperk tydens weerlig aktiwiteit.

Nuwe toerusting (uitval stuwingsafleiers en transformator deurvoerder gemonteerde sekerings) was ontwikkel en strategies op 4 verskillende distribusie lyne geïnstalleer. 'n Negentig persent vermindering in toerusting beskadiging is behaal terwyl die projek finansiël 'n goeie opbrengs op belegging meegebring het.

Stellenbosch University http://scholar.sun.ac.za

Acknowledgements

I would like to thank the following institutions:

Eskom for financial support and making facilities and data available.

Dr. Holtzhausen for his support and advice.

Ray Pohl of Eskom for his help with practical installation and performance monitoring.

DOC Mining Company for the production of the dropout arresters en bushing-mount fuses.

My family for their continued support.

Stellenbosch University http://scholar.sun.ac.za

THE PLACING OF LINE SURGE ARRESTERS AND FUSES ON 11 AND 22KV LINES TO PROTECT EQUIPMENT AGAINST LIGHTNING.

CONTENTS

Stellenbosch University http://scholar.sun.ac.za

Stellenbosch University http://scholar.sun.ac.za

Stellenbosch University http://scholar.sun.ac.za

1. INTRODUCTION

The performance of Eskom's distribution system in areas of high lightning activity has been negatively effected by failure of equipment (transformers, fuses, insulators and wood pole splitting). A study was done in the North Western Region (Wolmaransstad area) to investigate and prevent the equipment failures.

1.1. Background

Unshielded 11 and 22 kV distribution lines perform poorly during lightning activity. Direct lightning strokes cause extensive damage to transformers, fuses, poles, conductors, insulators and wood poles on distribution lines, which results in long outages. Repairs must be done in remote areas during bad weather and is very labour intensive.

Most equipment failures occurred unexpectedly during storms (lightning) and work scheduling is difficult. Secondly, the failures are not spread evenly during the year, which cause excessive work peaks in work load. This causes long outage times (frequently up to one day and sometime up to two days) to customers.

With aging of the equipment, more failures occur during stormy weather. However, if the overvoltage stress due to lightning on the lines can be decreased, the life expectancy of the above equipment can increase considerably.

During this study it was ensured that line faults that were not lightning related do not influence the results. This was done with the help of LPATS (Lightning Positioning and Tracking System).

This thesis investigates two methods of minimizing the effect of lightning surges on distribution lines. The first method is to rectify the pole-mounted supply point configuration and the second one is to install line surge arresters at strategic/problem areas on the unshielded 11 and 22 kV lines. The biggest challenge is to identify a strategic position for the line surge arrester and to do the earthing of the surge arrester efficiently. This concept has been applied to shielded transmission lines with excellent results. In the case of shielded lines, the purpose of the line arrester is to prevent a backflashover between phase and earth (pole or shieldwire) in order to prevent a power frequency fault. The main purpose of the line arrester in this thesis is to reduce equipment failure significantly by creating an additional low impedance path to earth.

The lightning performance of four unscreened 22kV poorly performing distribution lines were analyzed with the help of a manually populated performance database and compared to the electronic logging of a supervisory control system. An Alternative Transient Program (ATP) model of the lines was created for doing transient studies. During an on site visit the actual points where the lightning damaged the line were identified. A Lightning Positioning and Tracking system (LPATS) was used to verify all the above information and to determine the average lightning density around the line.

Stellenbosch University http://scholar.sun.ac.za

With the help of ATP the placement of additional line dropout surge arresters and newly developed bushing-mounted fuses were done to improve the line performance. The equipment was installed and the improvement in performance was assessed. A financial analysis was made to measure the cost effectiveness of the project.

1.1.1. Distribution network performance

The distribution line performance is based on the total duration and frequency of the outages over a one-month period. A reasonable figure is not to exceed a total of 2 hours outage time per month per customer. The failure of only one transformer requires 4 hours to repair, thus exceeds above targets.

A check was done one the accuracy of the performance database by comparing it with the equipment taken from the stores for repairs. This data is shown in table 1.1. It is clear that, despite the differences between the two databases, a large number of equipment failures occur.

	No of Transformers	No of Fuses	No of Surge arresters
Stores data	1384	17543	4837
NAPI data	1060	7567	651

Table 1.1. Equipment replacement annually

1.1.1.1. The fuse

The purpose of the fuse is to prevent the line from tripping for a transformer fault by disconnecting the faulty transformer. As seen in table 1.1, the fuses are the most vulnerable components. About 6% of the installed fuses blow annually - of these cases 90% are lightning related. According to Parrish [1] the lightning related fuse operations in a Florida, USA, test area was between 0.3% and 1.33%. However, different configurations are used in the pole-mounted installations in Florida. In their case surge arresters protect the fuses, which is not the case in the Eskom system.

Test done by Hamel [2] verified that fuses on the transformers can blow during lightning activity. The fuse operations are caused by long (few milliseconds) low amplitude (less than 1 kA) current causing overvoltage and saturation of the transformer. The result of the saturation of the transformer is an inrush current of up to 300 A. Hamel believes that the majority of cases of nuisance blowing of fuses are due to the transformer inrush current during lightning conditions.

Although the fuse manufacturers claim that their fuses will not blow due to lightning, they could not provide any characteristics (time/current graph) of the fuse operation below 10 milliseconds. Analysis of the network performance data shows that 90% of the fuse failures occur during lightning conditions. It was also found that reports of fuses blowing on clear days originate from installations that are not in daily use and the fuses most probably blew during a previous lightning storm.

In order to test whether the fuses will blow as a result of lightning currents, 8/20 μs impulse current tests were done at the CSIR. Two tests were done. The first test was

Stellenbosch University http://scholar.sun.ac.za

to establish the amplitudes at which the different K type fuses (5 A, 8 A, 15 A, 20 A) operate. Secondly, tests were done to establish whether the K type fuses degrade during impulses with smaller amplitudes that was found in the first test.

The first test showed that the 5 A, 8 A, 15 A and 20 A fuses operate at 15 kA, 16.6 kA, 25.5 kA and 37.8 kA. The second test showed that the 5 A and 8 A fuses do degrade after some lower amplitude (50% lower than the values in the first test) impulses. On average, the 5 A degraded by 21% and the 8 A by 13. The CSIR report is shown in Appendix D.

Hileman [3] compared 8 different research results on the crest current distribution for negative downward flashes and concluded that the average lightning crest current is 34 kA. According to the CSIR tests, a 34 kA 2.3/75 μs impulse will therefore blow K type fuses up to 15 A rating. Fuse failure statistics from the network performance database as shown in table 1.2 support this finding. The CSIR test also proved that a fuse degrades due to a surge even if the surge is only half the size needed to blow the fuse

Fuse size	8 A	10 A	15 A	20 A	25 A	30 A	40 A	50 A
Number of fuse blown/yr.	669	267	396	151	3	1	9	2

Table 1.2. Fuse failures over a year period in a certain area. About 6% of the installed fuses failed.

The fuses need to be graded with the power frequency protection as. Table 1.3 shows that the line protection operates correct on lines where only 8 A fuses are installed (fuse blows before the line protection operates due to a transformer fault). In most of the cases where 20 A fuses are installed on lines, the breaker protection operate before the fuses blow. This incorrect protection grading causes the line to trip. The 20 A fuses don't isolate a faulty installation correct from the line except in cases where the fault level is high.

	Fuses size used	Number of breaker T&L/O operations	Number of fuses blown for transformer fault	Number of transformer faults
Area 1	20 A	11	0	11
Area 2	20 A	3	0	3
Area 3	20 A	8	0	8
Area 4	8 A	1	17	18
Area 5	8/20 A	12	49	61
Area 6	20/8 A	28	37	65

Table 1.3. Incorrect protection/fuse grading cause line trips due to fuses not operating for a transformer fault.

Incorrect protection operation due to high rated fuses cause long outages while low rated fuses cause nuisance fuse operations. A possible solution to the grading of fuses with the line protection and lightning surges, is to prevent the lightning surge to pass through the fuse as shown in figure 1.1 by moving it to between the transformer bushing and surge arrester. With this option, the transformer surge arrester protects

Stellenbosch University http://scholar.sun.ac.za

the fuse. The fuse needs only to be graded with the line protection and transformer inrush currents.

Due to the required earthing arrangement, the space between the surge arrester and the transformer bushing is very limited. The 11 kV and 22 kV fuses on the market could not be used for two reasons:

i) The physical operation of the drop-out fuse requires adequate space.
ii) Severe arcing can occur during fuse operation as shown in the photograph in figure 1.2 and can result in a fault between phases.

To solve both problems a new fuse that mounts on the transformer bushing with very little arcing activity was developed. The bushing-mounted fuse can be seen in figure 1.3.

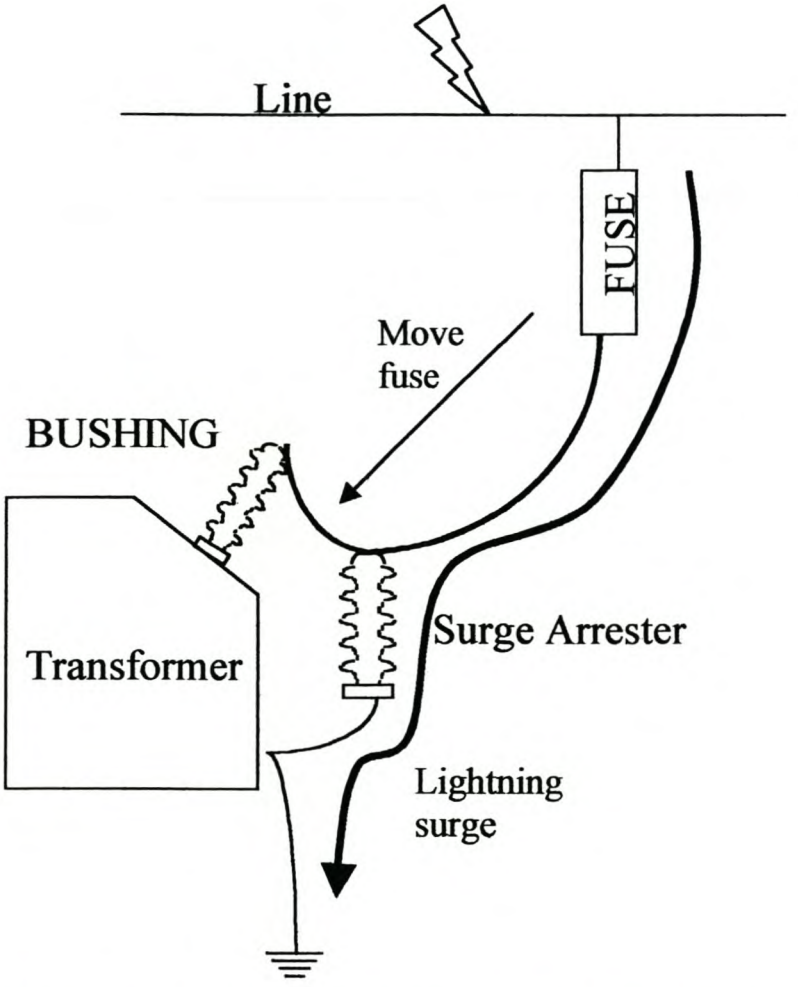

Figure 1.1. The lightning surge pass normally the through fuse and then through the surge arrester. If the fuse is moved to between the surge arrester and transformer bushing, no lightning surges will go through the fuse. Transformer inrush current will still pass through the fuse.

Stellenbosch University http://scholar.sun.ac.za

Figure 1.2. Arcing during fuse (standard type) operation.

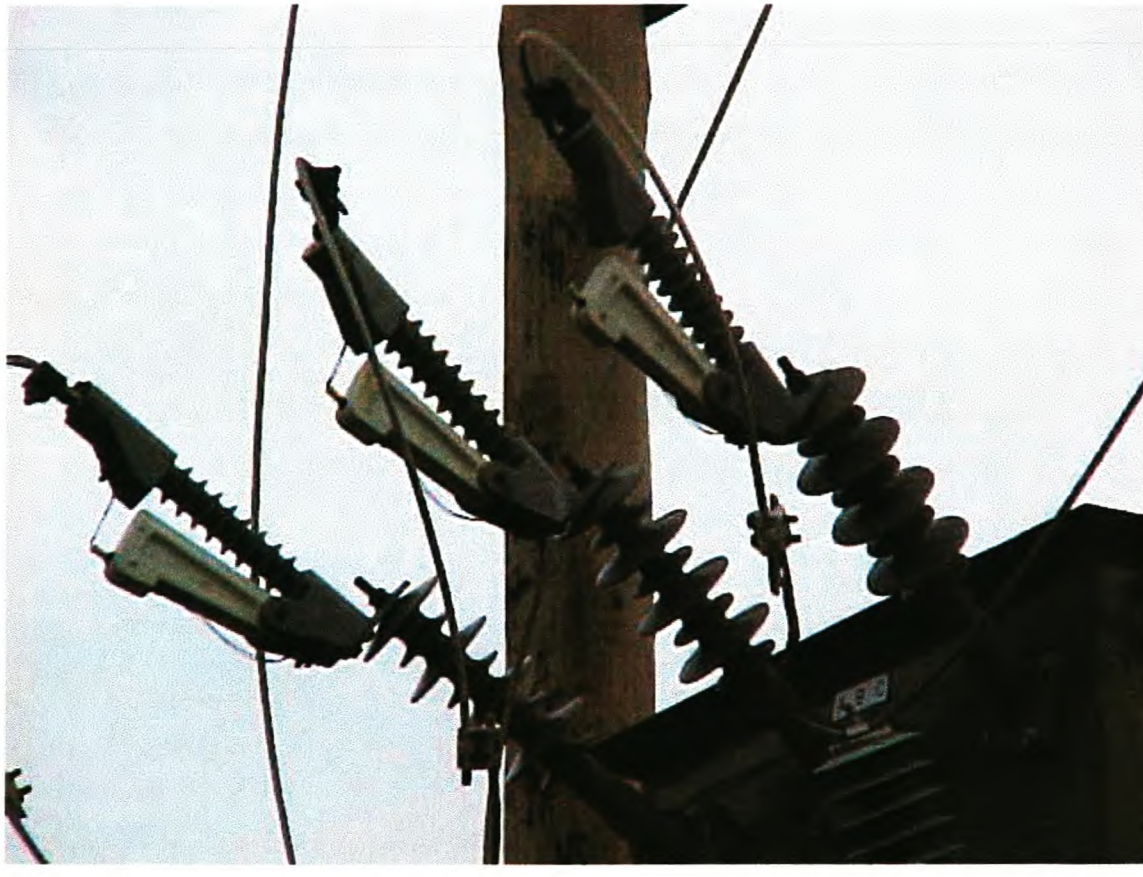

Figure 1.3. The newly developed bushing-mounted fuse developed and tested by the author of the thesis. It consists of a small explosion chamber (at the top) with a short fuse wire inside. The fuse cable comes from the bottom and fits tight through a small hole that prevents arcing downwards.

Stellenbosch University http://scholar.sun.ac.za

1.1.1.2. The transformer

Nearly all transformer failures were during lightning conditions. However in some cases it was clear that transformers failed because of overloading, especially in areas where extensive water pumping and irrigation are done. There was no relation to what make of transformers failed or any relation to the size of the transformers. In some cases (about 5%) it was found that the surge arresters, protecting the pole-mounted transformers also failed. It was not clear whether the surge arresters were blown long before the storm or during the storm. During the investigation it was also found that on some lines up to 40% of the surge arresters were not serviceable (tails blown out) due to poorly maintenance.

The 22 kV transformers are built to the SABS 780 specification. The surge level should therefore be 150 kV. Van Wyk [4] investigated transformer failures in Sub-Sahara Africa. The findings are shown in table 1.4 and it appears that about 75% of failures are lightning related ("internal failures").

It was also found that the earthing configuration is not always adequate (surge arresters effectively too far from the transformer) and differs from transformer to transformer. By far the most transformers do not have any lightning protection on the secondary side (400V) and it is possible that it can be damaged from the secondary side. The biggest installation in the study was 100 kVA while most installations were 25 kVA and 50 kVA.

Year	Bushing failures	Tapchan-ger fails	Internal failure mechanical	Internal failure electrical	Age related	Human Error	External related	Total failure
1996	132 (3%)	88 (2%)	1418 (32%)	1808 (41%)	576 (13%)	310 (7%)	100(2%)	4432(100%)
1997	180 (3%)	69 (2%)	932 (26%)	2099 (50%)	721 (17%)	52 (1%)	62 (1%)	4115(100%)
1998	190 (3%)	124 (2%)	1606 (26%)	2633 (43%)	1100(18%)	432 (7%)	93 (2%)	6178(100%)

Table 1.4. Breakdown of transformer (< 1 MVA) failures in Sub-Sahara Africa.

1.1.1.3. The surge arrester

The purpose of the surge arrester is to protect the transformer from being damaged by lightning. The surge arrester has a disconnecting device (Figure 1.4) that isolates the arrester from the line when the arrester is damaged.

Two types of surge arresters are used on the test lines. The porcelain types are known to be very unreliable due to some mechanical constraints. The polymer type surge arrester is very reliable with a failure rate of approximately 0.05% and was used on the test lines. Many of these failures were also due to mechanical reasons (bad handling).

Some important specifications of surge arrester are:

- Voltage:
  - Continuous operating voltage (U_c or abbreviated as COV or MCOV)

Stellenbosch University http://scholar.sun.ac.za

- Rated voltage (U_r) – knee point where arrester begins conducting.

- Current:
  -Continuous current (I_c) at U_c
  - Nominal discharge current (I_n) is the peak current value of a specified surge.

- Energy:
- Single surge energy capability (expressed in kJ or kJ/U_r) which is the energy absorbed by the arrester during an overvoltage or surge.

- Surge protection level (Voltage between terminals of arrester during discharge):
  - Lightning impulse protection level (LIPL) for lightning at I_n.
  - Switching impulse protection level (SIPL) for switching at I_n.

The Eskom standard specification of the arresters in use can be seen in Appendix E.

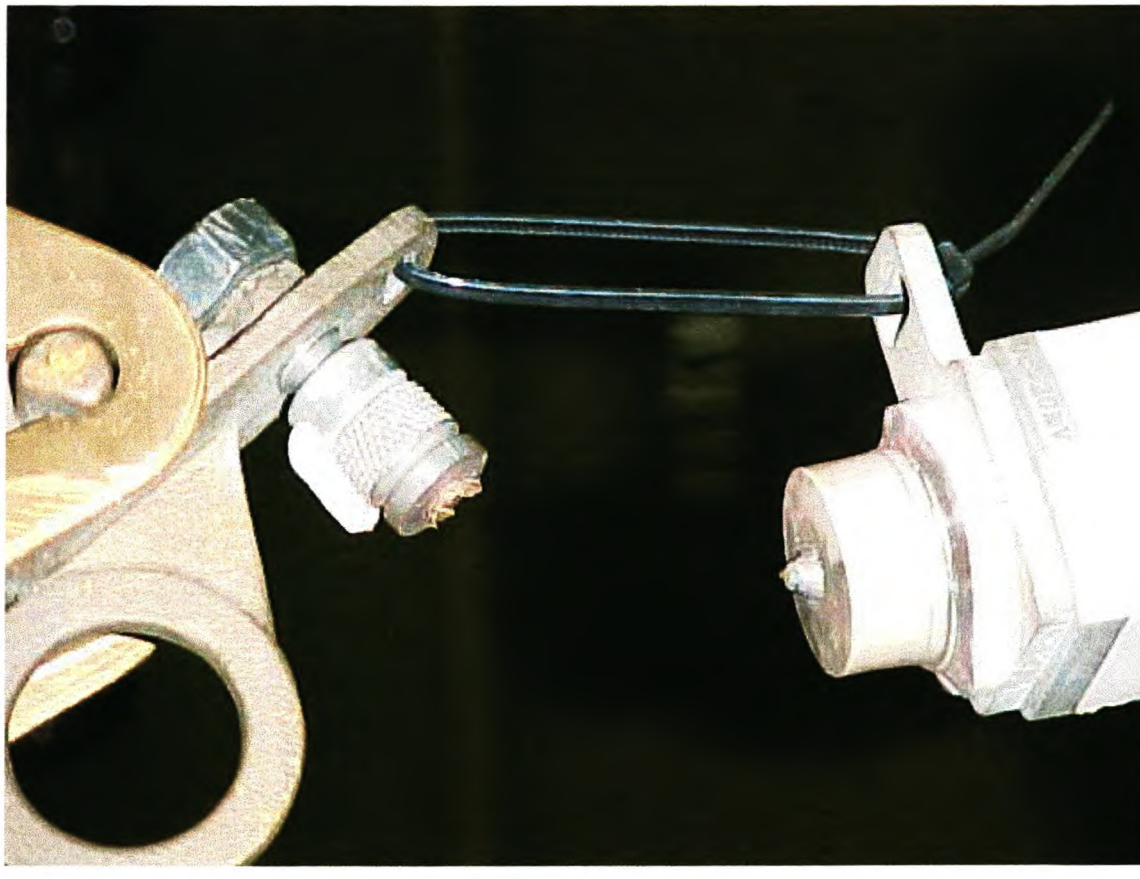

Figure 1.4. A surge arrester's disconnect device that operated.

Stellenbosch University http://scholar.sun.ac.za

1.1.2. Power system configuration

1.1.2.1. Distribution network configuration

Figure 1.5a shows the typical layout of a 22 kV distribution line. It is normally one of several feeders, feeding from a typical 10 MVA substation. The line consists of a backbone with T-offs and 400 V supply points along the line. Each supply point shown in Figure 1.5 consists of a 22 kV dropout fuse, a surge arrester on each phase and a 22 kV / 400 V three phase transformer. Figure 1.5c is a photo of a typical polemount installation.

The identification of positions on the line is done by the line code followed by pole numbers. For example, the code of the Kromdraai substation Mooiplaas feeder is KMP. The KMP feeder is also the feeder that was chosen for this study and will be mentioned regularly. The position of the point of supply named KMP59-40-3 means 59 poles down on the line there is a T-off, 40 poles down this T-off there is another T-off and 3 poles further on that T-off is the point of supply.

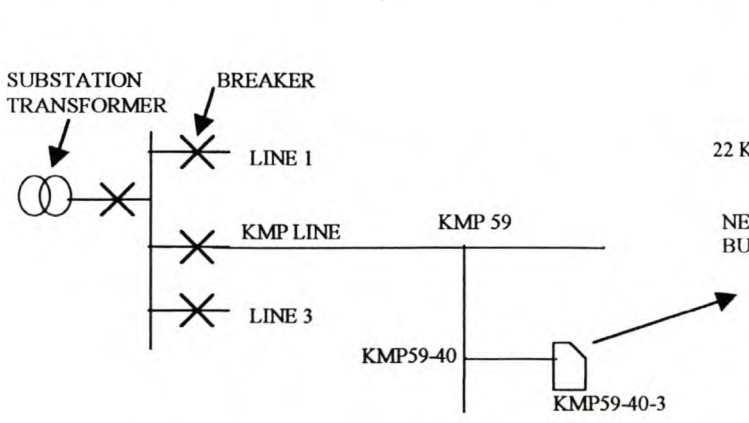

Figure 1.5a. Typical distribution line layout

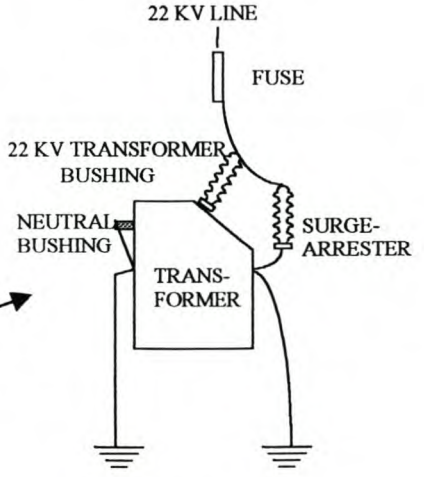

Figure 1.5b. Typical point of supply layout

1.1.2.2 The pole-mounted installation

As shown in figure 1.5b and c, the pole-mounted installation consists of three surge arresters, three dropout fuses and a transformer. The installations are responsible for most of the faults on the lines – especially during lightning storms. By studying figure 1.5b, it appears that a lightning surge from the line will go through the fuse and surge arrester to earth. The surge arrester should be able to effectively protect the transformer from being damaged by the lightning surge. The lightning surge current through the arrester may cause nuisance fuse-blowing.

Stellenbosch University http://scholar.sun.ac.za

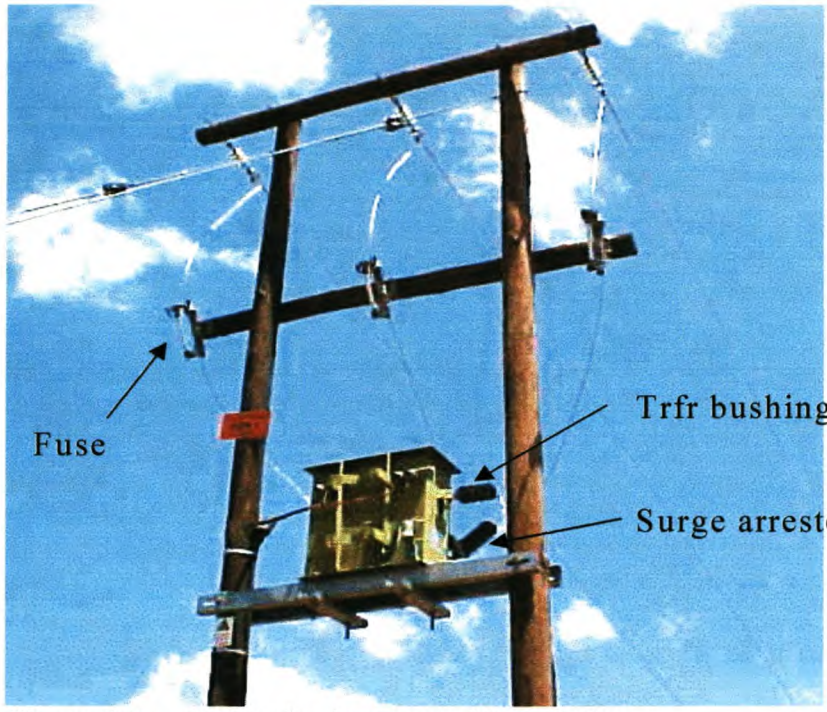

Figure 1.5c. A typical pole-mounted installation.

1.1.2.3. Earthing configuration

The earthing arrangement of the installation is of utmost importance. Incorrect earthing will result in poorly or no surge arrester protection for the transformer. The surge arrester earth as well as the LV neutral bushing should be bonded to the transformer tank, which is earthed. This earthing arrangement is known as bonded earthing (figure 1.6) while separate earthing means that the surge arrester is bonded to the transformer tank that is connected to the neutral bushing through a neutral surge arrester. The seperate earthing configuration ensure that there is no physical connection between MV and LV should the MV earth wire become alive.

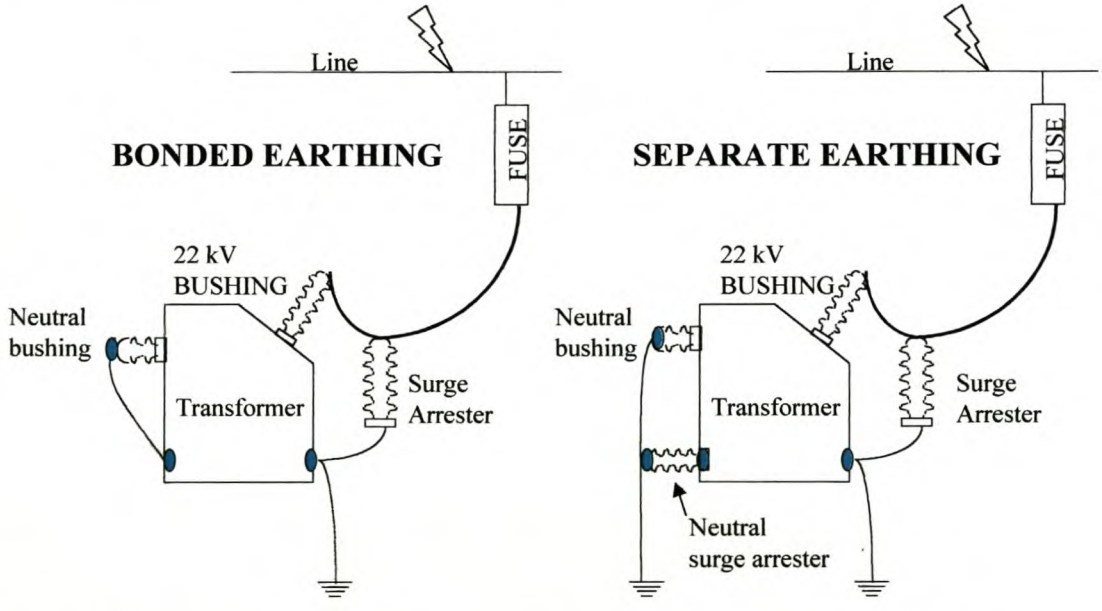

Figure 1.6. The difference between bonded earthing and separate earthing.

Stellenbosch University http://scholar.sun.ac.za

The MV surge arrester should be placed as close as possible to the equipment that must be protected. It is common practice that the surge arrester should be mounted on the transformer tank. The voltage across the transformer can be as much as double [5] when there is a high impedance connection (long jumper) between the surge arrester and the transformer.

1.1.2.4. The line

The KMP line was built in a time when the Wishbone configuration as shown in figure 1.7, was used as the standard. The insulation between phase and earth consists of two glass disc insulators in series with 600 mm of woodpole. An earthed wire is stapled to the pole from top to bottom to protect the woodpole from splitting due to lightning. The reason for using wood as part of the insulation is due to the substantial improvement of performance of the line during lightning storms [6]. Secondly, surge flashover along a wood path is usually characterized by relatively high residual arc voltage and therefore has good arc quenching properties [7].

According to Sadurski [8][9], the surge withstand level for positive surges over two glass disc insulators is 150 kV. The surge withstand strength for a 600 mm wood path is 200 kV. As most of the lightning surges have a negative polarity, the BIL of the KMP line can be taken as 350 kV.

Measurements done by Geldenhuys [10] showed that induced voltages on 8 – 10 m unshielded distribution lines occasionally exceeds 200 kV but seldom exceeds 250 kV. The KMP line should therefore be able to withstand all lightning induced voltages.

A direct lightning stroke on the line discharges currents in the range between 7 and 10 kA through the pole to earth [11]. This can cause the pole to splinter (figure 1.7) or split (figures 1.8 and 3.1.2)

Stellenbosch University http://scholar.sun.ac.za

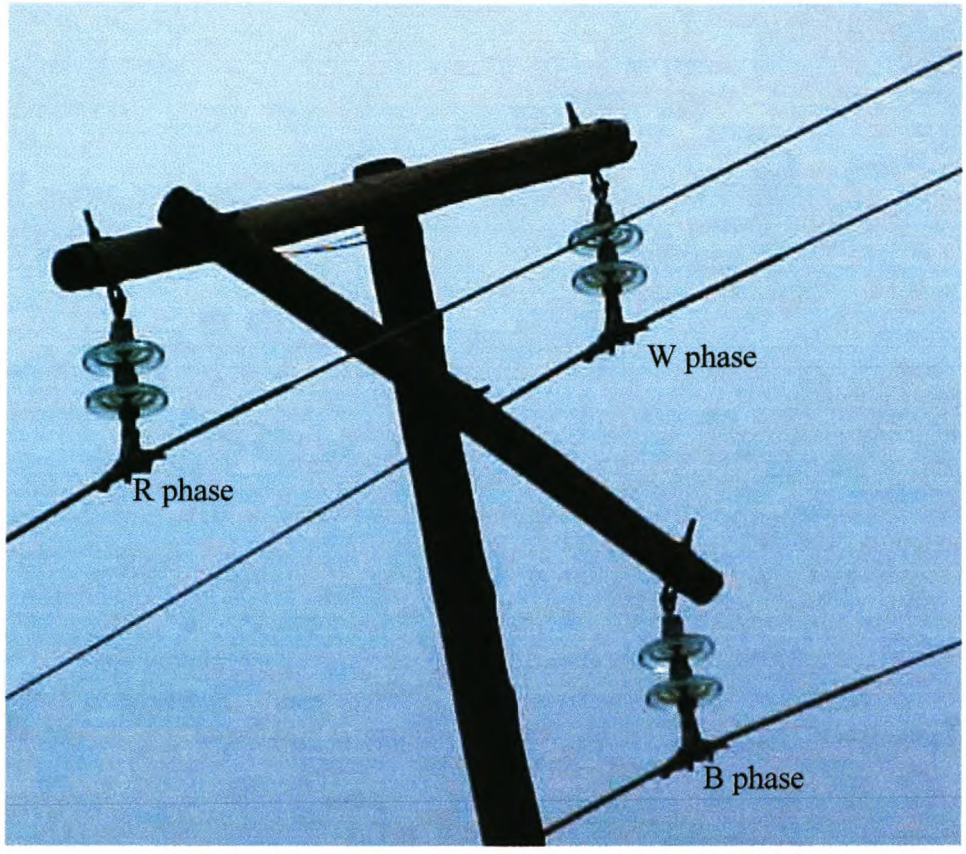

Figure 1.7. The Wishbone construction. Splintering due to lightning is visible in the top of the triangle.

Figure 1.8. Pole splitting. The lightning damage can be seen on the right top end of the cross arm.

Stellenbosch University http://scholar.sun.ac.za

1.2. Scope of the work

The purpose of this study is to limit the damage caused by lightning to equipment on distribution lines. Special attention is given to fuses, transformers as well as wood pole splitting and broken glass insulators. The emphasis is to reduce equipment failures rather than flashovers.

The goal is to identify problem zones and to effectively protect the equipment in that area against lightning. As there are many problem zones, the method and product must be cheap, easy to install and durable. The best point of installation must also be easy to identify. A dropout type line surge arrester as well as a bushing-mounted fuse were developed and this combination ensured on average a 95% decrease in failure of fuses and transformers.

Finally ATP (Alternative Transient Program) will be used to do surge studies on lines. The results will be used to accurately install the line surge arresters as well as to calculate the tolerance on accuracy that can be allowed.

1.3. Conclusion

In this chapter the background and motivation of the project was outlined. A brief description was given of the main equipment installed on the lines under consideration.

1.4. References

1. D.E. Parrish, Lightning caused distribution transformer outages on a Florida distribution System, IEEE Transactions on Power Delivery, Vol. 6. No. 2, April 1991, pg. 883.
2. A. Hamel, G. St-Jean, M Paquette, Nuisance fuse operation on MV transformers during storms, IEEE Transactions on Power Delivery, Vol. 5, No. 4, November 1990.
3. A.R. Hileman, Insulation Coordination for Power Systems, Marcel Dekker, Inc. 1999, p. 209 – 215.
4. I. Van Wyk, Transformer failures in Sub-Sahara Africa: A 1998 Review, Rotek Engineering.
5. ABB Switchgear, Application guidelines for station protection. Technical information publication SESWG\A 2310E, Edition 2, 1995-10, p. 2
6. M. Darveniza, Electrical properties of wood and line design, University of Queensland Press, 1980.
7. C.T. Gaunt, distribution line insulation, Seminar on the lightning protection of distribution lines, SAIEE, 1 – 2 August 1989, Pretoria.
8. K.J. Sadurski, H.H.K. Weihe, Lightning surge flashover voltages of pin and disc type insulators when used in combination with wooden crossarms, SAIEE Symposium on the Lightning performance of overhead lines, Pretoria, February 1982.
9. K.J. Sadurski, F.A. Auditore, Lightning surge tests on rural 11 and 22 kV wood-pole structures, Eskom report TRR/L/83/004, 1983.
10. H.J. Geldenhuys, C.T. Gaunt, A.C. Britten, Insulation co-ordination of unshielded distribution lines from 1kV to 36kV, SAIEE publication.

Stellenbosch University http://scholar.sun.ac.za

11. K.J. Sadurski, Woodpole splitting and its prevention, Seminar on the lightning protection of distribution lines, SAIEE, 1 – 2 August 1989, Pretoria.

Stellenbosch University http://scholar.sun.ac.za

2. LITERATURE STUDY: LIGHTNING PERFORMANCE OF EQUIPMENT

In this chapter work previously done in the field is investigated. Most of the work referred to the improvement of line performance by installing line surge arresters.

2.1 History

Much work was done worldwide on lightning and its impact on powerlines and other related equipment. However, to solve lightning problems on the power network is not easy as no two power networks are configured in the same way and no two lightning flashes have the same number of strokes, waveshape and intensity. It is therefore necessary to investigate, analyze and engineer each case separately. More than half of the electrical faults on overhead lines is due to lightning. Many counter measures are taken like improving tower footing resistance, install overhead screening wires, increasing insulation levels and lately most of the time install line surge arresters, to improve the lightning performance of lines [1].

The first equipment that was used for lightning protection was an open air spark gap. One major disadvantage of the spark gap was that once lightning bridged the gap, the air was ionized and then usually followed by an arc from the power system causing a short circuit. A second disadvantage was that a very steep change in surge voltage occurred when the arc was initiated causing impulse currents. The change in current $(\frac{di}{dt})$ in the transformer windings may cause high interturn potentials leading to insulation failure. The flashover voltage of the gap also depends on the air density, moisture and pollution.

The next generation of surge arresters used, was the silicon carbide (SiC) gapped surge arrester. A gap was put in series with the SiC blocks in order to eliminate leakage currents during normal operating voltages.

In 1971 Matsuoka [1] reported on experiments with Metal Oxide surge arresters (MOSA). Due to uncertainty of the stability and life of the MOSA, a spark gap was then still used in series with the MO blocks. The flashover voltage could be much better controlled and a follow through power arc was virtually impossible. More experiments [2] with line arresters was done in 1975 on a 33 kV line in Japan. In 1976 line arresters were installed on a 6.6 kV line also in Japan. In 1980 line arresters were for the first time applied on transmission lines (66 kV and 77 kV) in Japan. In 1982 line arresters were installed on a 138 kV line in the USA. Up to 1998 about 200 000 units were installed on lines (up to 500 kV) in all five continents. An estimate [2] of several ten millions line arresters are installed world wide on distribution and transmission lines.

S. Sadovic [3], R. Joulie, S. Tartier and E. Brocard did some calculations to show line surge arresters can be used and what the effect should be. They came to the conclusion that it can improve the line performance substantially, but no practical results were available. A good theoretical background on using line arresters is given by Hileman [4].

Stellenbosch University http://scholar.sun.ac.za

F De la Rosa [5], CA Nucci and VA Rakov just mentioned that line surge arresters will better line performance, but no practical results were available.

ISCOR, a steel and iron plant in South Africa, complained about numerous dips during lightning activity on their 275 kV supply. The problem area where the line went over a hill was identified. WC van der Merwe of Eskom installed line surge arresters on the hill with excellent results. No flashovers due to lightning occurred in the vicinity of the hill on these lines after the line arresters were commissioned.

2.2. Types of line arresters

Two types of surge arresters are used. The zinc oxide (ZnO) element type, named metal oxide varistor (MOV) have more non-linearity than the silicon carbide (SiC) element type. Both types can be used in series with an external or internal spark gap. An internal series gap will be used in cases where no leakage current during normal operating voltages is a requirement. Of importance is the amplitude and duration of these surges, as this will determine the energy to be absorbed by the surge arrester.

The resistance of arresters with ZnO blocks is sufficiently non-linear and no series spark gap is necessary. The current through this type of surge arrester is in the order of 100 μA at the continuous operating voltage. Figure 2.1 shows the typical voltage-current characteristics [6] of ZnO surge arresters.

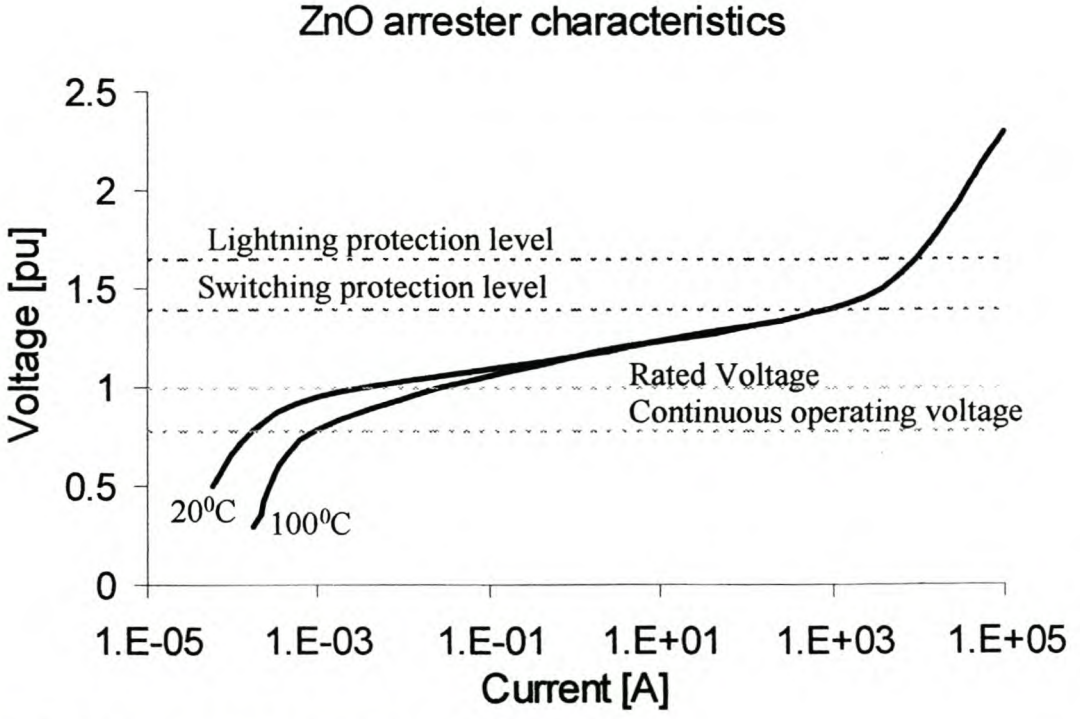

Figure 2.1. Typical characteristic of ZnO surge arresters

Stellenbosch University http://scholar.sun.ac.za

2.3. The purpose of the line arrester

CIGRE Working group [2] 33.11 consolidated most of the work done regarding line arresters up to 1998. Most of this work was done on shielded lines and the main purpose of installing line arresters were found to:

- prevent flashover between tower and phases (earth faults) due to direct stroke to overhead line.
- have an acceptable low failure rate and must be able to withstand possible direct strokes to the overhead line.
- be able to withstand environmental conditions and mechanical strength against natural atmosphere.

Special considerations should be given to the explosion possibility of the arrester (especially the porcelain type arrester) as it is installed at a high position above ground. An arrester that explodes can cause serious injuries to humans and animals. It must also be possible to install the line arresters on existing line towers. A line arrester that can be disconnected automatically from the line when faulty, will be an advantage.

From a functional point of view the arresters shall suppress the voltage across the insulator to prevent flashover and power frequency follow through at the instant of the lightning stroke while under normal circumstances act as an insulator. When the arrester get damaged, it shall not constitute a permanent short-circuit phase to ground fault.

In this thesis line arresters were installed on unshielded distribution lines to help protect equipment on the line and not necessarily to prevent a flashover.

2.4. Line performance improvement due to installation of line surge arresters.

For a start theoretical studies and surge simulations can be done in order to predict reduction in the number of flashovers. This will only give a vague idea of performance improvement, as there are too many unknown parameters involved in the modeling. Two of the biggest uncertainties are the earthing resistance and the lightning stroke parameters. Another two important uncertainties are the position (tower no.) where the lightning will hit the line and the influence of corona at the time of the stroke.

The earthing resistance change as soil ionization takes place. It also depends on the type of soil as well as the percentage moisture in the soil. There will also be a difference in outcome if a stroke terminates midspan instead of on the tower. Corona affects the surge steepness as well as the amplitude in the case of a stroke with a short tail.

No negative criticism could be found on the performance of lines after installation of line surge arresters. Looking at the number of line surge arresters installed as mentioned in 2.1, one can assume that the general conclusion of line surge arrester installations is positive.

Stellenbosch University http://scholar.sun.ac.za

A number of 66 kV and 77 kV double circuit lines in Japan experienced double circuit failures [2]. After installation of line surge arresters on every tower, on only one circuit of the double circuit lines, 36 lightning strokes terminated on the lines. No double-circuit failure occurred. In 22 cases out of the 36 strokes, faults occurred on the unprotected circuits. In the remaining 14 cases, line surge arresters operated and most probably prevent even single line faults.

In two cases of problem 115 kV lines in the USA, all phase on all structures were fitted with line arresters. No failures were experienced in over 4 years after installation.

A circuit breaker on a 13.8 kV line in Mexico [2] always tripped and reclosed several times during lightning storms. A section of 63 poles (5.5 km) that seems to be the problem area, were fitted with line arresters on al three phases at each pole. As shown in table 2.1, a drastic reduction in faults occurs since 1989 when the line arresters were commissioned.

Year	1986	87	88	89	90	91	92	93	94	95	96
No of trips	21	24	15	0	2	1	0	0	0	0	0

Table 2.1. Number of breaker operations before and after the installation of series-gap line surge arresters.

2.5 The difference between previous work done and this thesis.

The goal of all previous work was to improving lighting performance of the line during storms due to lightning strokes. Although not mentioned in previous work, it can be assumed that a second advantage of installing line arresters is that there were most probably less equipment failures (transformers, fuses, surge arresters) after installation of surge arresters.

In this case, the main objective was to reduce equipment failure and a second advantage will be fewer breaker operations. Areas where many equipment failures took place were identified. The failures were then linked to lightning activity using the Lightning Positioning and Tracking System (LPATS). A detail line inspection in that area was then done to find the exact position (pole) where lightning damaged the pole (splitting) or insulators. Line surge arresters were then installed on all three phases only on that specific pole.

2.6. Drop-out line surge arresters.

The porcelain type surge arresters were used in the past and had a poorly performance history. In most cases the porcelain arresters exploded. It many other cases the disconnect device failed to operate. This is also the reason why the fuse is installed on the line side of the surge arrester and is therefore not protected against lightning. The arrester can then easily be isolated for replacement by just opening the dropout fuses (see figure 1.7). The field services staff did not allow any surge arresters on lines, because if a faulty line arrester is not isolated correctly, the whole line will trip out. It will also be very difficult and time consuming to find a faulty line arrester in

Stellenbosch University http://scholar.sun.ac.za

areas where the fault level is low. In this low fault level case, the earth fault protection will operate before the arrester explodes (and physical damage is visible).

In order to get around this problem, a dropout surge arrester as shown in Figure 2.2 was developed. A polymer type surge arrester is used in the bracket. When the detonator operates, the surge arrester falls out of the bracket and is therefore completely isolated from the line. The arrester is tied with a steel tie to the bracket to avoid causing injury or damage when falling open. The faulty surge arrester can then be replaced from ground level while the line is alive using an insulated link stick.

In the rare case (1 in 30 000 from field experience with the polymer type arrester) where the detonator fails to operate, the suspect surge arrester can be pulled into the open position from ground level. The arrester can then be tested and replaced if faulty. The dropout concept makes operating very safe, as there is no need for climbing. The change for accidents is very small (falling and electrical contact).

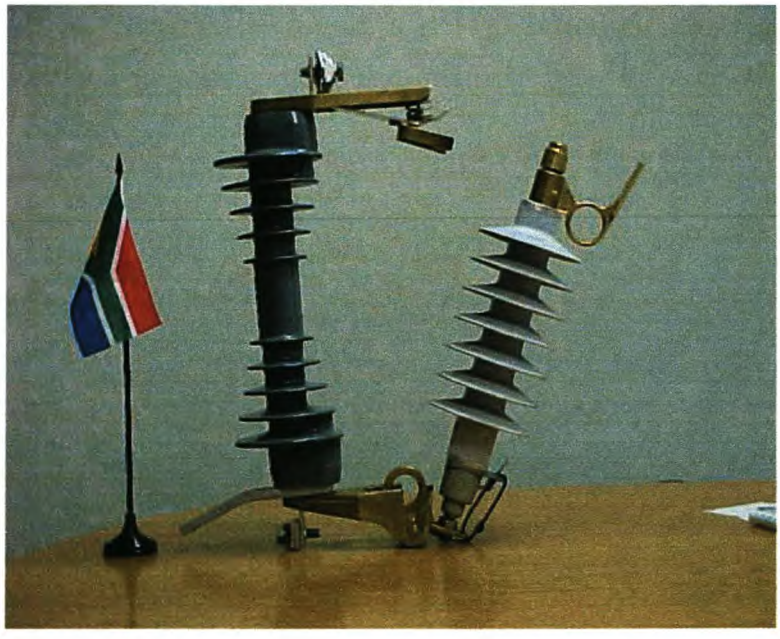

Figure 2.2. A 22 kV Drop-out line surge arrester

2.7. Conclusion

Line surge arresters are used worldwide to improve power line performance. However, the main purpose of this thesis is to use line arresters to minimize equipment failure. A dropout surge arrester was developed for easy isolation and replacement of faulty line arresters.

2.8. References

1. M. Matsuoka, Monohmic Properties of Zinc Oxcide Ceramics, Japanese Journal of Applied Physics, 10 June 1971, p.46.
2. A. Schei, Convenor of WG 33.11, Task Force 03, Application of metal oxide surge arresters to overhead lines, Electra No. 185, October 1999, p. 83 – 109.

Stellenbosch University http://scholar.sun.ac.za

3. S. Sadovic, R Joulie, S Tartier, E Brocard, IEEE Transactions on Power Delivery, Vol 12, No.3, July1997,p. 1232 – 1237
4. A.R. Hileman, Insulation Coordination for Power Systems, Marcel Dekker, Inc. 1999, p. 641 - 672
5. F. De la Rosa, CA Nucci, VA Rakov, CIGRE SC 33 Internation Conference, Zagreb, 1998, P.34, p.10
6. ABB, Selection guide for ABB HV surge arresters, Edition 3, 1995-02, p. 1

Stellenbosch University http://scholar.sun.ac.za

3. FACTORS AFFECTING LIGHTNING RELATED EQUIPMENT FAILURES

The overvoltages caused by lightning are affected by various factors. In this chapter the influence of the earthing resistance, corona and lightning is investigated.

3.1. Lightning

3.1.1. Background

There are about 8 million lightning flashes to ground per day worldwide that cause many deaths (about 100 deaths per year in the United States alone)[3]. Furthermore lightning causes damage to ships, vehicles, buildings, power lines and even airplanes (especially those with fuel leaks).

Before 1752, lightning has been feared as an atmospheric flash of the supernatural origins. In 1752 Benjamin Franklin [1] proved for the first time that thunderclouds are electrically charged using the famous kite experiment. A spark flew from a key which was tied to the damped kite string, that was insulated from earth, to Franklin's (who's body was earthed) knuckles. TF D'Alibard of France also proved in May 1752 and GW Richman[1] in July 1753 that thunderclouds contain electrical charge.

Two elements are necessary to charge a cloud electrically. There must be ice particles as well as convection present in the cloud. Ice particles are present when the temperature is below –10°C. Once the ice particles grow bigger, the crystals starts falling and capture supercooled cloud drops. As these built up, a structure called soft hail or graupel forms. As the graupel moves through the cloud of supercooled drops, it charges significantly. Crystals bounce from the growing graupel that leads to a separation of charge by a process that is still not clear. In any event, the graupel particles fall faster than the smaller ice crystals with the opposite charge, giving rise to a dipole [2]. The upper part of the cloud becomes normally positive charged while the lower part becomes negatively charged [1].

When the charge become large enough (charges up to 10 Coulomb per km^2 and Voltages up to 50 MV), air breakdown begins. First a leader (current between 50 A and 200 A) starts moving (at about 3×10^7 m/s) from the highly charged cloud towards earth. This leader which is invisible for the naked eye, can split up in more than one path. As it come closer to earth, streamers start from the earth towards the approaching leaders from the cloud. When they meet each other, a highly conductive (ionized) path is completed between the cloud and earth [3].

This results in the return stroke, which is highly visible and can be seen clearly many kilometers away. The actual core (current path) is less than 10 mm in diameter [2] and is surrounded by a corona sheath with radius of 10 m and less. A current in excess of 200 kA can pass through the core, but average about 34 kA [3].

The lightning current heats up the air between 20 000 degrees C [1] to as much as 27 000 degrees C [3] (five times the temperature of the sun's surface). This process causes a shock wave as the moisture "explodes", which is heard and known as thunder.

Stellenbosch University http://scholar.sun.ac.za

A lightning stroke can be between clouds or between clouds and earth. In the second case the cloud can be either charged negatively or positively. Between 85% and 95% of the flashes [3] are classified as negative downward. Only the cloud-ground flash influence power line performance.

About 45% of all lightning flashes consist of only one stroke. The rest of the flashes consist of a first stroke followed by a second stroke or by many subsequent strokes (on average three strokes per flash, but can be as many as 54 strokes per flash)[3]. The risetime of the subsequent strokes in a flash is also faster than that of the first stroke. Multiple stroke flashes discharge more energy and heats up arresters more than single strokes.

Due to the high current in a lightning stroke, a potential can be induced in circuits of metal, causing considerable high voltages. According to Geldenhuys [4] and Diesendorf [5] voltages of up to 200 kV and 300 kV respectively can be induced on a power line close to a lightning stroke.

3.1.2. LPATS

Lightning can be monitored/measured with Lightning Positioning and Tracking System (LPATS). This program was extensively used during this project. Accurate time-stamping as well as information about the magnitude, polarity and exact position of each lightning flash is stored in the LPATS database. This data is used to find lightning strokes that damage or cause flashovers on power lines. LPATS consists of 6 repeaters monitoring lightning activity in South Africa. This information is sent to a central master station where some calculations regarding the position, intensity and time are done.

The accuracy of the position of a stroke depends on how far the place of interest is from the sensors. Close to the sensors, the accuracy is better then 500 m while the accuracy around the KMP feeder (close to Wolmaransstad) is about 1 km. This means that it may appear in figure 3.1.1 as if there was a direct stroke on the line, while the striking point was in fact approximately 1 km away from the line.

Figure 3.1.1a shows some lightning activity that took place on 21 February 1999 between 02:04 and 17:50. During this period there were 9509 flashes consisting of 1106 positive, 8289 negative and 114 cloud – cloud flashes. Figure 3.1.1b and 3.1.1c are just zoomed in versions of figure 3.1.1a. Figure 1c shows the most northern part of the KMP feeder. A"×" in figure 1c indicates a flash between clouds, a "+" a positive and a "dot" indicates a negative flash to earth. Three lightning flashes, a positive flash at the top, a cloud to cloud in the middle and a negative flash at the bottom, are pointed out in figure 3.1.1c. The positive flash was 21 kA and occurred at 17:01:57,520.

Information about the flashes is 90% reliable in the Wolmaransstad area, implying that 10% of the flashes could be missed and not documented at all. Global Positioning System (GPS) time-stamping is done for each stroke, therefore the time as shown in figure 3.1.1c is extremely accurate (15 ms). One shortcoming of LPATS is

Stellenbosch University http://scholar.sun.ac.za

that it normally only shows the first stroke in a flash and it is not always known how many strokes were present in the flash. A second problem is that there is no information about the tail length of the lightning stroke.

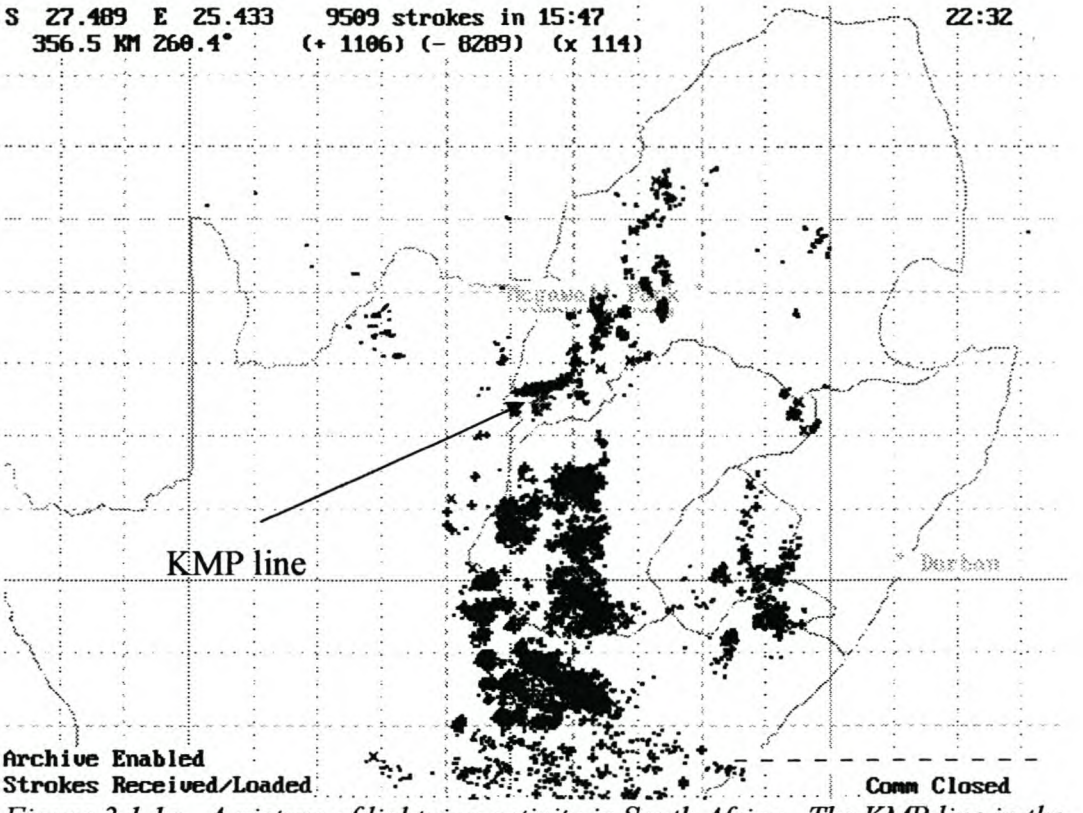

Figure 3.1.1a. A picture of lightning activity in South Africa. The KMP line in the North West Region will be studied closely.

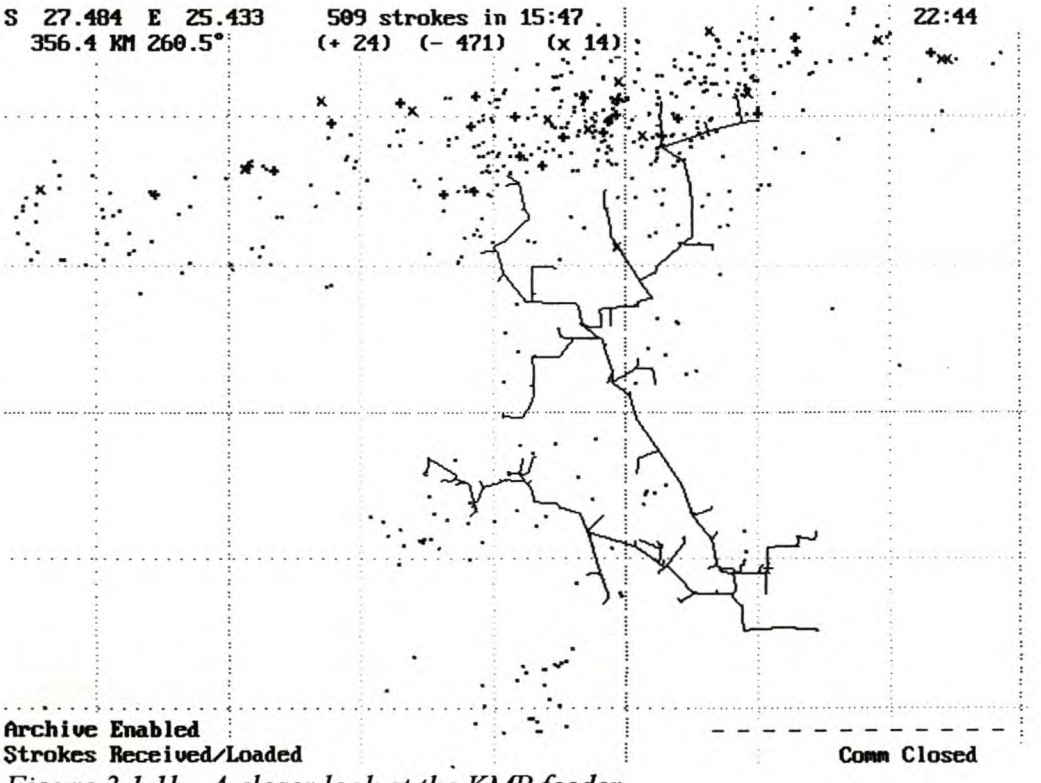

Figure 3.1.1b. A closer look at the KMP feeder.

Stellenbosch University http://scholar.sun.ac.za

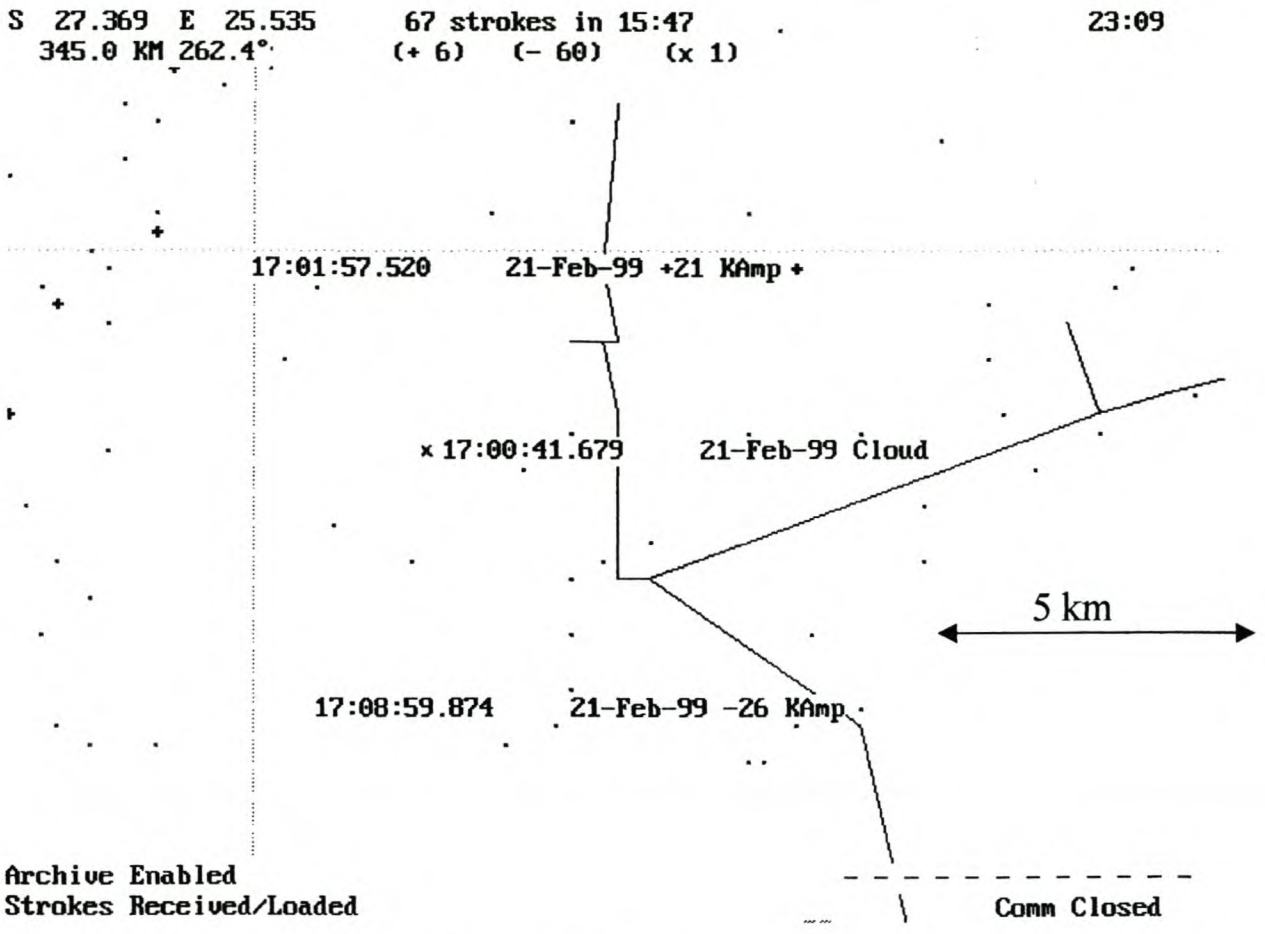

Figure 3.1.1c. The northern part of the KMP feeder.

3.1.3. Determining which stroke hit the line

A Supervisory control system is used by the Eskom Control Centre to monitor the power network. This system also makes use of GPS time-stamping of incidents. There is normally a breaker operation recorded if an unshielded distribution (11 kV/22 kV) line is hit by lightning. Other damages (fuse, transformer or conductor damages) or sectionalizer operations are normally quickly reported through the Customer Care Centre. The recorded times are useful to identify the stroke.

To find the exact location of the stroke, it is necessary to do a line patrol. Broken insulators, split woodpoles (see figure 3.1.2) and other damaged equipment are good indications of where the actual stroke hit the line.

3.1.4 Lightning density

In order to calculate the chances of a line being hit by lightning, the lightning ground flash density must be known. It is normally given as the number of lightning flashes per km^2 per year. This information is available in documentation [4] but can also be calculated more accurately with LPATS. The lightning density around the KMP line is between 2 and 7 flashes/km^2 /year. Figure 3.1.3 shows that the lightning density change from year to year between 1994 to 1997 is relative small.

Stellenbosch University http://scholar.sun.ac.za

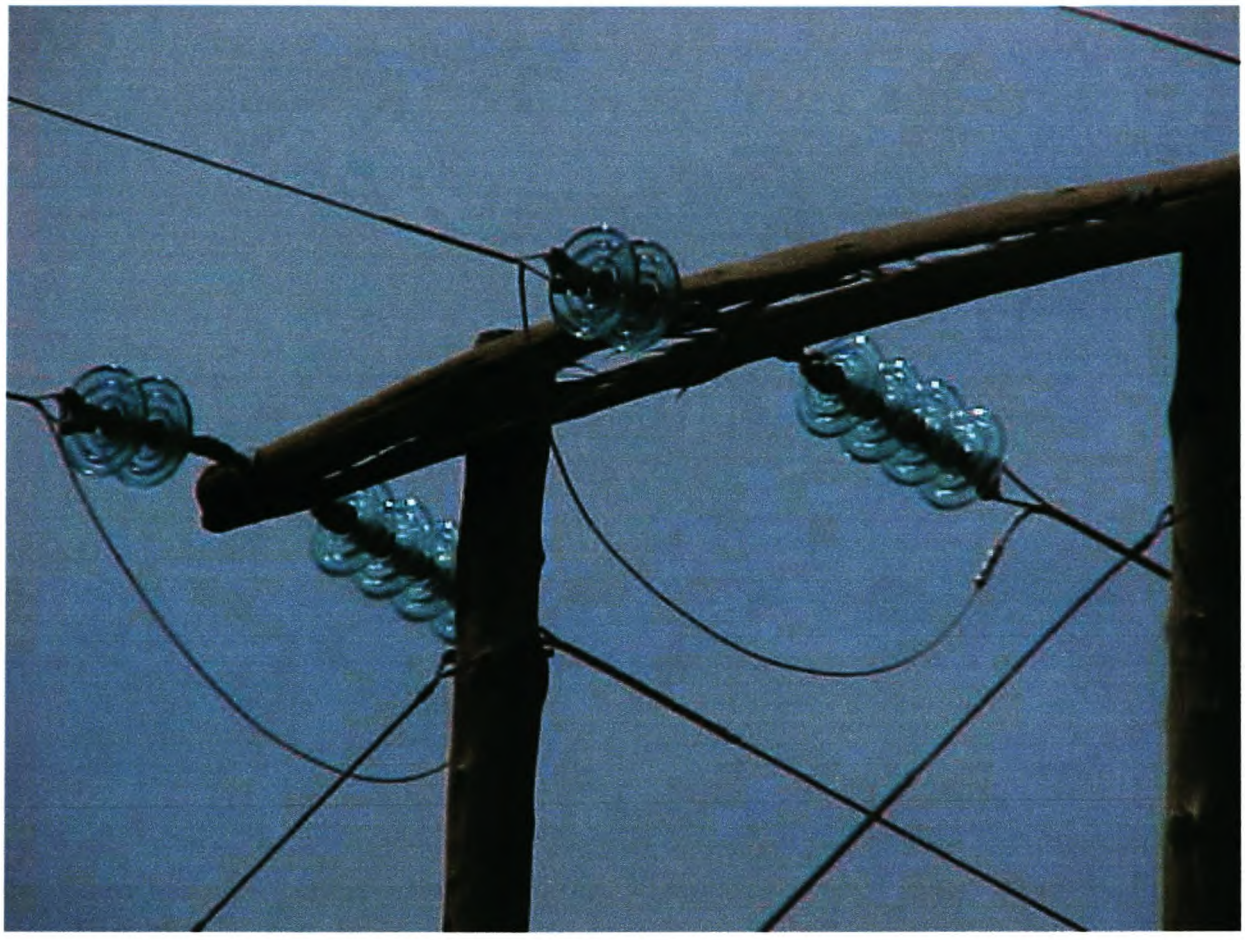

Figure 3.1.2. Lightning damage to a crossarm.

3.1.5. Probability of lightning stroke hitting a line.

Detail about the probability of a stroke terminating on the line is given in Appendix A The average number of direct strikes (Ns) per year to a line is given by Eriksson [6] as:

$$Ns = Ng(28H^{0.6} + w) \times L \times 10^{-3} \text{ per year}$$

Where Ng = average ground flash density in km^{-2} /year
w = line width in the absence of shield wires in m
L = line length in km
H = average tower height in m.

For the KMP line, which is 163 km long in total, the height = 8 m, the line width = 1.2 m and using a value of Ng = 4 flashes/km²/year, *Ns* will be:

$$Ng(28H^{0.6} + w) \times L \times 10^{-3} = 4(28 \times 8^{0.6} + 1.2) \times 163 \times 10^{-3}$$
$$= 64.3$$

Stellenbosch University http://scholar.sun.ac.za

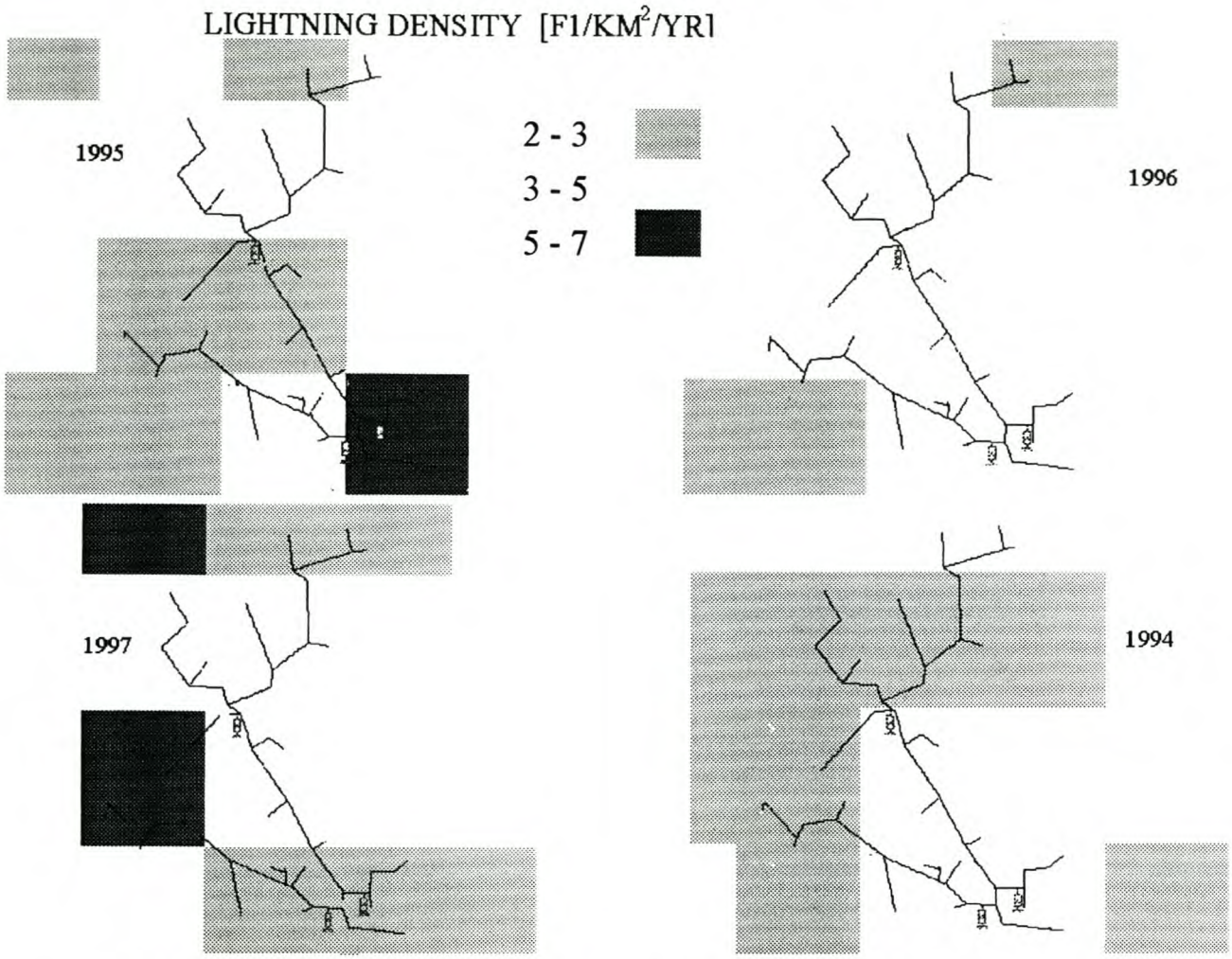

Figure 3.1.3. The lightning density over 4 years around the KMP feeder.

3.1.6. The amplitude and duration of a lightning flash.

The average current amplitude of a lightning flash is 35 kA according to CIGRE [9]. The average first stroke is 40 kA [8] and the subsequent stroke 8 kA. Figure 3.1.4 shows the frequency distribution of the lightning peak current.

The average duration of a lightning flash [9] is 200 ms as shown in figure 3.1.5.

Stellenbosch University http://scholar.sun.ac.za

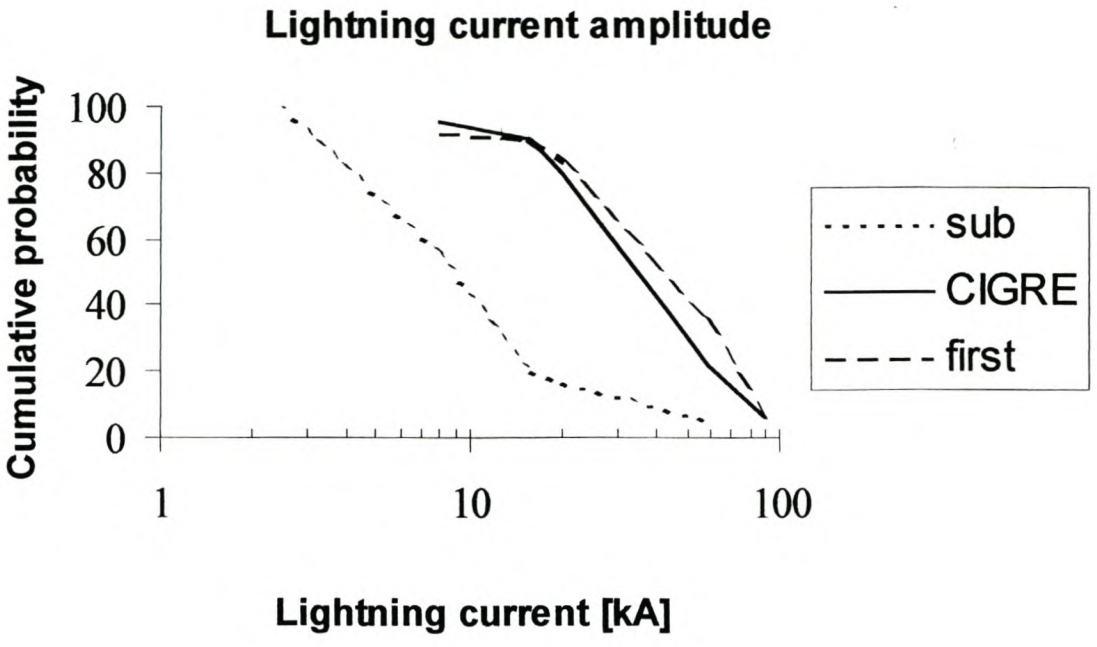

Figure 3.1.4. Cumulative frequency distribution of lightning current peak amplitudes [8]. The first and subsequent strokes as well as a CIGRE [9] reference are shown.

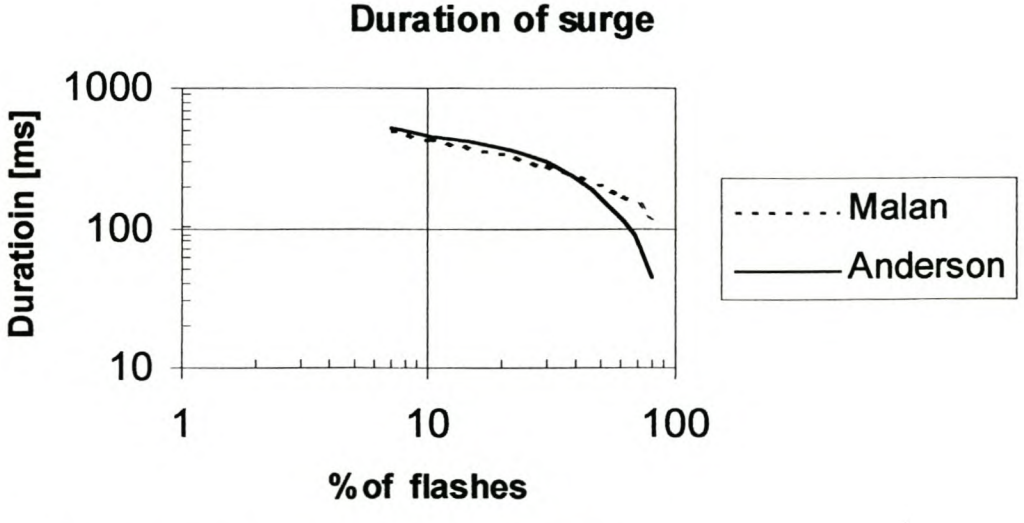

Figure 3.1.5. The duration of a lightning flash [9].

3.1.7. Direct and indirect lightning strokes

A direct stroke is referred to when the lightning stroke terminates on the overhead line. The current surge divides into two surges that proceed at the speed of light down the line in both directions. Based on Ohm's law, the voltage v at the struck point is:

$$v = i\frac{Z_c}{2}$$

where i = peak current

Stellenbosch University http://scholar.sun.ac.za

v = peak voltage
Z_c = surge impedance of the line

If the surge current is equal to 30 kA and the surge impedance 350 ohm, the surge voltage will be 5.2 MV. This will cause a flashover on a distribution power line, which will most probably result in a power frequency fault.

An indirect stroke is referred to as a stroke close to the line and affects al three phases of the line. If a leader from a negatively charged cloud approached the power line, a positive charge will be induced on the line due to capacitive coupling between the leader and the line. As the leader terminates on a nearby object and discharges the cloud, the charge on the line is "released" and travels in the form of a surge on the line. The amplitude of the voltage is normally less than 200 kV [4]. Although no flashover may occur, unprotected equipment can get damaged.

3.1.8. Conclusion

With the help of LPATS, lightning statistics were available. The average lightning density was determined and other lightning flash parameters were studied. Lightning related line faults and equipment failures could be identified.

3.2. Corona on a line during a lightning surge

Corona is a partial discharge that occurs when the electric field strength exceeds the ionization threshold for the air surrounding the conductors. Proper line design ensures that power frequency corona losses and interference is kept to acceptable levels.

However, if a voltage surge appears on a line due to lightning (direct or induced stroke), severe corona can occur on the affected line. The corona sheath around the conductor increases the effective radius of the conductor, leading to a reduction in the steepness of the wave, thus reducing the effects of the surge.

3.2.1. Capacitive effect of corona

When a ramp-shaped surge travels at a speed of c (3×10^8) m/s along the line, the voltage at a specific point will increase as the surge passes that point. When the voltage at that point reaches the corona inception voltage (V_i), corona will commence and the effective radius of the conductor and therefore the capacitance will increase as shown in Fig 3.2.1. The propagation speed, $U = \frac{1}{\sqrt{LC}}$, of the wave corresponding to the part where $V>V_i$, will be slower. The effect will therefore be to reduce the effective steepness of the wave. Increased capacitance therefore decreases the effective wavefront steepness en therefore the voltage magnitude if the tail is short. Figure 3.2.1 presents CIGRE's [10] interpretation of the capacitance increase as the voltage increase due to corona.

Stellenbosch University http://scholar.sun.ac.za

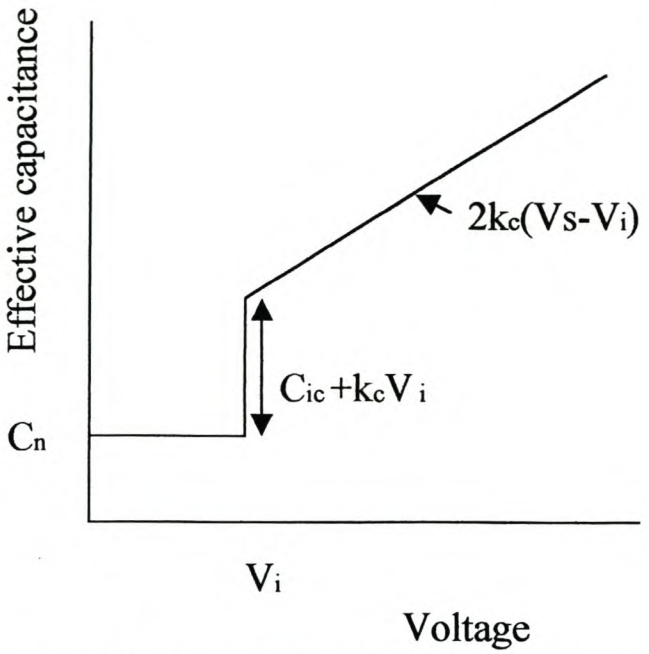

Figure 3.2.1. Line capacitance increase with an increase in conductor voltage above the corona inception voltage V_i [3, p 360].

According to figure 3.2.1, the line capacitance C below V_i is:

$$C = C_n \qquad (3.2.1)$$

where C_n is the natural capacitance of the conductor

At V_i the capacitance is:

$$C = C_n + C_{ic} + k_c V_i \qquad (3.2.2)$$

where C_{ic} is the initial jump in capacitance above V_i and k_c is a constant.

And above V_i

$$C = C_n + C_{ic} + k_c V_i + 2k_c (V_s - V_i) \qquad (3.2.3)$$

where V_s is the surge voltage.

The approximate values for C_{ic} and k_c differ between publications [3, p 363-365]. For a single conductor, the value of k_c varies from 0.9 to 3.3×10^{-3} pF/kV-m and C_{ic} from 0.85 to1.82 pF/m.

3.2.2. Wavefront steepness.

The decrease in steepness of the wavefront due to the increase of capacitance is defined in terms of $\Delta T/d$ meaning the time delay per unit length traveled by the wave. This is illustrated in figure 3.2.2.

Stellenbosch University http://scholar.sun.ac.za

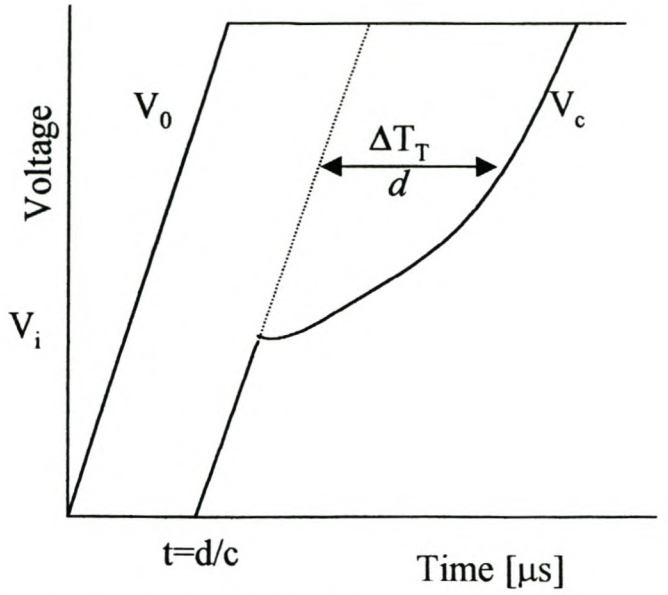

Figure 3.2.2. The time delay in steepness of a wavefront after the wave traveled a distance d in the presence of corona. Vo is the initial voltage and Vc the voltage at distance d.

A surge travels at the speed of light ($c = 3\times10^8$ m/s) on a resistance free line in air. Due to capacitance of the line, the surge speed decreases to a slower speed, *v*. Note that the increase in effective radius only affects the capacitance and not the inductance.

Therefore:

$$\frac{\Delta T_T}{d} = \frac{1}{v} - \frac{1}{c} \tag{3.2.4}$$

$$c = \frac{1}{\sqrt{LC_n}} \tag{3.2.5}$$

Below the corona inception voltage:

$$\frac{\Delta T_T}{d} = \frac{1}{v} - \frac{1}{c} = 0 \text{ because } v = c$$

Using Eq. 3.2.2 - at the corona inception voltage:

$$\frac{\Delta T_T}{d} = \frac{1}{v} - \frac{1}{c} = \sqrt{L(C_n + C_{ic} + k_c V_i)} - \sqrt{LC_n}$$
$$= \sqrt{LC_n}\left[\sqrt{1 + \frac{C_{ic} + k_c V_i}{C_n}} - 1\right] \tag{3.2.6}$$

Using the Taylor series, Eq. 3.2.6 is approximately:

Stellenbosch University http://scholar.sun.ac.za

$$\frac{\Delta T_T}{d} \approx \sqrt{LC_n}\left[1+0.5\frac{C_{ic}+k_cV_i}{C_n}-1\right]$$
$$\approx 0.5Z_0(C_{ic}+k_c V_I) \qquad (3.2.7)$$

Where Z_0 is the surge impedance before corona.

In the same way it can be shown that above the corona inception voltage:

$$\frac{\Delta T_T}{d} \approx 0.5Z_0k_c(Vs - V_i) \qquad (3.2.8)$$

where Vs is the applied voltage.

3.2.3. The surge impedance of a line due to corona

The surge impedance Z_c of a line above the corona inception voltage is:

$$Z_c = \sqrt{\frac{L}{C_n+\Delta C}} = Z_0\sqrt{\frac{C_n}{C_n+\Delta C}} \qquad (3.2.9)$$

Where ΔC is the increase in the line capacitance due to corona.

For a single line with radius r at a height h meter above a ground plane:

$$L = 0.2\ln\frac{2h}{r} \qquad (3.2.10)$$

$$C = \frac{10^{-3}}{18\ln\frac{2h}{r}} \qquad (3.2.11)$$

Let the corona radius be R_c, then Eq. 3.2.11 becomes

$$C + \Delta C = \frac{10^{-3}}{18\ln\frac{2h}{R_c}} \qquad (3.2.12)$$

From Eq.3.2.12, the corona radius is:

$$R_c = 2h\times e^{-\left(\frac{10^{-3}}{18(C+\Delta C)}\right)} \qquad (3.2.13)$$

Anderson [11] provides an estimate of the corona radius:

$$R_c\ln\frac{2h}{R_c} = \frac{V}{E_0} \qquad (3.2.14)$$

Stellenbosch University http://scholar.sun.ac.za

Substitute Eq. 3.2.10 and 3.2.12 in 3.2.9

$$Z_c = \sqrt{0.2\ln\frac{2h}{r}18\ln\frac{2h}{R_c}10^3} = \sqrt{3.6\times10^3\ln\frac{2h}{r}\ln\frac{2h}{R_c}} \qquad (3.2.15)$$

3.2.4. The critical electric field strength [3, p 363-365]

The critical electrical field E_0 (CIGRE value) where corona starts, is:

$$E_o = 23\left(1+\frac{1.22}{d^{0.37}}\right) \text{ kV/cm} \qquad (3.2.16)$$

Where d = the diameter of the conductor in cm

Skilling-Dykes uses the equation in another format:

$$E_0 = 23\delta^{0.67}\left(1+\frac{0.3}{\sqrt{r}}\right) \qquad (3.2.16a)$$

Where δ is the relative air density

The corona inception voltage V_i is:

$$V_i = \frac{Z_0 r E_0}{60} \qquad (3.2.17)$$

Where r is the radius of the conductor

The conductor used in the study is 1.1 cm in diameter and is 8.5 m above ground.

From Eq. 3.2.16

$$E_0 = 23\left(1+\frac{1.22}{1.1^{.37}}\right) = 50.1 \text{ kV/cm}$$

Substituting Eq. 3.2.10, 3.2.11 and 3.2.16 into Eq. 3.2.17

$$V_i = \frac{\sqrt{L/C}\times r\times E_0}{60} = \frac{482\times.55\times50.1}{60} = 221\text{kV}$$

Table 3.2.1 is a comparison of E_0 and V_i values by Hileman [3, p 363-365]. The actual value of the 50.8mm conductor is questionable but is not relevant to this thesis. Looking at the thinner conductors, it seems that Skilling and Dykes is more accurate.

Stellenbosch University http://scholar.sun.ac.za

There is a considerable difference in the value of E_0 . In addition to the above values, Anderson [11] uses an average value for E_0 of 15 kV/cm.

Conductor diameter in mm	E_0 : Skilling-Dykes in kV/cm	E_0 : CIGRE kV/cm	V_i : Skilling-Dykes in kV	V_i : CIGRE kV	V_i : Actual kV
50.8	27.3	38.4	515	723	420
41.25	27.8	39.5	443	630	570
23.5	29.8	43.5	283	420	270
11	32.3	50.1	141.8	221	

Table 3.2.1. Comparison of corona inception voltages.

3.2.5. The effective corona radius

From Eq. 3.2.12:

$$\Delta C = \frac{10^{-3}}{18\ln\frac{2h}{R_c}} - C$$

$$= \frac{10^{-3}}{18\ln\frac{2h}{R_c}} - \frac{10^{-3}}{18\ln\frac{2h}{r}} \qquad (3.2.18)$$

Using Eq. 3.2.2 and 3.2.3 to calculate the line capacitance and substituting the result in Eq 3.2.13, the corona radius can be calculated. The result with the conductor height taken as 8 m is shown in figure 3.2.3 on different scales. To compare Anderson's method of calculating the capacitance and corona radius, Eq. 3.2.14 is used. Substituting the calculated value of R_c (from Eq 3.2.14) in Eq. 3.2.12, C+ΔC is known. Figure 3.2.4 shows a comparison of the corona capacitance between CIGRE, Weck, Anderson and Lee [13]. Lee differs substantially with CIGRE. The CIGRE values were taken for further calculations.

Stellenbosch University http://scholar.sun.ac.za

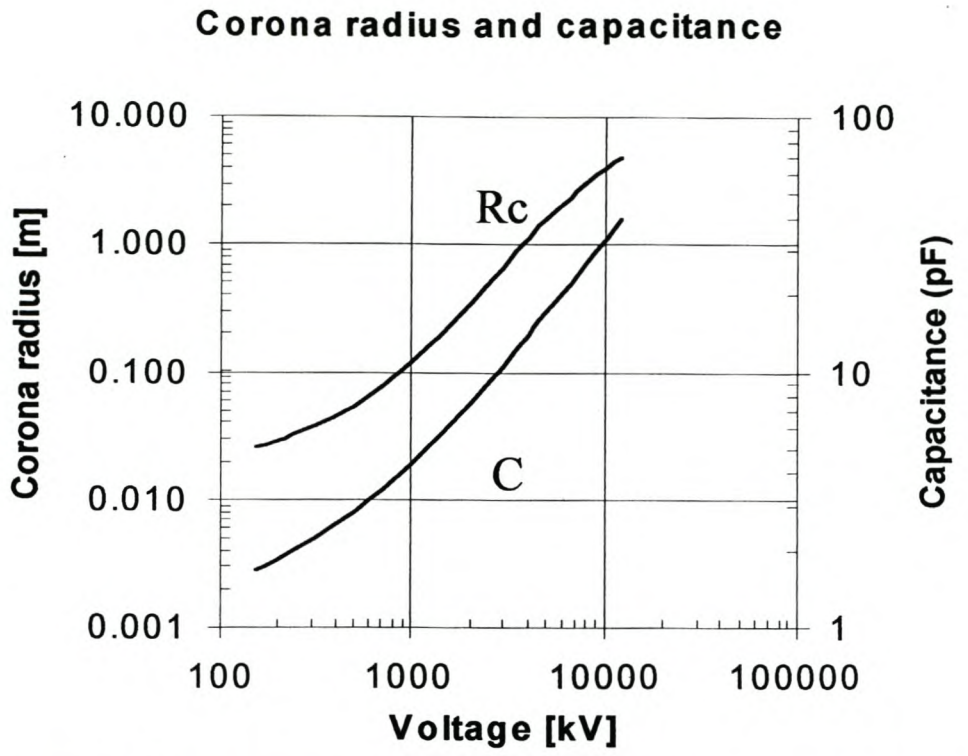

Figure 3.2.3. The corona radius and line capacitance increase as the surge voltage increase above V_i. CIGRE's formula was used.

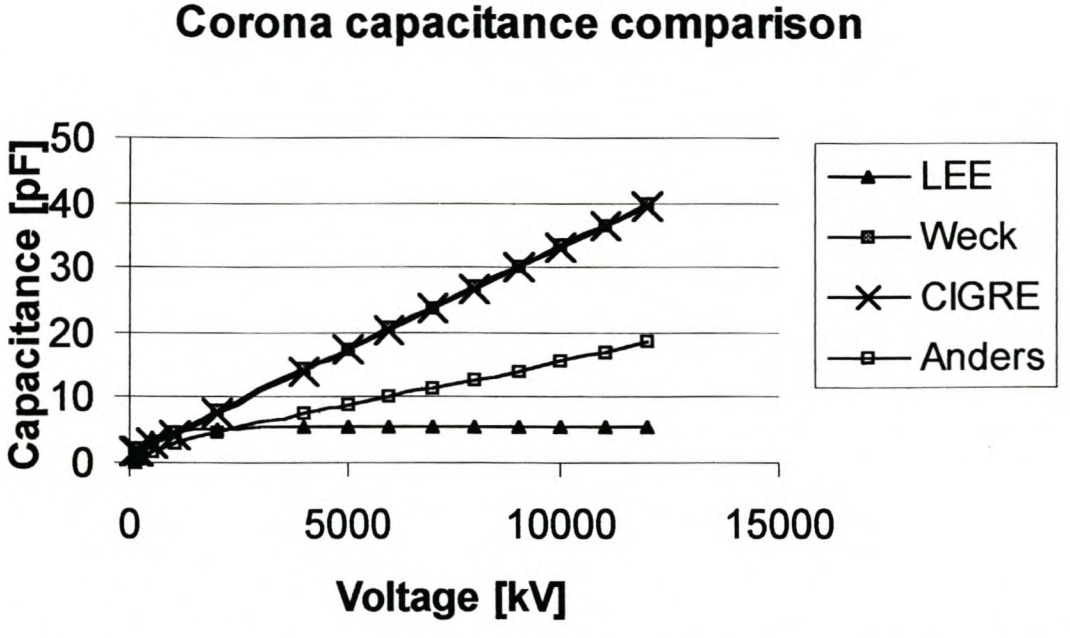

Figure 3.2.4. Comparison of corona capacitance as calculated by CIGRE, Weck, Anderson and Lee.

Table 3.2.2 is 'n summary of Gary's [12] information regarding the line capacitance with different surges. V_i was taken as 150 kV, which compare well with Skilling and

Stellenbosch University http://scholar.sun.ac.za

Dykes in table 3.2.1. On average, the capacitance increases due to corona, correlates well. However, Gary did not do tests higher than 500 kV.

	1.2/50μs positive	1.2/50μs negative	10/90μs positive	10/90μs negative
C_g	7.63 pF/m	7.63 pF/m	7.63 pF/m	7.63 pF/m
C_{cor} / C_g	1.91	1.41	1.35	1.2

Table 3.2.2. Line capacitance (C_g) below V_i and the) increase (ratio C_{cor}/C_g) of line capacitance (C_{cor}) above V_i (150 kV) for a 10 mm conductor.

Lee [13] modelled C_c (capacitance due to corona) in parallel with G_c (the conductance due to corona) as shown in figure 3.2.5 using the following formulas:

$$C_c = 2k_c\left(1-\frac{V_{co}}{V}\right)$$

$$G_c = k_r\left(1-\frac{V_{co}}{V}\right)^2$$

Where $k_c = \sigma_c\sqrt{\frac{r}{2h}}\times 10^{-11} F/m$ σ_c

σ_c = 15 for negative and 30 for a positive surge
r = radius of conductor
h = height of conductor
V_{co} = Corona onset voltage
V =voltage of line

$k_r = \sigma_G\sqrt{\frac{r}{2h}}\times 10^{-11} mho/m$

$\sigma_G = 10\times10^6$ for negative and 20×10^6 for a positive surge

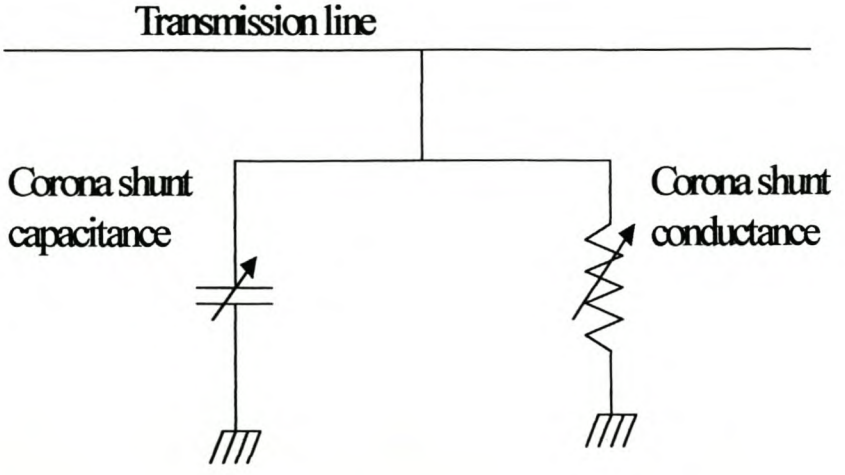

Figure 3.2.5. Lee's model for studies including corona capacitance.

Stellenbosch University http://scholar.sun.ac.za

3.2.6. Corona losses

Practical work in this regard was done by Dragan [12] et al. He studied the corona losses due to charge build up. Below the conductor critical voltage V_i (voltage where corona starts), the charge q_g is 'n linear function of capacitance times the applied voltage. Above V_i , q is equal to q_g plus the supplementary charge q_{sp} due to corona. The supplementary charge is not linear and is a function of the voltage as well as the wave front steepness. He used three different conductors and the thicker the conductor, the higher V_i. Of interest are the tests on the 10mm diameter conductor. Figures 3.2.6a and b give a summary of the relevant losses. The positive surge is in particular sensitive to the wavefront steepness.

Only negative surges will be considered during this study. From figure 3.2.6 the losses due to corona is about 100 mJ/m × 5000 m = 500 J over 5 km. For the study the line lengths will be approximately 5 km and the surge energy approximately 80 kJ. The corona losses will therefore not be taken into account.

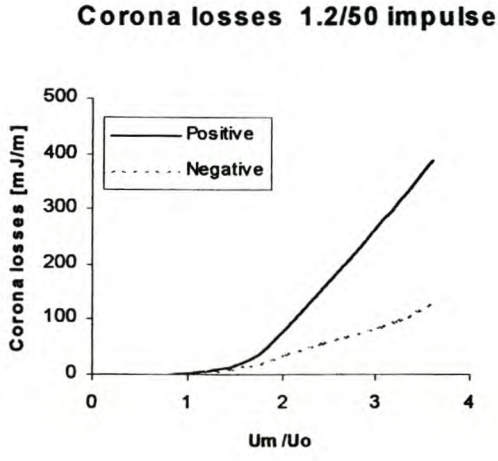

Figure 3.2.6a. Corona losses with different voltage magnitudes 1.2/50 us surges [12]

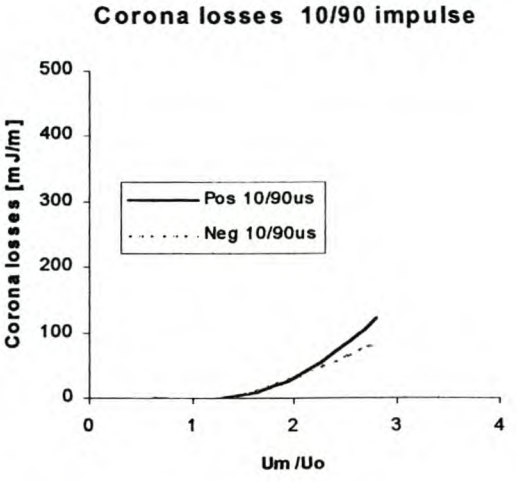

Figure 3.2.6b. Corona losses with different voltage magnitudes 10/90 us surges [12]

3.2.7. Including the effect of corona in ATP studies.

In order to include the increase in capacitance (ΔC) in the ATP calculations, ΔC can be lumped every 70 m to 350 m depending on the line configuration. Lee [13] compared field measurements with lumping ΔC every 70 m and 350 m. The surge peak voltage value was very much the same, but the retardation of the front varied between 5% and 10%. Lumping ΔC will result in additional reflections when doing the calculations.

Another option is to make provision for the corona radius in the line model by increasing the conductor diameter. The rest of the parameters can be kept the same. Although this will result in a manual iteration process (to model the right corona radius for the relevant voltage) as well as modeling the line as short pieces of line, no

Stellenbosch University http://scholar.sun.ac.za

additional reflections will occur. This seems to be a better option and will be used in the simulations.

3.2.8. Conclusion

Corona has a significant influence on the effective conductor radius and therefore line capacitance. A surge wavefront's steepness decreased as the line capacitance increase due to an increase in the corona level. The line inductance does not change with an increase in corona.

3.3. Earthing resistances

The earthing resistance of substations and line towers plays an important role in the magnitude of overvoltages. Earth resistance depends heavily on the type of soil, the soil moisture content and the presence of soil ionization.

3.3.1. Earth resistance calculations

Normally earthing on distribution substations (11 and 22 kV) is designed around the power frequency. This is normally known as the low-current, low frequency resistance R_0. The current is normally low enough that no soil breakdown occurs and the frequency is normally below 100 Hz. Measurement of earth resistance for DC currents is easier than for high frequencies and can easily be done with cheap equipment.

Distribution systems normally use the crowfoot earthing configuration in the area where the study was done, and due to many reasons it was decided to keep this standard. Formulas to calculate the low frequency resistance of the earthing electrodes are readily available. Such formulas for different earthing configuration can be found in the Green Book [14] and work done by Saraoja [15]. The formula used to calculate the earth resistance for the crow foot with vertical electrodes, one in the middle and one at the end of each strip is:

$$R = \left[\frac{8\pi l}{\rho \ln \frac{4l}{1.36d} \times \frac{2h+l}{4h+l}} + \frac{6\pi L}{\rho \ln \frac{9L^2}{0.767hD}} \right]^{-1}$$

Where l = length of vertical electrode in cm
L = length of strip in cm
d = diameter of vertical rod in cm
D = width of strip in cm
d = depth below surface in cm
ρ = soil resistivity in Ω.cm

The four distribution lines (22kV) that were used for the test are only earthed at the substations, switching equipment and at the points of supply. Unlike transmission lines the insulator spindles are not bonded. There is only a downwire along the pole from about 400 mm below the bottom crossarm to the bottom of the hole where the

Stellenbosch University http://scholar.sun.ac.za

pole is planted in. The purpose of the wire is to protect the woodpole from lightning damage and to provide a 300 kV BIL. If the line voltage increase to 300 kV due to a lightning surge, there is a 20% change of a flashover between phase and earth. In a case where a flashover occurs and the earth resistance of the downwire is high, a flashover will most probably occurs at the next pole as well. A standard earthing configuration called the crowfoot, is used at the pole-mounted point of supply. Sensitive earth fault protection is used to take care of high impedance earth faults.

3.3.2. Earth impedance characteristics for high currents and frequencies

The following information is largely based on work done by Oettlé [16] and Hileman [3, p 433-446]. The self-inductance of the electrodes comes into play when the overall dimensions of the earthing configuration are bigger than 20 m. Only "concentrated" earthing (overall dimensions of earthing smaller than 20 m) was used to earth the line surge arresters.

In the following sections the frequency-dependant properties of the soil and the effect of soil ionization are considered.

3.3.2.1. The frequency-dependant properties of the soil.

The conduction in soil is nearly entirely electrolytic. Current flow take place through the movement of positive and negative ions which are dissolved in microscopic layers of water around the soil particles resulting in the frequency-dependant electrical properties of soil [17, 18]. Figure 3.3.1 is redrawn from Oettlé [19] and illustrates the magnitude of soil resistivity at different frequencies. The soil that was used had a resistivity of 250 Ω.m at 100 Hz.

Figure 3.3.1 indicates that up to about 1 MHz there is little change in the soil resistivity. Oettlé [19] defined the 66% frequency value, at which point the soil resistivity falls below 66% of the DC resistance value. At higher frequencies the soil resistivity changes drastically.

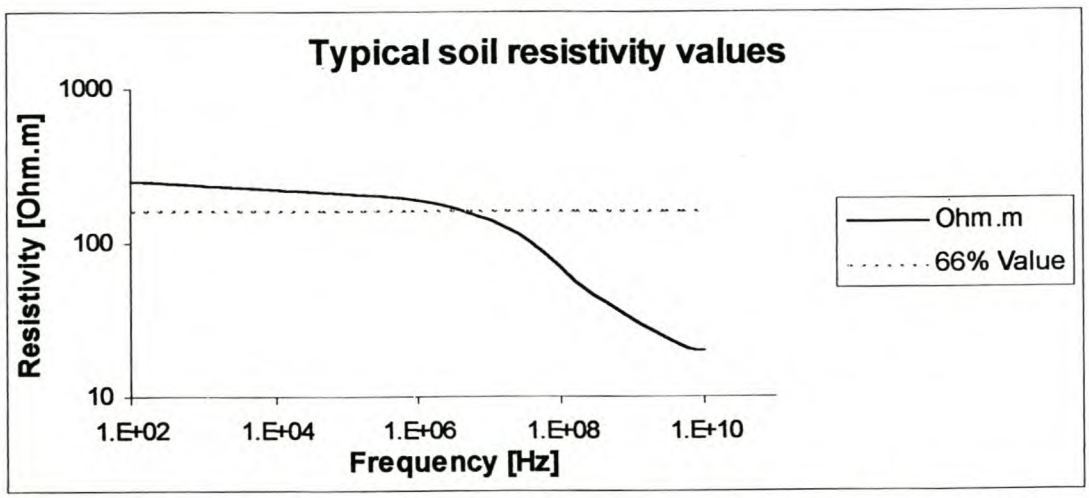

Figure 3.3.3. Typical values for ρ as the frequency increases. The dotted line presents the 66% frequency value.

Stellenbosch University http://scholar.sun.ac.za

The type of soil (clay, sand or rock) as well as the water content in the soil has a large influence on the soil conductivity. According to Anderson [11], the earth resistivity of swampy ground is between 10 and 100 Ω.m, dry earth 1000 Ω.m, and sandstone 10^8 Ω.m. The type of soil and water content differ continuously along a line and one cannot just use one value for ρ to calculate the earth electrode impedance of all the poles.

Results on surge test done by Oettlé [19] (below soil ionization) on concentrated earthing electrodes are shown in figures 3.3.2 and 3.3.3. The 66% frequency (as shown in figure 3.3.2) for a soil with high resistivity, shows an appreciable reduction in the frequency range 10kHz to 1MHz, associated with lightning. It appears that the frequency-dependant properties of the soil with high resistivity will assist in reducing the earthing resistance for most soils.

Figure 3.3.3 shows an initial low resistance for the first 3 μs. However, after 5 μs the surge impedance is more than 95% of the low frequency impedance.

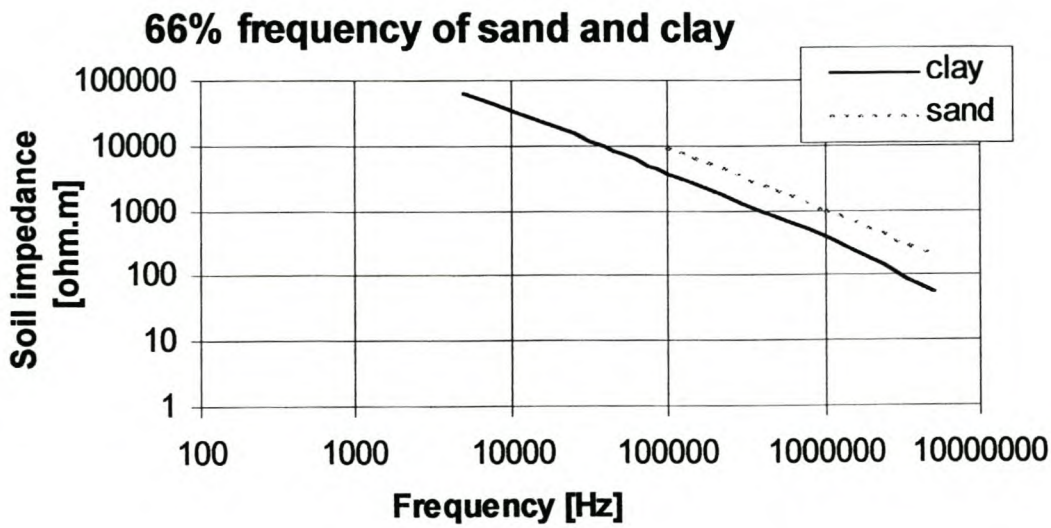

Figure 3.3.2. The relationship between the soil resistivity and frequency. Clay soil with high DC resistivity tends to drop in resistivity if the current frequency exceeds 10 kHz. [19]

Stellenbosch University http://scholar.sun.ac.za

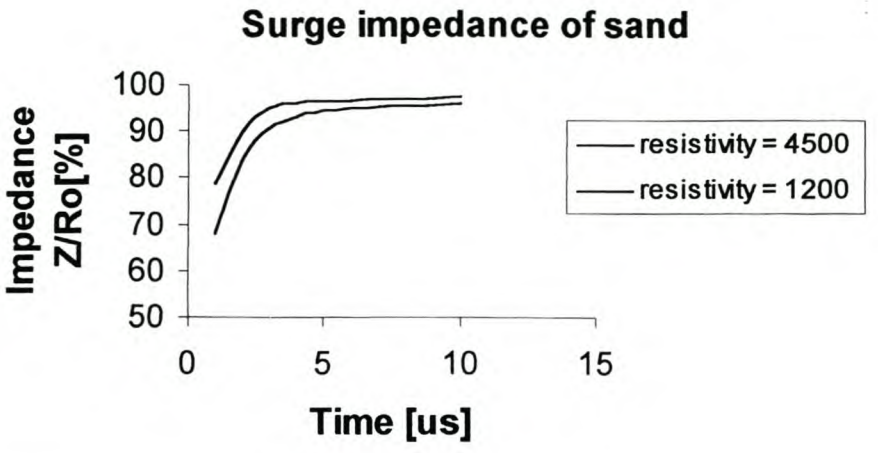

Figure 3.3.3. Surge impedance as a percentage of the low frequency impedance for a surge wavefront with a 2 μs time to peak [19].

3.3.2.2. Ionization and discharge processes in soil

As the magnitude of the current surge increases, the electric field strength, E, increases in the soil around the electrode. The soil becomes ionized when the electric field strength reaches the critical soil ionization electric field strength E_0 . If the electric field strength increases further, streamers will develop, followed by arcing in the soil.

In a concentrated earthing configuration, ionization will start around each electrode and progress to a point where it embraces the earth electrode as a whole. As the current increases, the earthing configuration becomes less important. Korsuntev [20] and Liew [21] describe this ionized zone as a uniform conductor with zero resistivity. This zone extends up to the point where $E < E_0$. Table 3.3.1 gives some values for E_0 . To generalize, it appears that the higher the soil resistivity, the higher the critical electric field strength where soil ionization starts.

Ionization and breakdown of soil does not start as soon as the surge is applied. Due to the fundamental electrical properties of soil, ionization up to a magnitude where breakdown is possible, takes place about 5 μs after the surge is applied.

According to Geldenhuys [24] and Oettlé, the streamer impedance can reach 'n minimum between 5 μs and 30 μs. The higher the current (and therefore the electric field strength) the quicker the minimum streamer impedance is reached. Figure 3.3.4 shows three different surges – a 80 kV surge where soil breakdown just started, a 180 kV surge reaching the minimum soil resistivity at 130 μs and a 245 kV surge where the soil resistivity is minimum within 50 μs. The soil resistivity was within 20 μs already close to the minimum. During this surge test the rod resistance was 834 Ω and the soil resistivity 2000 Ω.m.

Stellenbosch University http://scholar.sun.ac.za

Reference	Soil resistivity (ohm.m)	E_0 (kV/m)
Bellaschi [22]	100	300
	100	270
	85	127
	75	220
	300	425
Petropoulos [23]	290	8.3
Korsuntcev [20]	470	1 200
	180	1 000
	100	800
Liew and Darveniza [21]	50	100-300
	60	50
	150	200
	300	50
Oettlé [19]	Sand:	
	180 000	1 700
	19 200	1 850
	8 000	1 620
	3 500	1 600
	2 000	1 500
	960	1 650
	900	900
	680	1 080
	610	1 280
	470	1 000
	380	750
	Red clay:	
	340 000	1 800
	500	900
	330	600
	200	1 130
	70	80
	Black clay:	
	3 100	1 300
	800	1 180
	170	800
	50	710
	65	700
	Mixture of previous types	1 280
	525	830
	180	850
	50	

Table 3.3.1. Electric field strength at soil breakdown for different soil samples.

Stellenbosch University http://scholar.sun.ac.za

An EPRI [25] report confirms that the soil resistance does decrease as the current increase up to 40kA as shown in figure 3.3.5. The percentage decrease in the soil resistivity depends on the type of soil. However, the electrode's resistance does not decrease to such low levels as described by Oettlé. For currents higher than 20 kA it seems like the type of soil does not make a difference in the electrode's resistance.

During this study, the modelled earth resistance will be based on figure 3.3.5. The measured DC earth resistance of the electrodes will be decreased as the current increases using a model in ATP. The earth resistance characteristic of gravel soil as shown in figure 3.3.5 will be used. In cases where the measured DC values are below 6 Ω, the measured value will be used as a constant in the model.

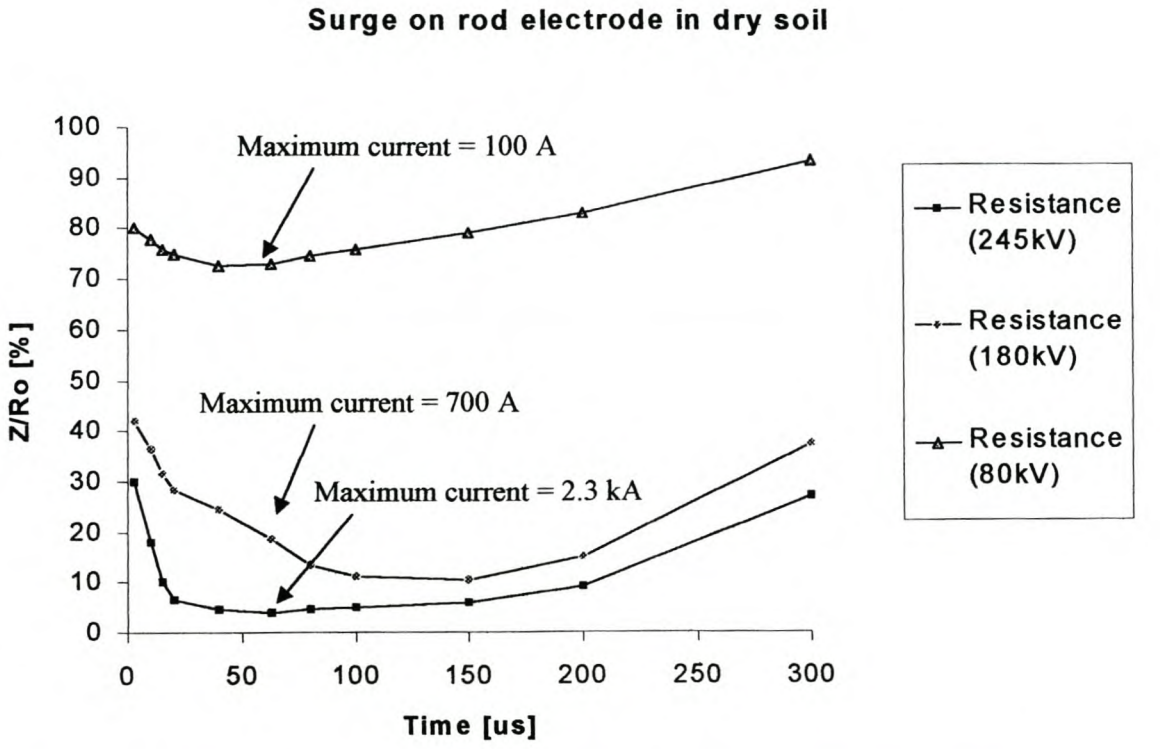

Figure 3.3.4. An increase in surge current above soil ionization causes a decrease in soil resistivity [24].

Stellenbosch University http://scholar.sun.ac.za

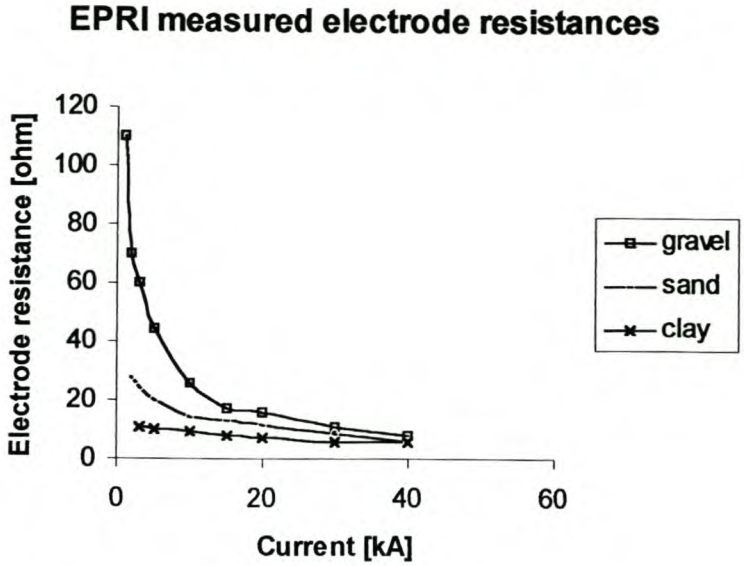

Figure 3.3.5. Minimum transient resistance values as a function of the current surge magnitude for a counterpoise in three different types of soil [25].

3.3.3. Conclusion

The frequency-dependant properties of soil plays only a minor role at lightning surge frequencies. Soil ionization plays a major roll in reducing soil resistance. A lightning surge current of 40 kA will decrease the soil resistance by 90 %.

3.4. References

1. S. Goodman, A lightning Primer from the GHCC, NASA, p. 2.
2. R.A. Black, J. Hallet, The Mystery of Cloud Electrification, November-December 1998, Vol. 86, No. 6.
3. A.R. Hileman, Insulation Coordination for Power Systems, Marcel Dekker, Inc. 1999, p. 195 - 205.
4. H.J. Geldenhuys, C.T. Gaunt, A.C. Britten, Insulation co-ordination of unshielded distribution lines from 1kV to 36kV, SAIEE publication.
5. W. Diesendorf, Insulation Co-ordination in High Voltage Electric Power Systems, Butterworths, London, 1974.
6. A.J. Eriksson, The incidence of lightning strikes to power lines, IEEE/PES Winter Meeting, New York, February 1986.
7. H.J. Geldenhuys, H.M. Rautenbach, D.V. Meal, Progress report on the 11 kV test line project (85/86 season) including preliminary study of shield wire effects, I ELEK 173, NEERI, CSIR, August 1985.
8. H.J. Geldenhuys, Lightning parameters, The lightning Protection of distribution lines Seminar, August 1989.
9. R.B. Anderson, A.J. Eriksson, Lightning parameters for Engineering Applications, Electra, No. 69, March 1980, p. 65 – 101.
10. CIGRE Technical Bulletin 63, Guide to Procedures for Estimating the Lightning Performance of Transmission Lines, Oct 1991.

Stellenbosch University http://scholar.sun.ac.za

11. J.G. Anderson, Lightning performance of Transmission lines, Transmission Line Reference Book 345kV and Above, EPRI, Second Edition, Chapter 12, pg. 554 - 560.
12. C.Gary, G. Dragan, D. Critescu, Attenuation of travelling waves caused by corona, Study Committee No.33, 1978 session, Aug 30 – Sept. 7.
13. K.C. Lee, Non-linear corona models in an electromagnetic transients program, IEEE Transactions on Power apparatus and Systems, Vol. PAS-102, No. 9, September 1983.
14. Green Book, Practice for grounding of industrial and commercial PS., IEEE, Chapter 4, p. 4.
15. E.K. Saraoja, Lightning earths, Westend, Finland.
16. E.E. Oettlé, The surge impedance of concentrated earth electrodes, M Thesis, 1987.
17. E.I. Parkhomento, Electrical properties of rocks, Plenum Press, New York, 1967
18. G.F. Tagg, Earth resistances, George Newnes Ltd., London, 1964.
19. E.E. Oettlé, The influence of the frequency-dependant properties of soil on the surge impedance of concentrated electrodes below the ionization threshold.
20. A.V. Korsuntov, Application of the theory of similitude to the calculation of concentrated earth electrodes, Electrichestvo, No. 5, May1958, pg. 31-35.
21. A.C. Liew, M. Darveniza, Dynamic model of surge characteristics of concentrated earths, Proc. IEE, Vol. 121, No. 1, February 1974, pg. 123-135.
22. P. Bellaschi, R.E. Armington, A.E. Snowden, Surge and 60 cycle characteristics of driven grounds, Part II. Trans. Am. Inst. Elec. Eng., 1942, p. 349-363.
23. G.M. Petropoulus, The high voltage characteristics of earth resistances, J. IEEE, 1948, Vol. 95, Part II, p. 59-70.
24. H.J. Geldenhuys, E.E. Oettlé, Results of surge tests on practical electrodes at the high voltage laboratory of NEERI.
25. EPRI, 1998 Annual Report on the Lightning and Grounding Project, February 1999, p3-24.

Stellenbosch University http://scholar.sun.ac.za

4. LIGHTNING SURGE SIMULATION MODEL

In order to be able to investigate the effect of lightning on the line it was decided to use the ATP transients program. Suitable models also had to be chosen to represent the system components.

4.1. ATP software [5]

The 32-bit version of ATPDraw, which runs on Windows 95/NT, is a graphical, mouse-driven preprocessor to the ATP version of the Electromagnetic Transients program (EMTP). ATP is free of any royalty and any person may use this software free of charge. However, an interested person has to register as an ATP user and will receive a license free of charge.

The advantage of ATPDraw is its assistance to populate the EMTP database correctly. Numerous models for lines, transformers, generators, switches and other linear and no-linear components are available. Calculation can be done in the frequency and time domain.

Node voltages are used as state variables in EMTP. The branch currents are therefore expressed as functions of node voltages. The equations are converted into the Laplace transform and written in a matrix format where it is solved.

4.2. The line model

The first line models used in transient studies were cascade connections of π-circuits [1]. Travelling wave solutions were first used for simple lightning arrester studies where lossless single phase line models were adequate. It was often called the Bergeron or Bewley method. Travelling wave solutions were much faster for computers to solve than cascaded π-circuits. In some cases it became also necessary to include the frequency-dependence. J. Marti did a re-evaluation of existing frequency-dependant models, which led to the reliable Electromagnetic Transient Program (EMTP) and later ATP.

The line model that is used for simulating a travelling surge on the line must take the change in line impedance with frequency into account. On the other hand the model should not cause mathematical instability. This can happen when a piece of line is broken up into smaller pieces of line to include other influencing factors. Different line models are available in ATP. The three types of models are:

- Frequency dependent models for example the JMarti model.
- Nominal PI-equivalent models (for short lines) called the PI model.
- Constant parameter KC Lee or Clark models for example the Bergeron model.

Frequencies in a lightning stroke depend on the crest current of the stroke. It can vary between 1 MHz (for subsequent strokes) and 60 kHz (for a 250 kA first stroke) and will be discussed later in 5.2. The AIEE Working Group [2] selected a 4 μs (250 kHz) front risetime as the best representative value for the time to crest. It will therefore be necessary to use a frequency dependant model, especially if the accuracy

Stellenbosch University http://scholar.sun.ac.za

of the wavefront modelling and simulation is important. The JMarti model is a frequency dependant model. More detail about the JMarti frequency-dependent model is given in Appendix B. To evaluate the JMarti model, a 100 km line connected to a surge source and open ended on the other side was modelled. A shorter line will not show the surge reflection very clearly. The reflected surge wave will overlap with the surge generated at the source.

Two surges with different risetimes were used to demonstrate the effect of different frequencies on the JMarti line model (shown in figure 4.1).

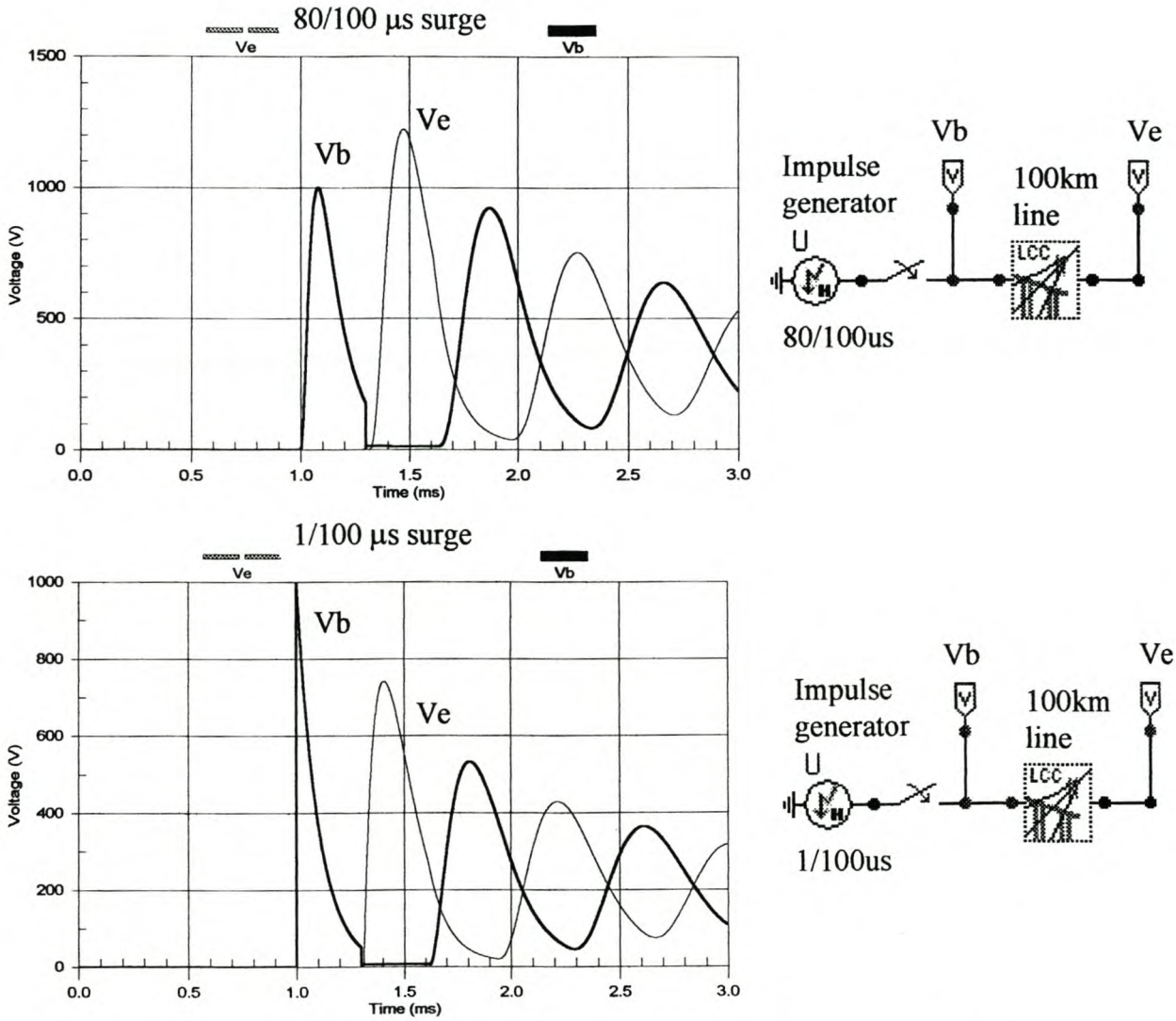

Figure 4.1. The travel time and attenuation of surges with different wave fronts on a 100 km JMarti line model.

The speed of travelling wave on a lossless line is [3]:

Stellenbosch University http://scholar.sun.ac.za

$$v = \sqrt{\frac{1}{LC}} \tag{4.1}$$

where:

$$L = 2\times10^{-7}\ln\frac{d}{r}\ \text{H/m} \tag{4.2}$$

$$C = \frac{2\pi\varepsilon}{\ln d/r}\ \text{F/m} \tag{4.3}$$

Substituting 4.2 and 4.3 in 4.1

$$v = \left(\sqrt{2\times10^{-7}\ln\frac{d}{r}\frac{2\pi\varepsilon}{\ln d/r}}\right)^{-\frac{1}{2}}$$

$$v = \left(\sqrt{2\times10^{-7}\times2\pi\times\frac{1}{36\pi}\times10^{-9}}\right)^{-\frac{1}{2}}$$

$$= 3\times10^{8}\ \text{m/s}$$

For distance = 100km the travel time will be 333μs. Figure 4.1 verify this calculation. The wave takes about 330μs to the open end of the line.

The amplitude of the voltage and current gets attenuated exponentially while travelling over the line. The characteristic impedance Z of the line is:

$$Z = \sqrt{\frac{L}{C}} \tag{4.4}$$

From 4.2:

$$L = 2\times10^{-7}\ln\frac{d}{r}\ \text{H/m}$$

$$= 2\times10^{-7}\ln\frac{800}{0.55}\ \text{H/m for Mink conductor}$$

$$= 1.456\times10^{-6}\ \text{H/m}$$

From 4.3:

$$C = \frac{2\pi\varepsilon}{\ln 800/0.55}\ \text{F/m}$$

Stellenbosch University http://scholar.sun.ac.za

$$= \frac{2\times10^{-9}}{36\ln\frac{800}{0.55}}$$

$$= 7.629\times10^{-12}\ \text{F/m}$$

Substitute the values of L and C in 4.4:

$$Z = \sqrt{\frac{1.456\times10^{-6}}{7.629\times10^{-12}}}$$

$$= 437\ \Omega$$

The voltage V at a point x km away from source is [3]:

$$V = V_0\varepsilon^{-0.5(R/Z+GZ)x} \qquad (4.5)$$

where V_0 is the initial magnitude of the surge voltage, R the line resistance/km, G the leakage/km and Z the surge impedance.

Substituting V_0 = 1 kV, R = 0.4 Ω (for Mink conductor), G = 0.0 siemens, x = 100 km in 4.5:

$$V_0 = 1\times2.718^{-0.5(0.4/437)100}$$

$$= 0.955\ \text{kV}$$

The surge voltage will double [4] at the end of the open circuit line and will therefore be 0.955×2 = 1.91 kV for a lossless line. Figure 4.1 shows that the voltage (Ve) at the remote end of the line is only 1.25 kV due to an 80/100 μs surge. The difference in amplitude is due to the skin effect (that will be discussed in more detail in 5.2) which was taken into account with the JMarti model. The JMarti model does not take the conductance (G) as zero as in the above calculations. As the risetime increase (frequency increase) to 1/100 μs, the reflected wave amplitude decrease further to 750 V due to the increasing skin effect.

4.3. The surge model

In order to determine the effect of a 50 Hz source on the surge model, the same circuit was modelled with both a 50Hz and a surge current source and then only with an current surge source. No difference was found on the initial amplitude of the current surge. The substation surge arresters are seen by the surge as a low impedance circuit to earth. For the purpose of this study it is therefore not necessary to model the 50Hz source. See figure 4.2.

The shape of every lightning initiated travelling wave differs. The rise time is longer if the surge amplitude is higher and will be discussed in more detail in chapter 5.

Stellenbosch University http://scholar.sun.ac.za

Depending on the accuracy needed, the waveshape can be described with a first, second or a third order formula. A third order formula is a more accurate description and does not cause transitional distortions which is possible in the case of a first order formula.

An existing ATP current surge source as modelled by Heidler (Type 15) was used to represent a lightning stroke. Figure 4.3 shows a surge wave shape using the Heidler source model supplying a pure resistive load. The wave front and tail will be varied during different studies to simulate each lightning wave shapes.

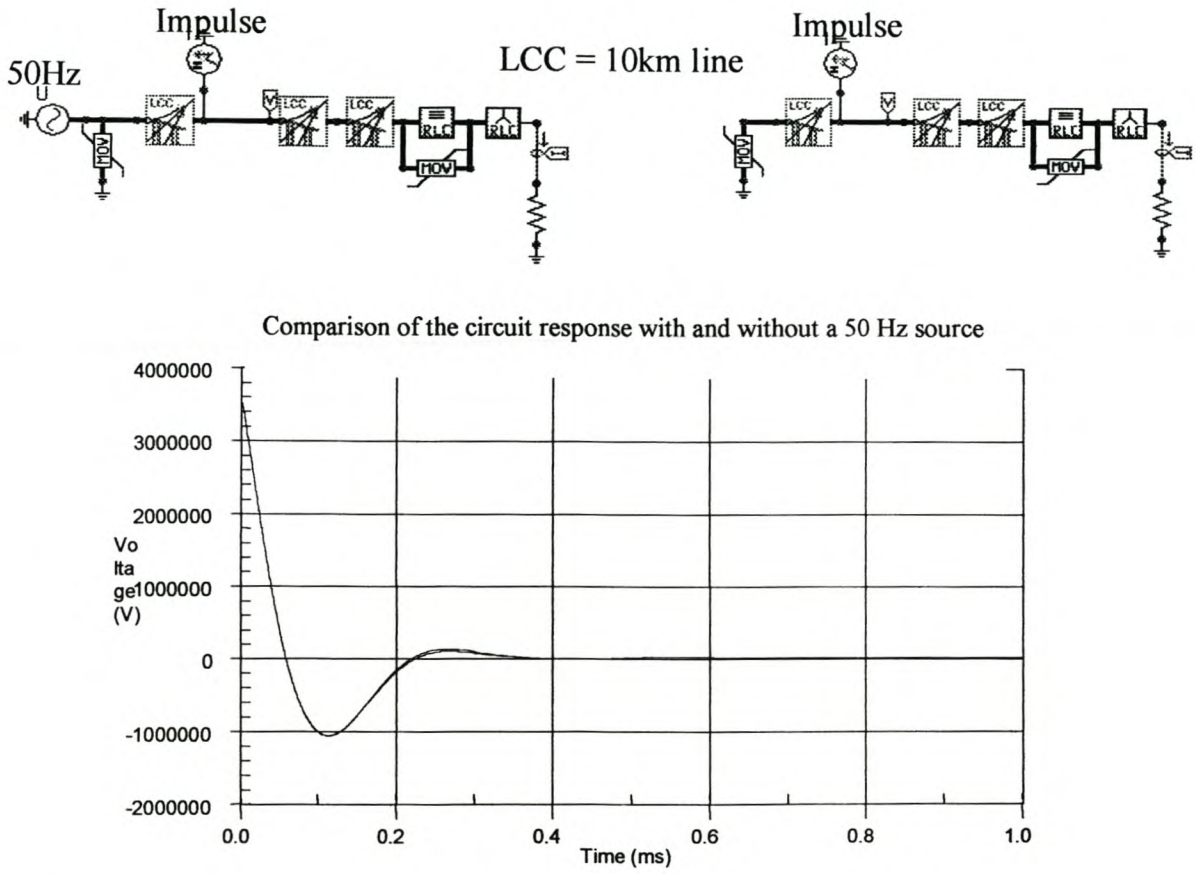

Figure 4.2. The surge waveshape is not influenced by the 50 Hz source. The two curves are nearly identical and are lying on each other.

Stellenbosch University http://scholar.sun.ac.za

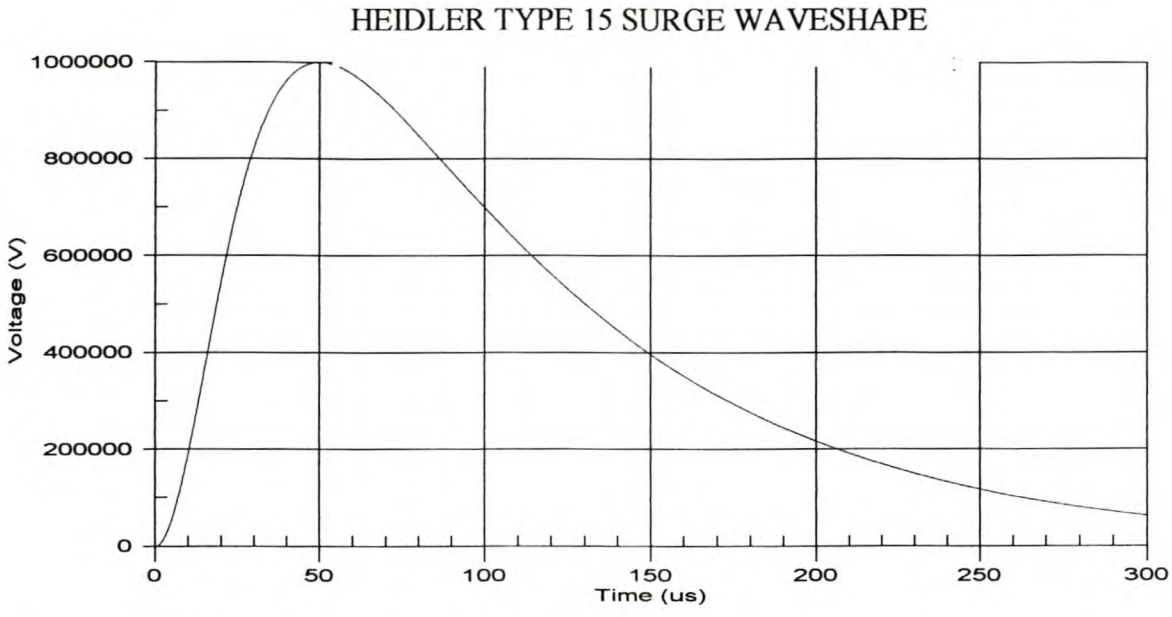

Figure 4.3. The Heidler surge source model of a 30/130 wave. A long risetime was used to demonstrate the shape of the wavefront properly. Three concave waveforms with a smooth transition between them are visible.

4.4. The surge arrester

The metal-oxide surge arrester is a highly nonlinear resistor. Below the normal operating voltage, the voltage/current characteristic has almost an infinitive slope. This part of the graph is represented by a linear function. Between 10 mA and 10 kA and above a 100 kA the characteristics are described by two power functions of the form:

$$i = p\left(\frac{v}{v_{ref}}\right)^q$$

where p, v_{ref} and q are constants. Typical values for q = 20 to 30.

Data from the ABB catalogs [6] was put into the arrester model in ATP which then used a "ZNO fitter" to characterize the arrester. Typical characteristics of the ZNO arrester are shown in figure 2.1.

4.5. The pole-mounted installation

The fuse was left out in the model due to its low impedance. In the scenarios where there was interest in the current through the fuse (whether it will blow or not), a current probe was used to monitor the current.

The surge arrester has the biggest impact on the surge studies and was always modelled as discussed in paragraph 4.4.

Detailed modelling of the transformer is necessary if a study on stresses inside the transformer needs to be done. In this case, the main interest is to minimise the surge amplitude on the line before reaching the pole-mounted installation. When modelling

Stellenbosch University http://scholar.sun.ac.za

a transformer for surge studies on a network, it can be modelled as a capacitor only. Tests show that the value of the capacitor vary between 1 nF and 4 nF [6]. Due to the short risetime of the lightning surge, the inductive reactance at this frequency become very high – in fact an open circuit. In the majority of the cases, the surge arrester is mounted on the transformer tank. The voltage across the surge arrester will therefore be the same as the voltage across the transformer.

4.6. The flashover model

There is a possibility of a flashover at each wood pole that depends on the magnitude of the surge voltage as well as the BIL of the pole. The BIL of the test lines are 350 kV. Therefore, if the voltage magnitude reaches 350 kV, there is a 10 % change that a flashover will occur as discussed in chapter 3.

ATP has a flashover model as part of the program software. As soon as the preset voltage is reached, the model creates a short circuit between phase and earth. The switch opens again after a preset time and minimum current are reached.

4.7. Conclusion:

ATP has adequate models with all the features to simulate the circuit that will be used. However, there is no model that includes the influence of corona. The JMarti model will be modified manually to include corona simulation.

4.8. References

1. W. Scott Meyer, Tsu-huei Liu, BPA EMTP Theory Book in WP 5.1, July 1995, p. 4-56 - 58.
2. AIEE Committee Report, A method of estimating the lightning performance of transmission lines, AIEE trans. 69(3), 1950, p. 1187 – 1196
3. C.L. Wadhwa, High Voltage Engineering, New Age International Limited, Publishers, First reprint, September1995, p230-233
4. L.V. Bewley, Travelling waves on Transmission Systems, Wiley New York, 1951, p55.
5. L. Prikler, H.K. Hoidalen, ATPDraw for Windows 3.1/95/NT User Manual, Version 1, November 1998, p 7 – 12
6. ABB, Selection guide for ABB HV surge arresters, Edition 3, 1995-02

Stellenbosch University http://scholar.sun.ac.za

5. SIMULATION OF LIGHTNING SURGES ON OVERHEAD LINES

In this chapter the models developed in the previous chapter are used to analyze the effect of lightning strokes with various current amplitudes on a section of line. The influence of surge arresters and flashovers on the lightning surge waveshape is studied.

5.1. Overview of the lightning surge study

It will be much easier to study a section of line with no T-offs (no additional reflections) when struck by lightning. A 60 km line will therefore be modelled with a lightning surge in the middle of the line. Each section of 30 km line at both sides of surge is symmetrical. The woodpoles of the lines are 100 m from each other. For the first 300 m a voltage measurement will be taken at each pole. The next voltage measurements will be taken at the 5th, 8th, 12th, 20th, 40th, 80th, 140th, 300th poles. Figure 5.1 shows the single line electrical diagram of the model. Most of the activity and changes takes place close to where the line is struck by lightning and at the remote end of the line, as the studies will show.

The line will first be modelled excluding any provision for corona and flashovers. Then the model will be changed to include the corona model, then include corona and flashover models. Soil ionization as discussed in chapter 3.3 will be taken into account in the flashover model. Lastly, a 3 phase surge arrester will be placed at different locations on the line to study the benefit of line arresters. The main objective of the line surge arrester is to minimise the amplitude of the lightning surge drastically, thereby protecting the pole where it is installed and cross arm while decreasing the stress on fuses, transformers and other surge arresters. This will give an indication of the accuracy needed for the placement of the line arrester.

5.2. A surge on a line without modeling of corona or flashovers.

Anderson and Eriksson [1] studied lightning stroke current waveshapes and found that the peak currents correlate with the surge risetimes and can be given as:

$T_f = 0.3I^{0.6}$ for the first strokes and

$T_f = 0.03I^{0.94}$ for subsequent strokes.

where T_f = the wavefront risetime in μs
and I = the current amplitude in kA.

The lightning surge tail time to the 50% value is 75 μs for first strokes and 32 μs for the subsequent strokes [1].

As discussed in paragraph 4.3, an exponential and not a biconcave waveshape was used for the studies to avoid possible transitional phenomenon. A 30 kA first stroke and a 30 kA subsequent stroke are regularly used in this chapter to illustrate the surge voltages along a line. Using the above formulas, the risetime of a 30 kA first stroke is:

Stellenbosch University http://scholar.sun.ac.za

$$T_f = 0.3I^{0.6}$$

$$T_f = 0.3 \times 30^{0.6} = 2.3 \ \mu s$$

The risetime for a 30 kA subsequent stroke is:

$$T_f = 0.3I^{0.6}$$

$$T_f = 0.03 \times 30^{0.94} = 0.73 \ \mu s$$

No corona compensation was done for the first simulation. The flashover and surge arrester models as shown in Figure 5.1 were ignored for this study. A 30 kA 2.3/75 μs surge model is used. As the line is symmetrical on both sides of the surge, the surge current will divide into two equal current surges. Measurements will only be taken on the one side of the surge.

Figure 5.2 shows the voltage between the three phases. With the surge injected into the W phase, a significant voltage is induced in the R and B phases due to coupling between the phase conductors. The coupling factor (K) between two phases, phase 1 (with a surge) and phase 2 is given as [2]:

$$K = \frac{V_2}{V_1} \tag{5.1}$$

where V_1 is the voltage on phase 1 and V_2 the voltage on phase 2.

$$V_1 = i_1 Z_1 \tag{5.2}$$

where i_1 is the current in phase 1 and Z_1 the surge impedance of phase 1.

The mutual surge impedance Z_{12} between the two phases is defined as [2]:

$$Z_{12} = 60 \ln \frac{D_{12}}{d_{12}} \tag{5.3}$$

where D_{12} and d_{12} is defined in figure 5.3.

$$V_2 = i_2 Z_{12} \tag{5.4}$$

$$= \frac{Z_{12}}{Z_1} V_1 \tag{5.5}$$

For the Wishbone construction, the B phase is 1.8 m from the W phase (d_{12} = 1.8 m). D_{12} =17.5 m and Z = 437 ohm from paragraph 4.1. From figure 5.2 the W phase (V_1) = 3.95 MV. Substituting this values into equations 5.2 and 5.3, the induced voltage on the B phase (V_2) should be:

$$V_2 = \frac{60 \ln \frac{17.5}{1.8}}{437} \times 8.4 = 2.6 \text{ MV}$$

Stellenbosch University http://scholar.sun.ac.za

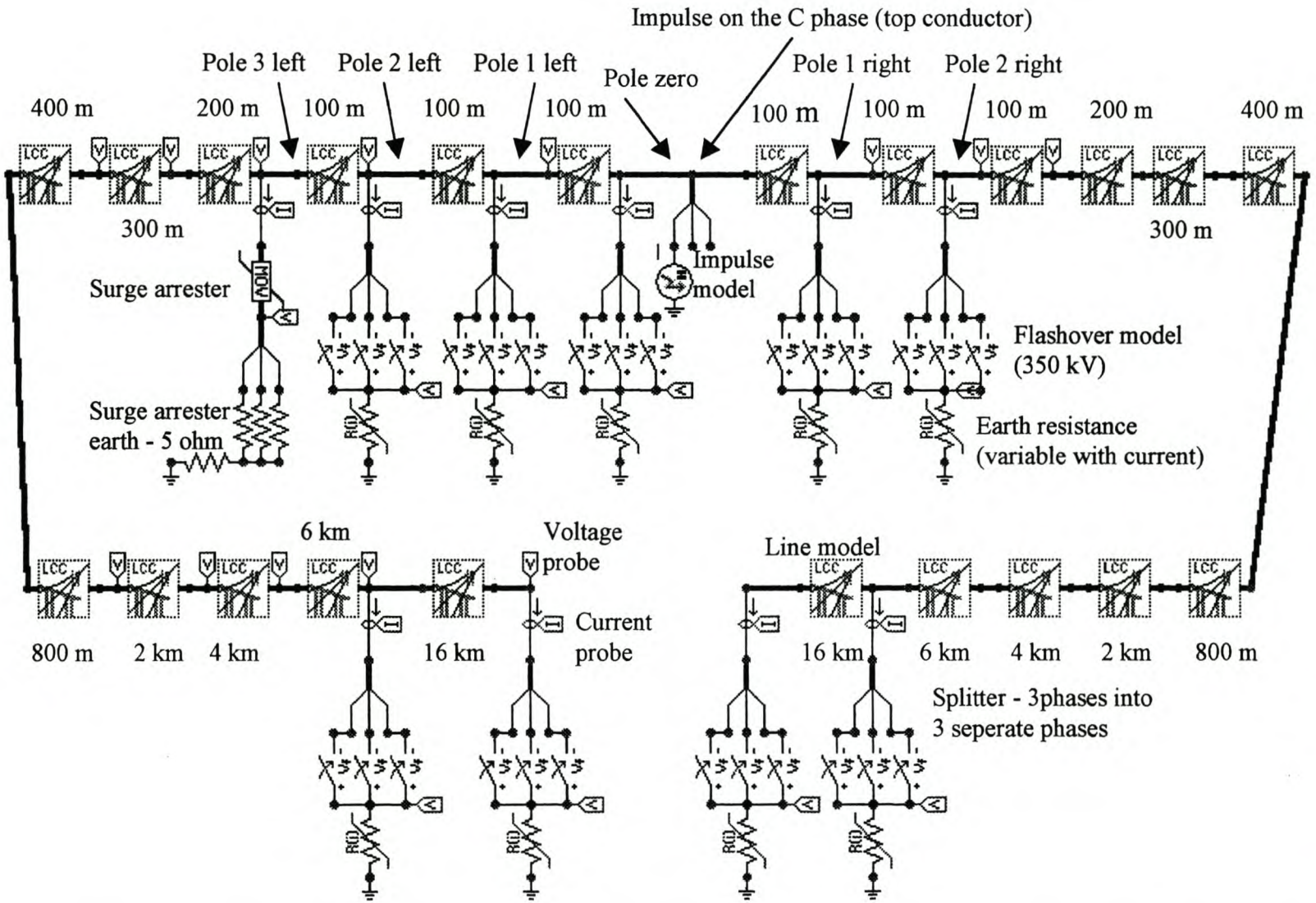

Figure 5.1. A model of a 60 km line - 30 km on both sides of the impulse. The line is symmetric to both sides. Flashovers are simulated on the relevant poles

Stellenbosch University http://scholar.sun.ac.za

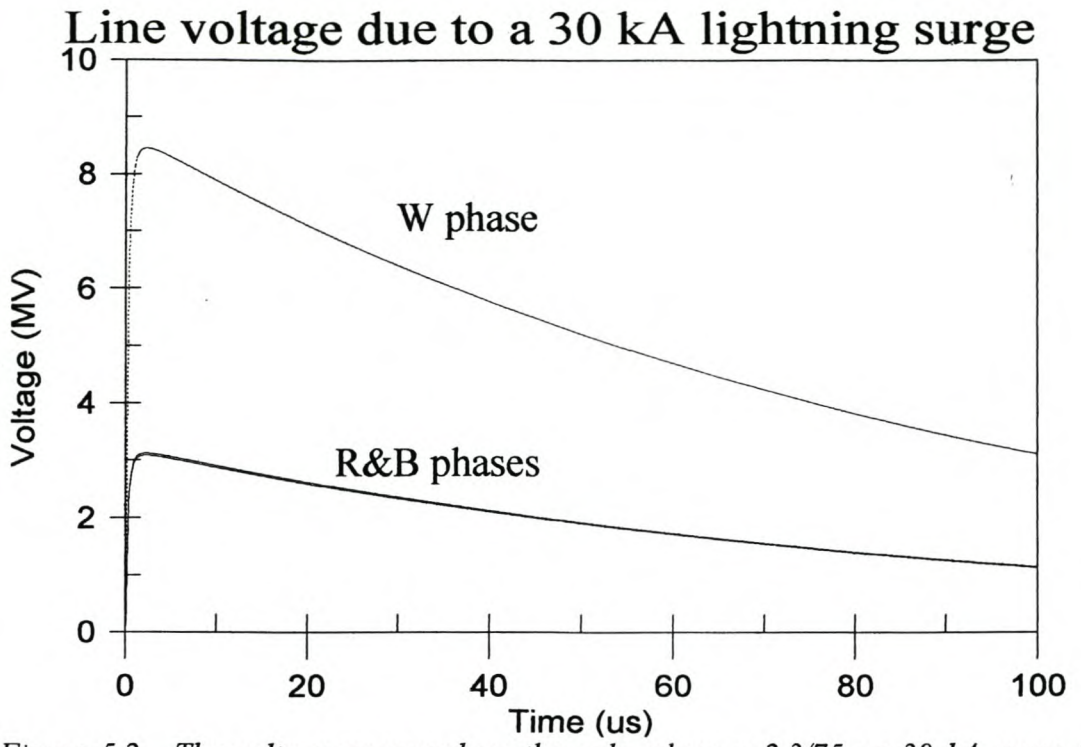

Figure 5.2. The voltage measured on the pole where a 2.3/75 μs 30 kA surge is injected. As the distance between the W&B phases is nearly the same as between the W&R phases, the induced voltages on the R&B phase are virtually the same

From Figure 5.2, the B phase is 3 MV which is reasonably close to the calculation, taking into account the lumped model approach. The W phase is 1.82 m from the R phase and there is also coupling between the B&R phases, therefore the induced voltage on the R phase differs marginally from the B phase.

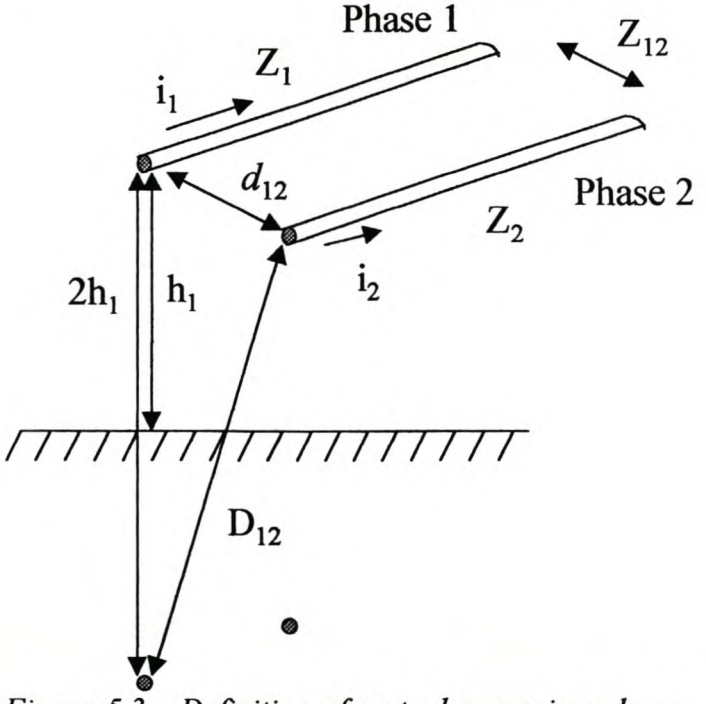

Figure 5.3. Definition of mutual surge impedance. Phase 1 induce a voltage on phase 2.

Stellenbosch University http://scholar.sun.ac.za

Figure 5.4 shows the W phase voltage along the line. In a lossless line (R=0) , as shown before, pulses are propagated at 3.10^8 m/s without distortion. However, since the injected pulse consists of various frequency components and as, in a lossy line, both the attenuation and propagation speed are frequency dependent, the wave becomes distorted as it propagates along the line. As the higher frequencies experience a higher attenuation and a decrease in propagation speed the steepness of the wave decreases. This effect is therefore more pronounced in the case of the steeper wave front. The frequency dependence is included in the Jmarti model, described in Appendix B.

The main reason for the frequency dependence of the attenuation is skin effect.

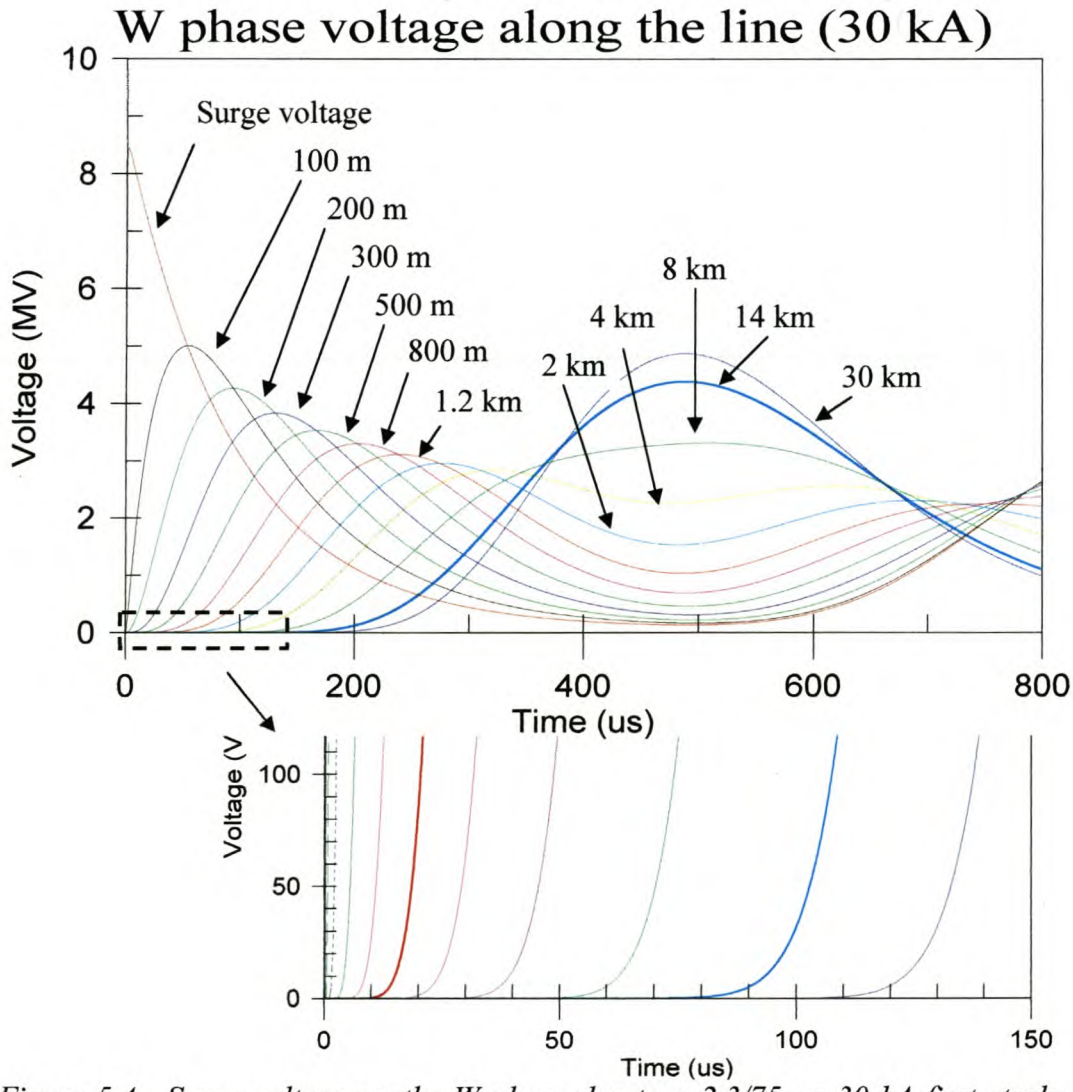

Figure 5.4. Surge voltage on the W phase due to a 2.3/75 μs 30 kA first stroke at different positions along the line. Due to the waveform attenuation, it looks if the surge travels slowly. Zooming into the origin of the graph, it shows that the surge takes 105 μs to travel the 30 km distance along the line (speed of 2.86×10^8 m/s).

The skin depth δ for a surge with a risetime of .73 μs along an aluminum wire is [5]:

Stellenbosch University http://scholar.sun.ac.za

$$\delta = \frac{1}{\sqrt{\pi f \mu \sigma}}$$

$$= \frac{1}{\sqrt{\pi\left(\frac{10^6}{.73}\right) \times (4\pi 10^{-7} \times 1.00000065) \times 3.82 \times 10^7}}$$

$$= 0.07 \text{ mm}$$

The resistance R per length L = 1 km along an aluminum wire with a radius r = 5.5 mm is [5]:

$$R = \frac{L}{2\pi r \sigma \delta}$$

$$= \frac{10^3}{2\pi 5.5 \times 10^{-3} \times 3.82 \times 10^7 \times .07 \times 10^{-3}}$$

$$= 10.8\ \Omega$$

The skin depth and resistance for a surge risetime of 2.3 μs will be 0.123 mm and 6.2 Ω respectively. The conductor resistance decreases by 46% if the surge risetime decreases from 0.73 μs to 2.3 μs. This explains the lower amplitude of the 0.73/32 μs surge compared to the 2.3/75 μs surge along the line (compare figures 5.4 and 5.5).

No corona

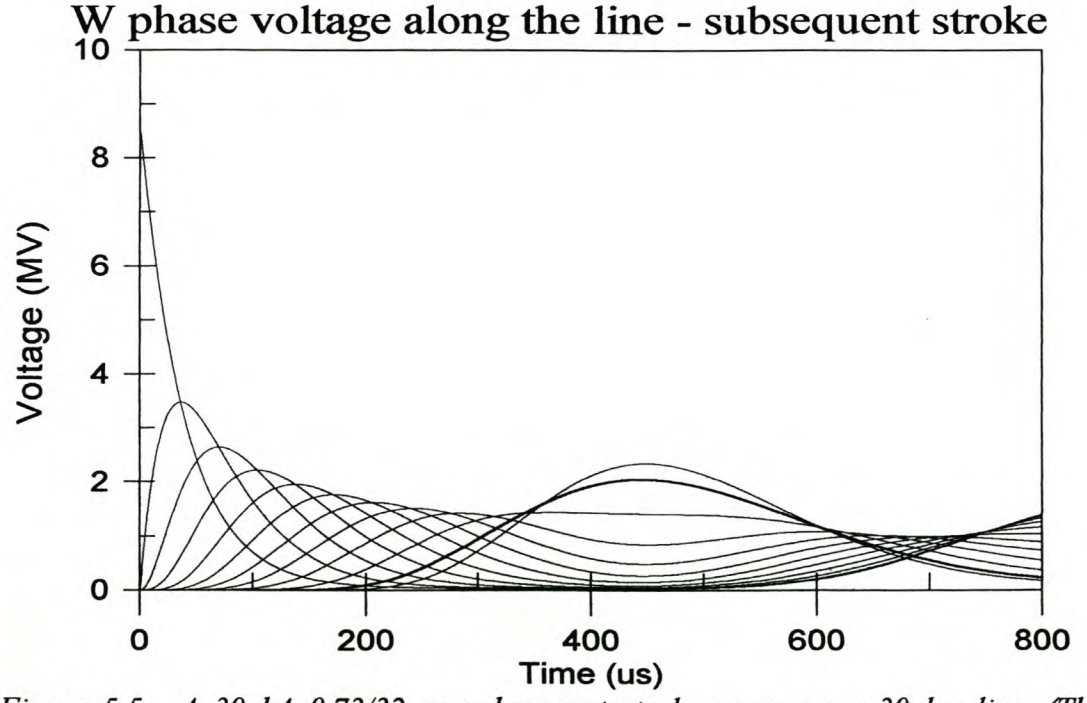

Figure 5.5. A 30 kA 0.73/32 μs subsequent stroke surge on a 30 km line. (The different curves identify different positions along the line – see fig 5.4)

Stellenbosch University http://scholar.sun.ac.za

In short, a long duration surge results in a higher surge voltage along the line than a short duration surge.

5.3. A line model with compensation for corona

As discussed in paragraph 3.2.7, the effective radius R_c of the conductor increases above the critical voltage for corona. To simulate this, the existing JMarti model's conductor radius will be increased firstly to an estimated value using the graph in figure 3.2.3. A surge study is then done and if necessary, the conductor radius is adjusted. This manual method is then repeated until the voltage amplitude and radius match the values in figure 3.2.3. Figure 5.6 shows a flow diagram of the above procedure.

Figure 5.7 illustrate the corona on a wishbone construction (shown in figure 1.10) line due to a 40 kA surge. The ATP line models were printed on scale and shows how the corona radius decreases non-linearly with distance. A surge voltage of 5.2 MV is generated at the pole where the surge is injected and will cause a flashover because the line's BIL is only 350 kV.

Figure 5.8 shows the result of a 30 kA 2.3/75 μs surge injected into a line with corona compensation. Using figure 3.2.3, the capacitance of the line increase from 6.7 pF to 14 pF and the effective corona radius increases to 1 m. This retards the wavefront risetime even more and halves the voltage at the injection point. As shown in figure 5.9, the coupling between phases is also stronger (compare to figure 5.2) due to the larger effective conductor radius.

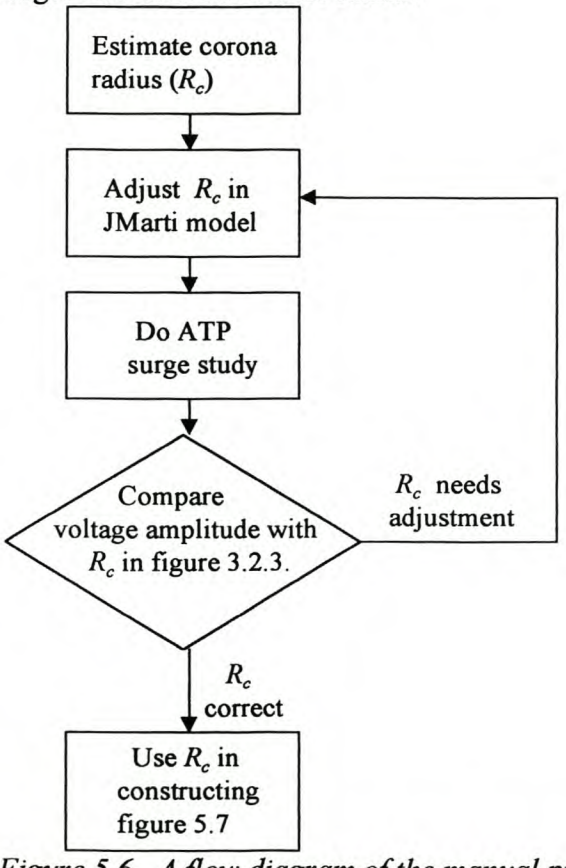

Figure 5.6. A flow diagram of the manual process to calculate the corona radius.

Stellenbosch University http://scholar.sun.ac.za

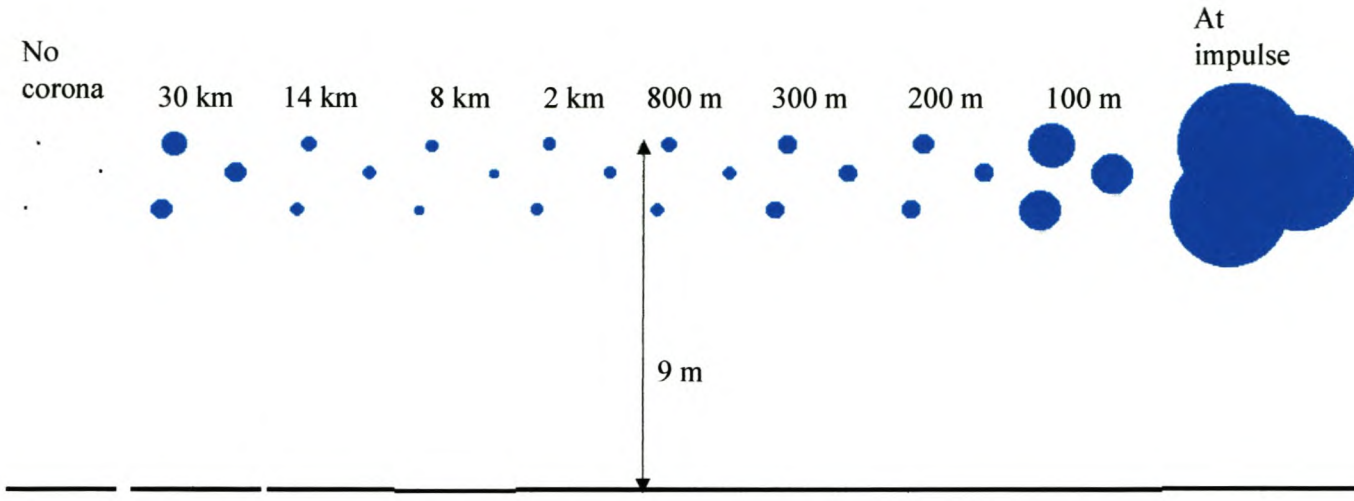

Figure 5.7. Corona due to a 40 kA surge on a 30 km line if no flashover to earth occurs.

When the steepness of the wavefront increases and the tail length decreases, corona has a larger effect on the line voltage. This is due to the same reason as discussed in paragraph 5.2. Along the line the wavefront slope is less steep due to the additional corona capacitance. The retarded wavefront reaches its peak when crossing the initial surge's tail. As the surge has a relative short duration, this happen quite low down on the initial surge's tail. Figure 5.10 shows the result of a 0.73/32 μs 30 kA surge injected into the test line. Although the voltage amplitude at the point of injection is the same for a 2.3/75 μs and 0.73/32 μs, the peak voltage along the line is 50% less for the short duration surge (compare figures 5.8 and 5.10).

In short, the longer the duration of the surge, the less influence the corona has on the surge.

Stellenbosch University http://scholar.sun.ac.za

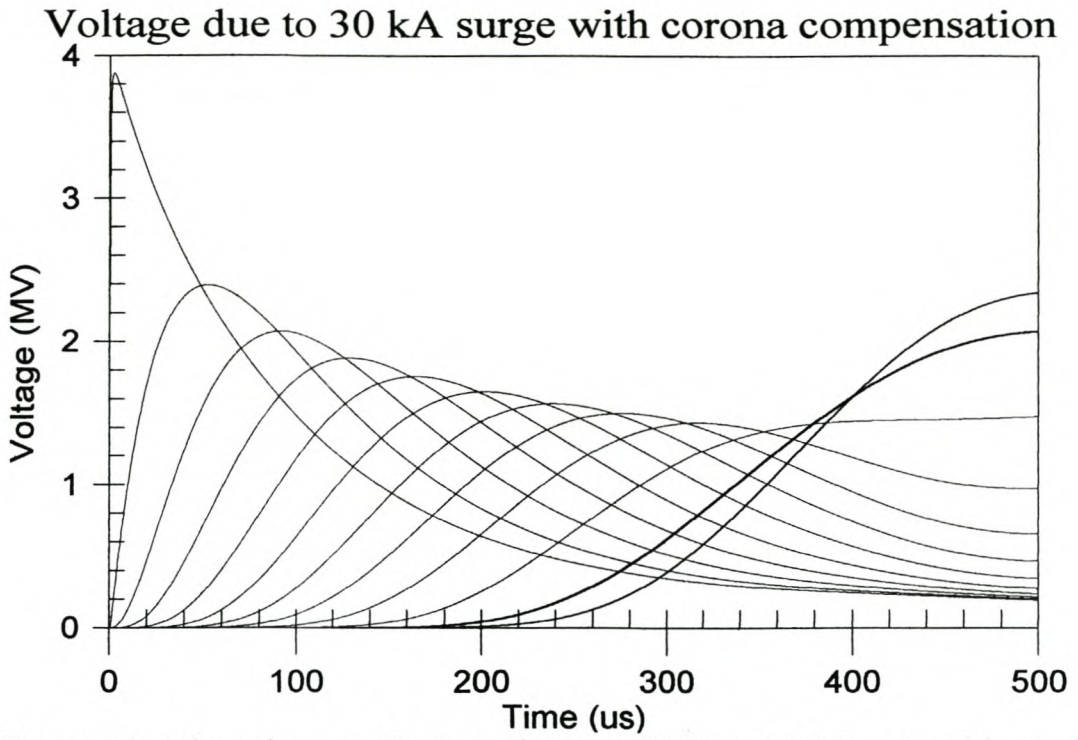

Figure 5.8. The voltage on W phase due to a 2.3/75 μs 30 kA surge. The model included compensation for corona.

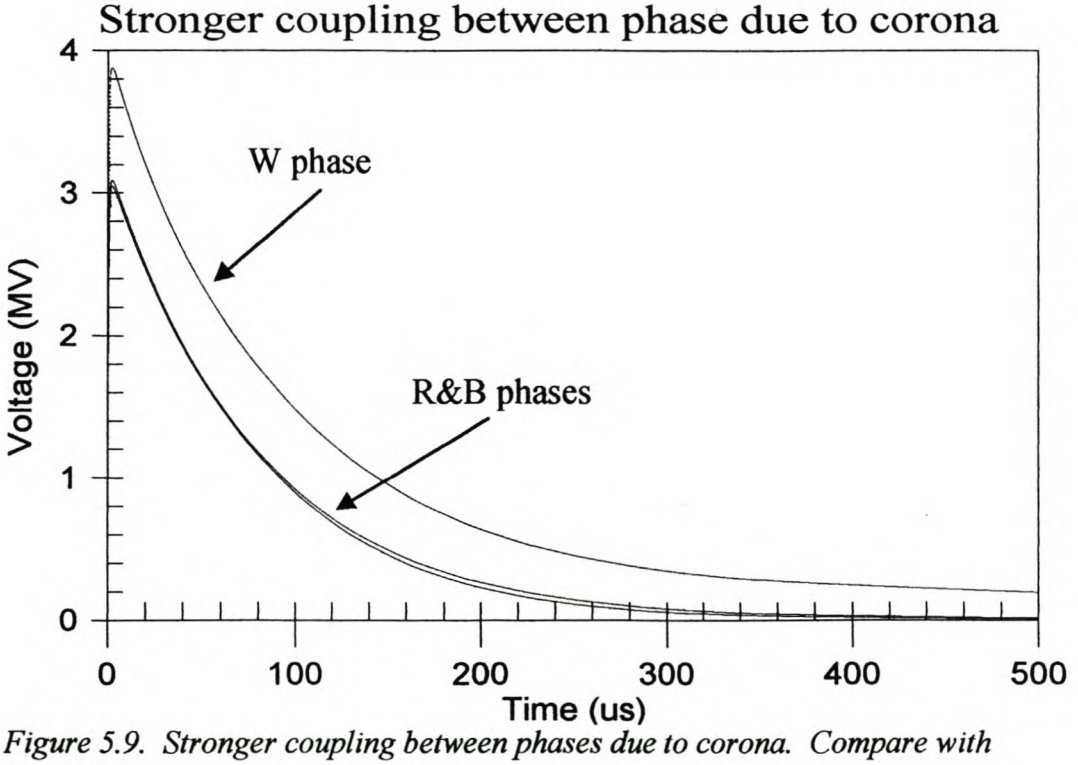

Figure 5.9. Stronger coupling between phases due to corona. Compare with figure 5.2

Stellenbosch University http://scholar.sun.ac.za

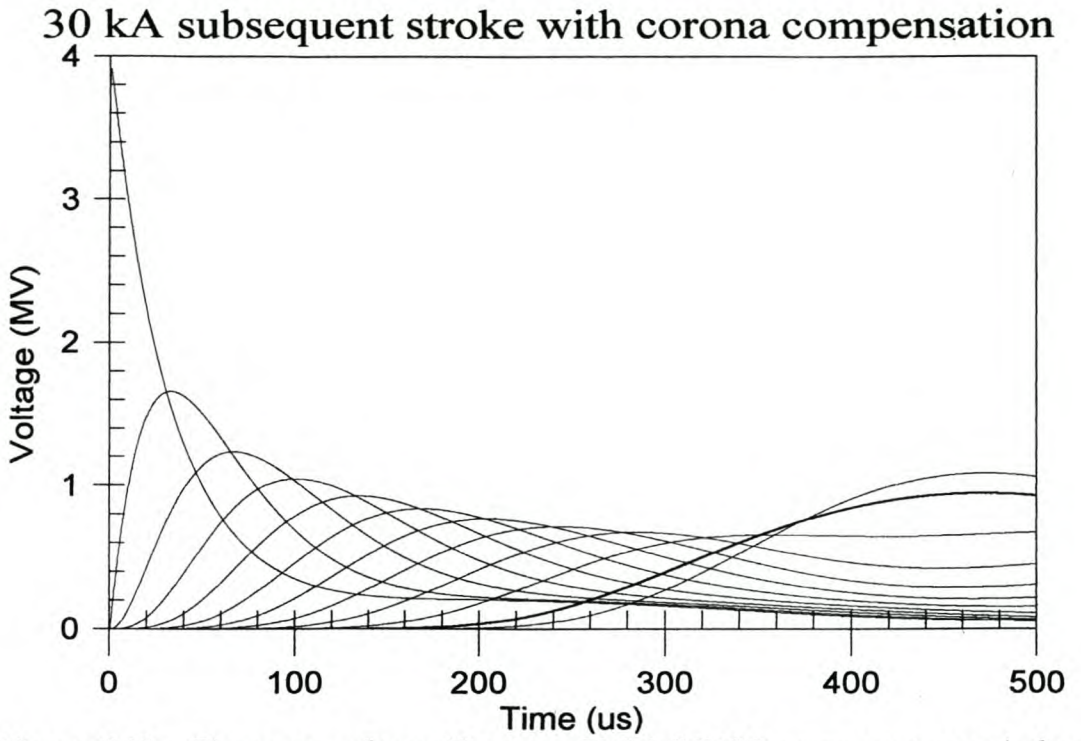

Figure 5.10. The surge voltage (due to a 30 kA 0.73/32 μs current surge) drops rapidly along the line due to the short rise time.

5.4 The influence of a flashover on the surge voltage.

The BIL of the test line is 350 kV. This means that there is a 10% [2, p. 4] chance that a flashover will occur with a potential of 350 kV between phase and earth. Depending on the downwire earth resistance, the phase voltage will then be limited to much lower values as discussed previously in this chapter. The single line electric diagram of the test line that was used, was the same as figure 5.1, with the surge arrester omitted.

After some experimental surge studies, it became clear that it is unnecessary to model a flashover at each pole on the line. To ensure a good safety margin, allowance was made in the simulation for flashovers on pole zero (where surge is injected) and two poles on each side of pole zero. The previous studies showed that the surge amplitude increases towards the end of the line. The last two poles that were modelled on each end of the line were then fitted with flashover models as well.

Figure 5.11 is the result of a 30 kA 2.3/75 μs surge study on the test line where a flashover occurred only on the pole where the surge was injected. The flashover occurred at 350 kV and the line voltage dropped to 290 kV due to the voltage drop across the earth impedance.

A 250 kA 8.2/75 μs surge caused 7 flashovers – at pole zero, pole 1 left and right, pole 2 left and right (see figure 5.1) and on both sides at the end of the line as shown in figure 5.12. The multiple flashovers are due to the earth impedance at the poles. Due to earth impedance, the pole top voltage at pole zero peaked at 900 kV (figure 5.12). A 100 m further on both sides of the surge, the W phase flashed over causing

Stellenbosch University http://scholar.sun.ac.za

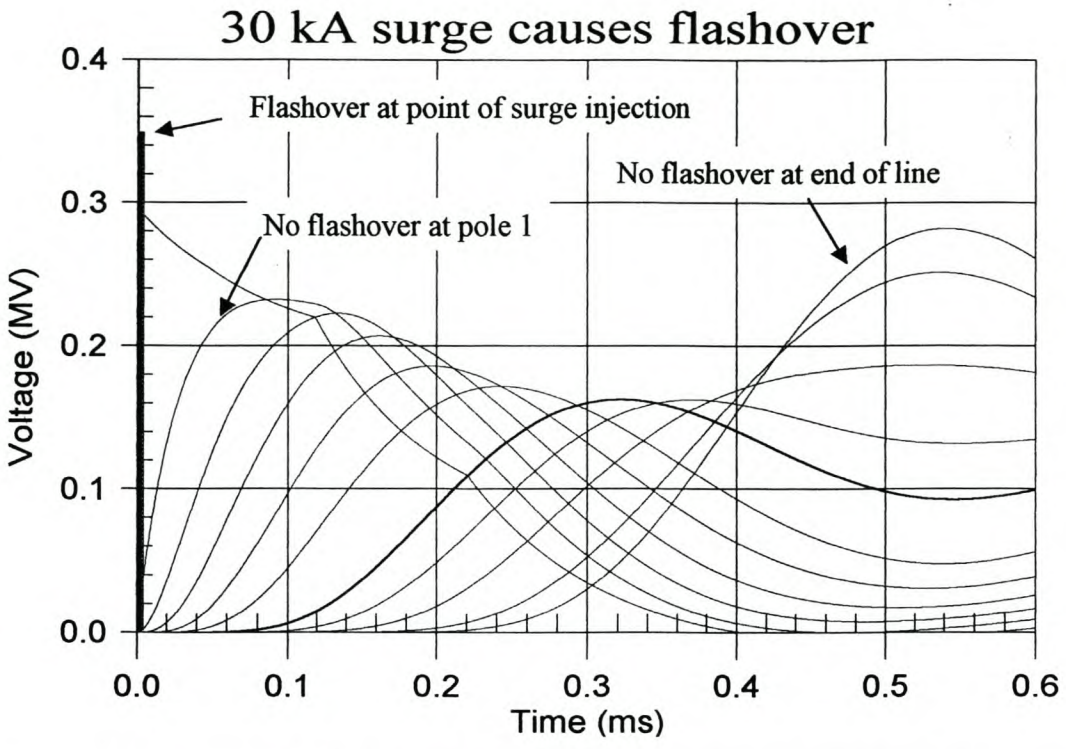

Figure 5.11. A 30 kA 2.3/75 μs surge caused a flashover at the pole where the surge was injected (no surge arrester).

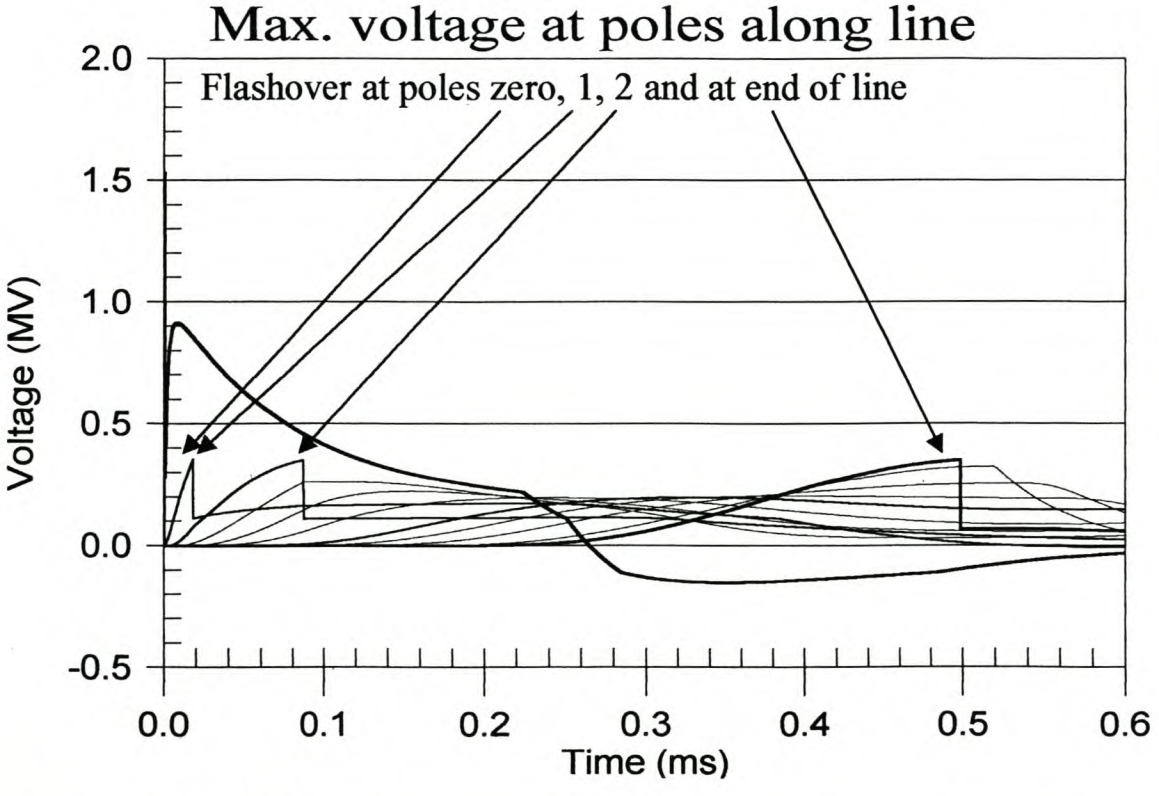

Figure 5.12. A 250 kA 8.2/75 μs surge causes flashovers at poles zero, 1, 2 and at end of line.

Stellenbosch University http://scholar.sun.ac.za

the earth lead's potential to rise. As shown in figure 5.13, the R and B phases did not flash over due to the earth lead potential also being high.

Flashovers also occurred on pole 2 (200 m from the surge injection). This time the B phase flashed over because this phase's voltage was the highest at the previous pole. No flashover occurred on the next poles (300 m away from surge) as all the phase voltages were below 350 kV. The last flashover occurred at the end of the line where the surge was reflected, causing the voltage to rise. This is also shown in figure 5.12.

To conclude, current surges as little as 2000 A can cause a flashover on the pole of injection. High amplitude surges cause multiple flashovers due to a rise in potential because of earth impedance. Flashovers limit the line voltage to much lower values (compare figures 5.8 and 5.11).

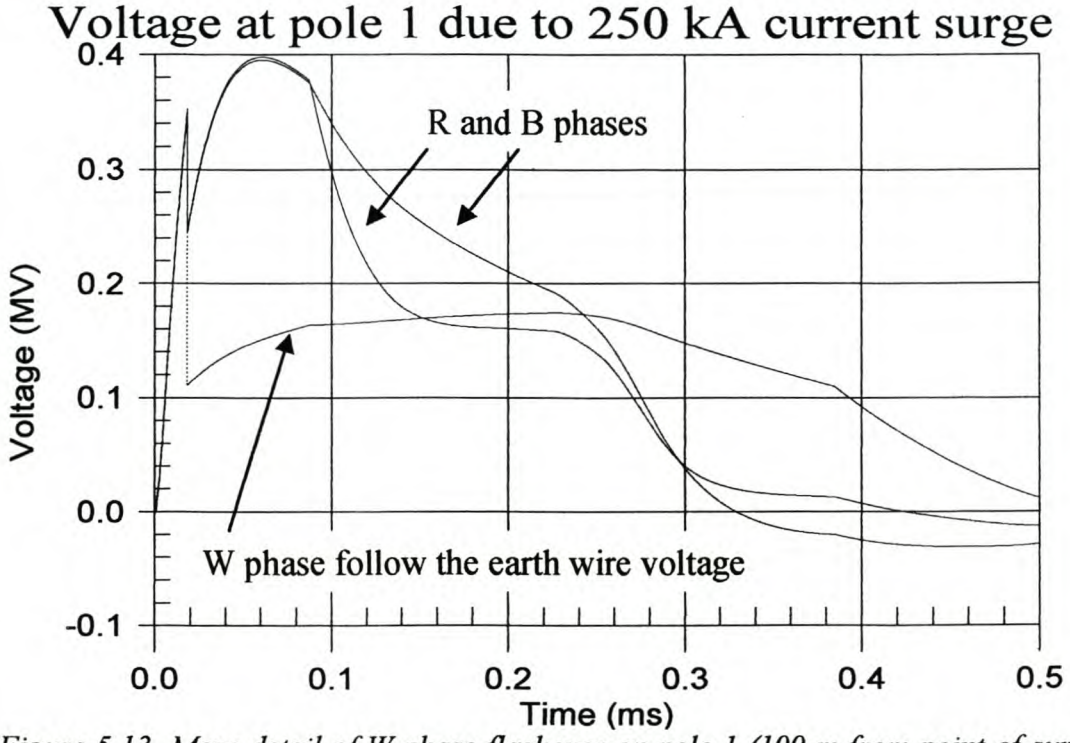

Figure 5.13. More detail of W phase flashover on pole 1 (100 m from point of surge injection) as shown in figure 5.12. Although the R and B phase voltage exceeds 350 kV, no flashover occurs due the potential rise in the earth lead.(same as Fig 5.12).

5.5. The effect of a line surge arrester.

A three phase line surge arrester was put at different locations on the test line to find the optimal placement and accuracy necessary to be effective. First the arrester was placed as shown in figure 5.1 on the pole 300 m away from the surge. A 2.3/75 μs 30 kA surge was injected at pole zero. The line arrester did not prevent a flashover at pole zero. The results are shown in Fig 5.14. Comparing figures 5.11 and 5.14, the arrester has not much influence on the surge amplitude, especially at the point of surge injection and on the first two poles. The surge amplitude at the end of the line decreased from 280 kV to 140 kV.

Stellenbosch University http://scholar.sun.ac.za

If the surge arrester is placed 200 m or 100 m from surge, it still does not prevent a flashover on the pole where the surge is applied, as shown in figures 5.15 and 5.16 respectively. Figure 5.17 shows that the surge amplitude is 3 times higher on the side where there is no line surge arrester. The surge arrester on the left side of the surge does not help at all to reduce the surge amplitude on the right side – even if the arrester is only 100 m from pole zero.

Figure 5.18 presents the final test with the arrester placed at pole zero where the surge is injected. The arrester not only prevents flashover at pole zero, but also reduces the surge amplitude at the other poles with 50% in comparison with the case where no surge arrester is installed (compare figures 5.18 and 5.11). A 250 kA 8.2/75 μs surge causes only two flashovers (at the first pole on both sides) instead of seven flashovers where no surge arresters is installed (compare figures 5.12 and 5.19). The earth resistance and the lead connected to the line arrester together were modelled as 5 ohm. This value was practically measured. Due to coupling between phases, no flashover occurs between phases (maximum voltage difference is 300 kV)

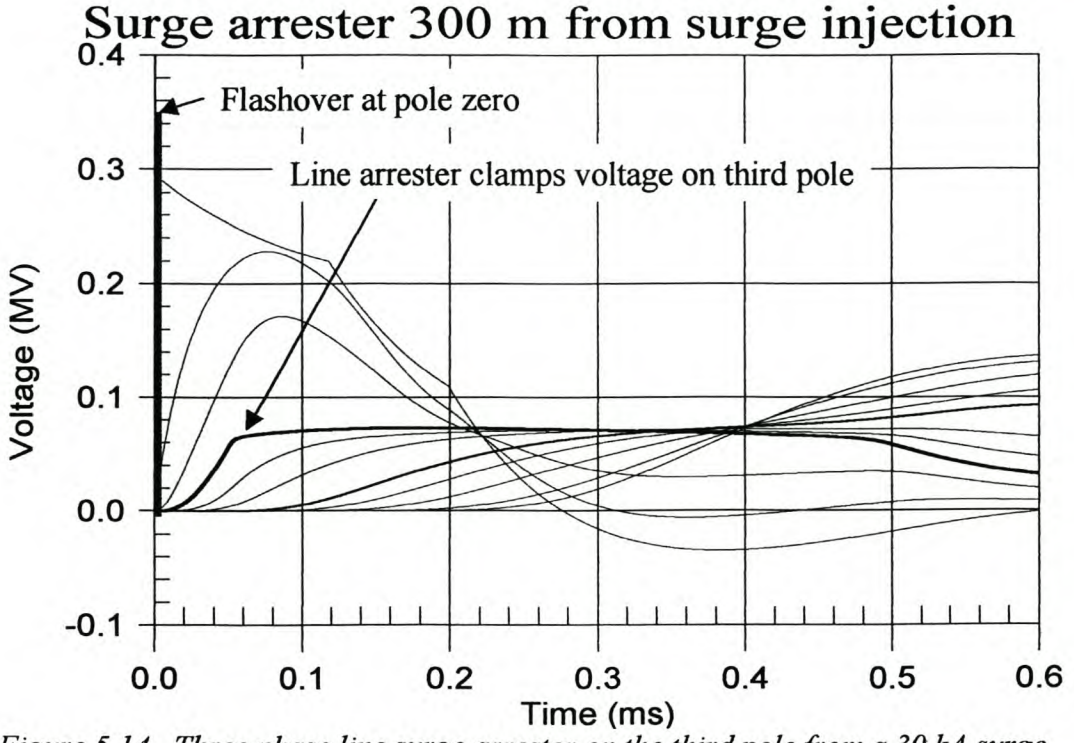

Figure 5.14. Three phase line surge arrester on the third pole from a 30 kA surge.

Stellenbosch University http://scholar.sun.ac.za

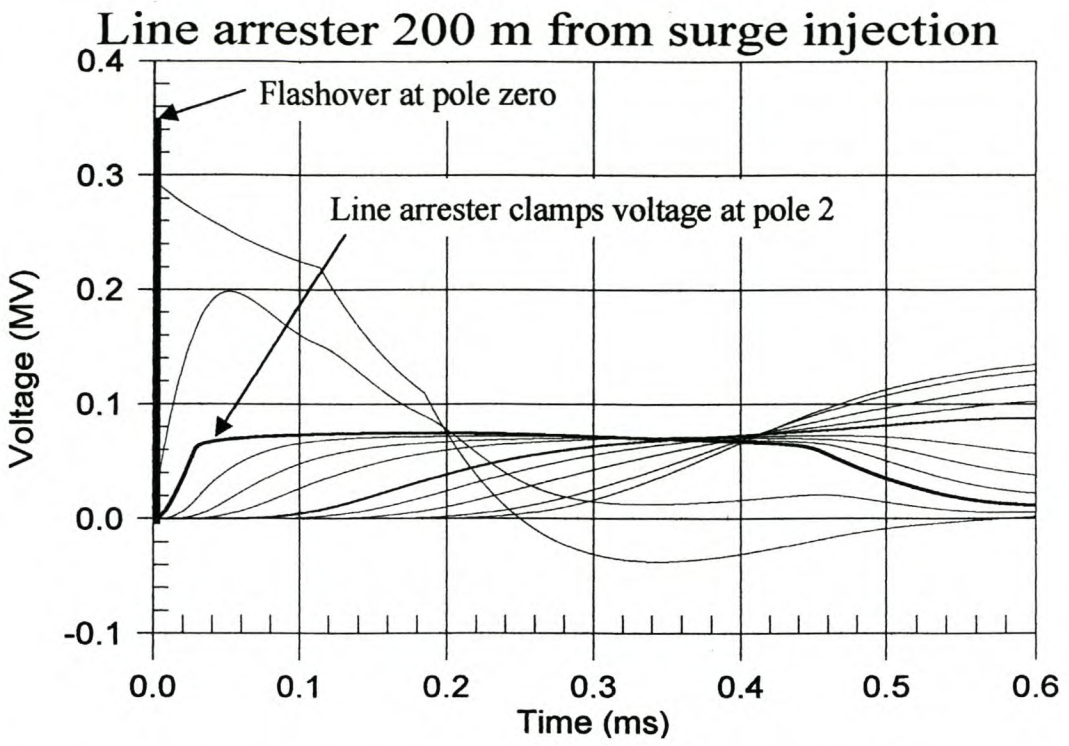

Figure 5.15. Line arrester placed on second pole from a 30 kA surge

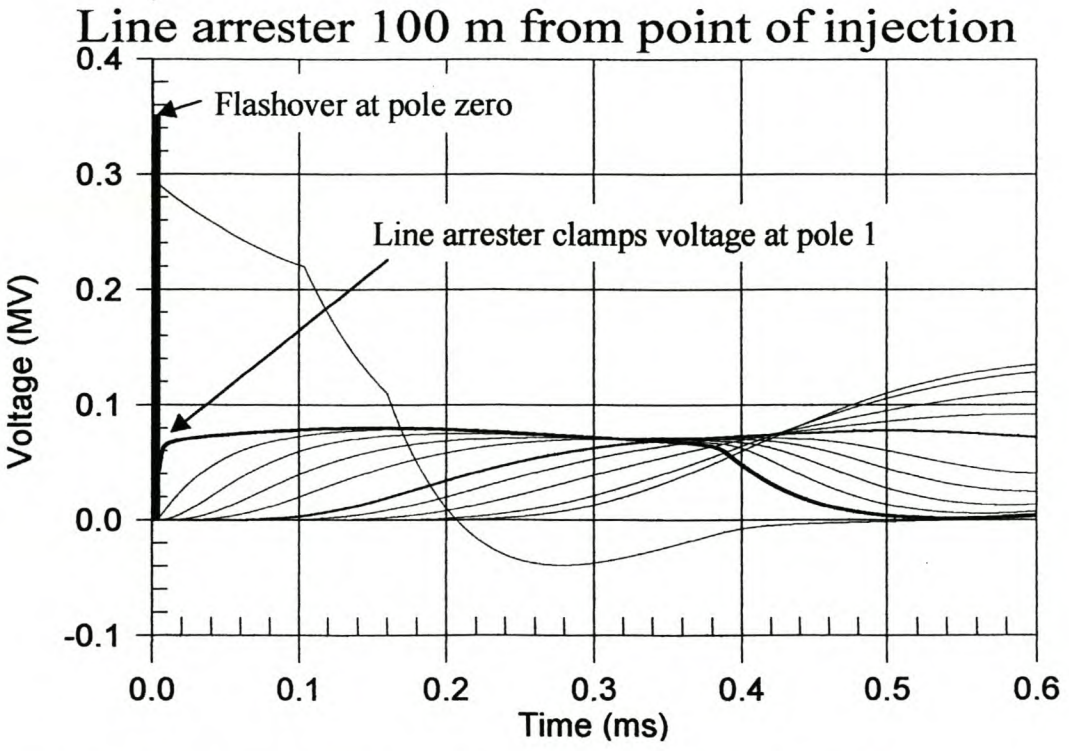

Figure 5.16. Line arrester on the first pole away from the 30 kA surge.

Stellenbosch University http://scholar.sun.ac.za

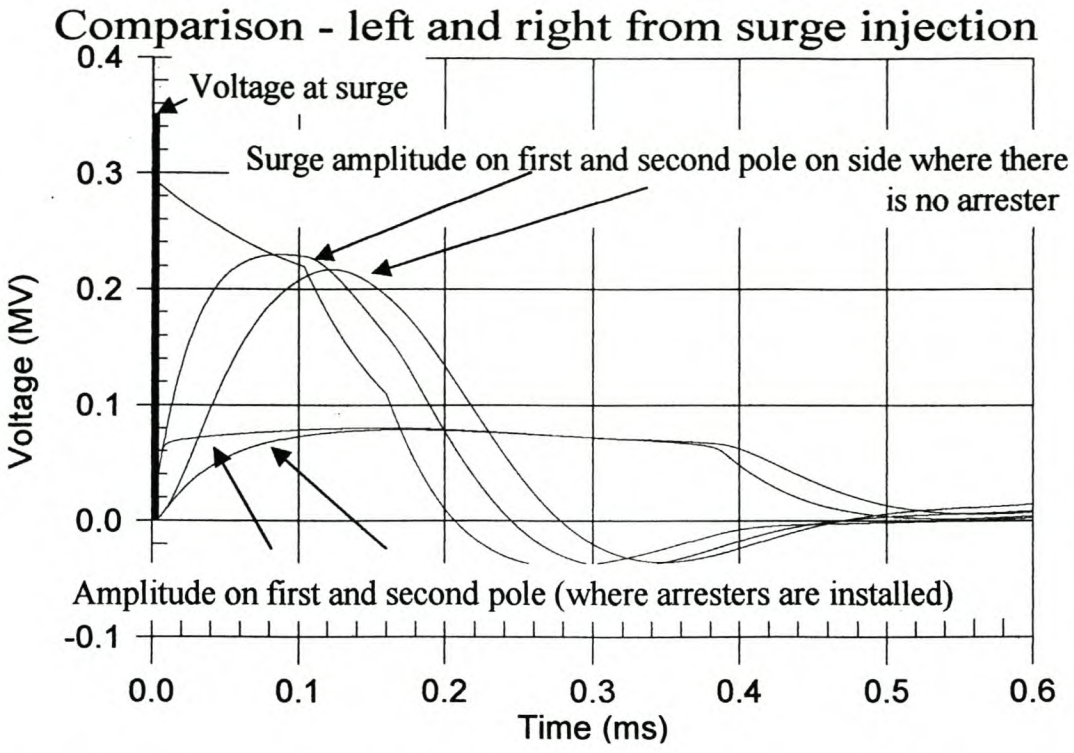

Figure 5.17. Comparison of voltage amplitude on both sides of surge. The two lower amplitudes are due to the voltage clamped by the surge arrester 100 m (first pole) from the surge.

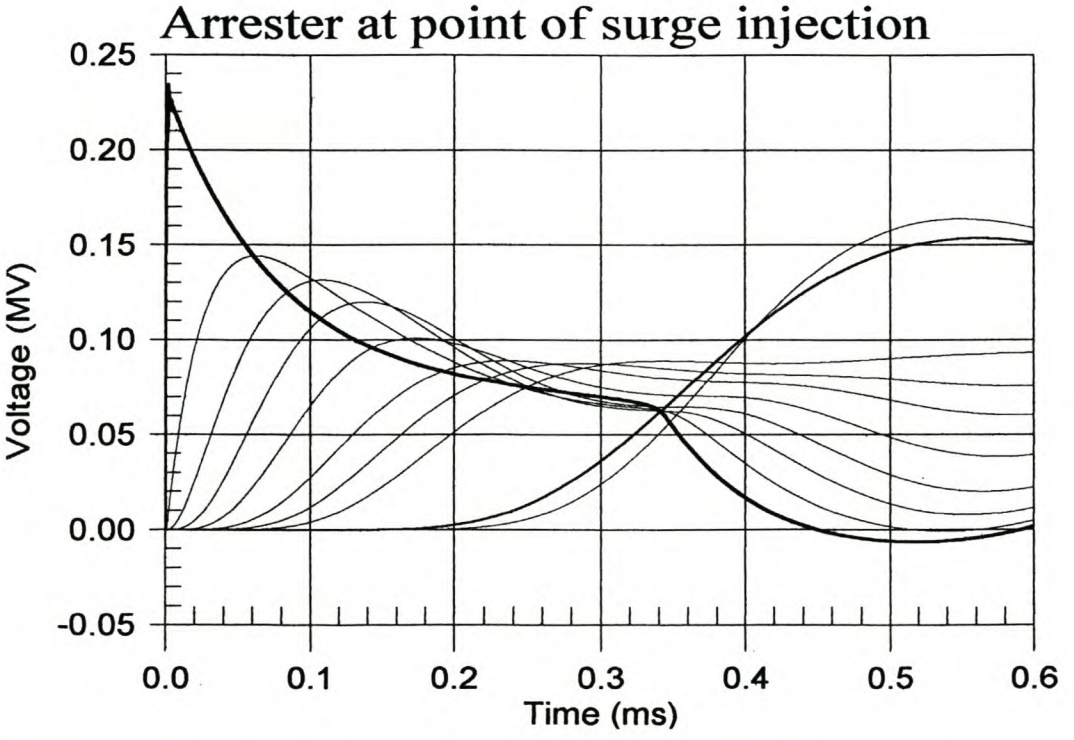

Figure 5.18. Line arrester installed on pole where 30 kA surge is injected.

Stellenbosch University http://scholar.sun.ac.za

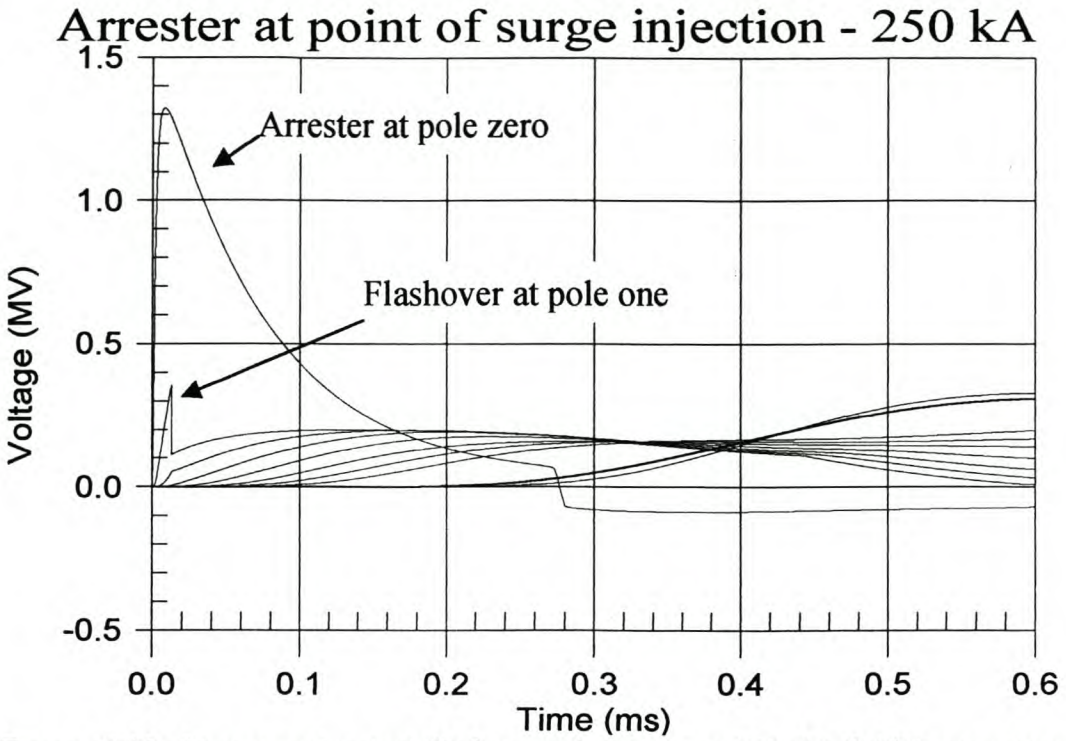

Figure 5.19. Line arrester installed on pole where a 250 kA 8.2/75 μs surge is injected.

5.6. Transformer and fuse failures

Theoretically it seems impossible for pole-mounted transformers (protected by arresters on transformer tank) and fuses to fail due to lightning surges, even if no line surge arresters are fitted. In the first place, the voltage is limited to the BIL of the line. For higher voltages the line flashes over. Secondly, most of the lightning energy is dispensed to earth with the flashover. Then there are also line losses, including corona.

An example of a typical lightning flash shows that except for the stroke surges, there is also a continuing current of between 100 A and 600 A [4]. The average interval between strokes is 30 ms [4]. Figures 5.20 and 5.21 show a simulation of a 30 kA first stroke followed by two 22 kA subsequent strokes and a continuing current of 300 A. The stroke surges (at 0, 10 and 40 milliseconds) have little influence on the I^2t value through the fuses (figures 5.20 and 5.21). Most of the energy in the flash was released by the 300 A continuing current. Although the stroke amplitude was much higher than that of the continuing current, the duration was too short to release a large quantity of energy.

The energy rating of the surge arresters used is 3.6 kJ/kV. For a 22 kV arrester, the permissible energy dispensed in the arrester is 79.2 kJ. In the case where line arresters were installed (figure 5.21) as well as in the case with no line arresters installed (figure 5.20), the maximum energy absorbed by the line arrester was more

Stellenbosch University http://scholar.sun.ac.za

than 79.5 kJ. The W phase line arresters, that is at the pole where the surge was injected, had to absorb 900 kJ as shown in figure 5.22. None of the installed line arresters failed after several lightning storms and it can therefore be assumed that the continuing current of the lightning strokes was not as severe as in the simulation.

Figure 5.20 shows that the I^2t specified limit of 1 600 A^2s for a 10 A fuse was exceeded where no line arresters were installed. In the case were line arresters were installed, the fuse should not operate as shown in figure 5.21.

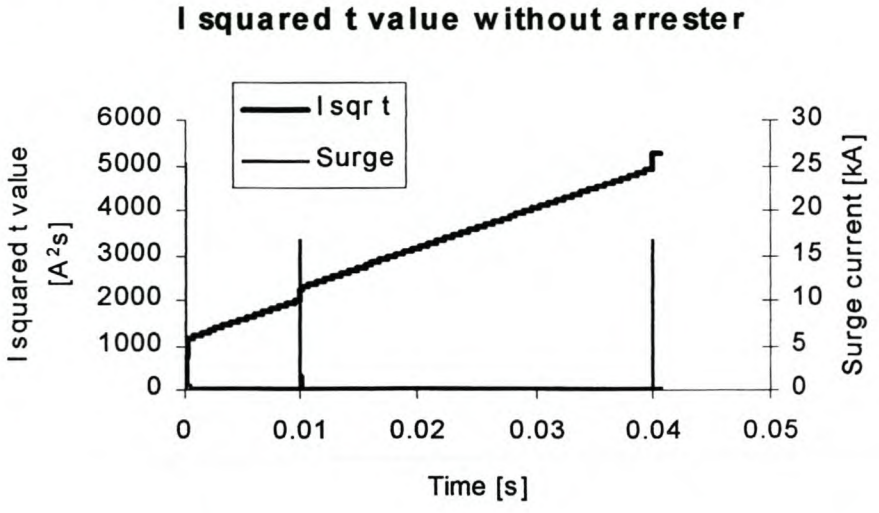

Figure 5.20. Stress on a fuse due to a flash consisting of 30 kA, 22 kA and 22 kA strokes and a continuing current of 300 A. No line arresters are installed. A 10 A fuse has an I squared t value of 1 600 and will therefore operate. The flash was injected into the line 2 km from the pole-mounted installation

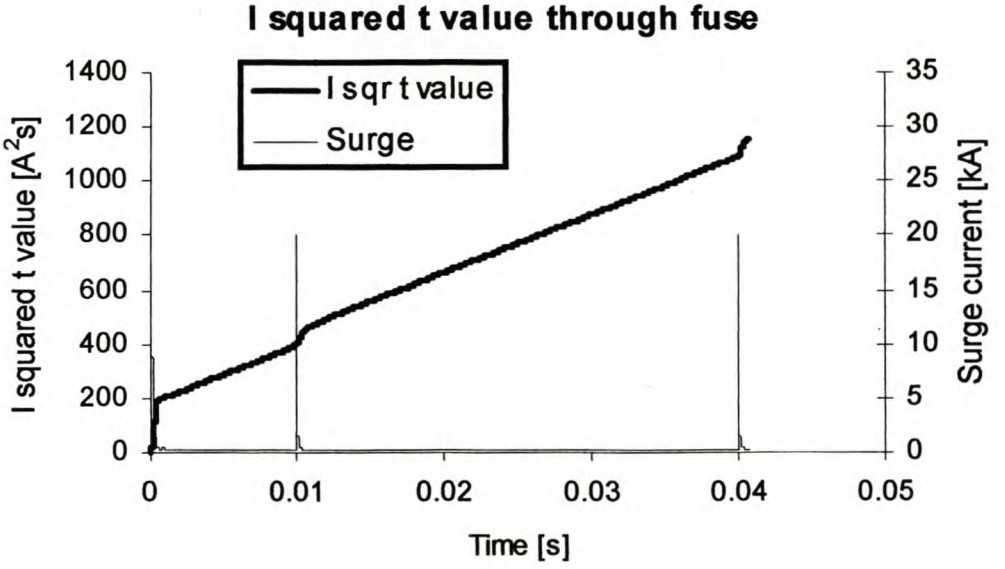

Figure 5.21. Stress on a fuse due to a flash consisting of 30 kA, 22 kA and 22 kA strokes and a continuing current of 300 A. Line arresters are installed. A 10 A fuse has an I squared t value of 1 600 and will therefore operate. The flash was injected into the line 2 km from the pole-mounted installation

Stellenbosch University http://scholar.sun.ac.za

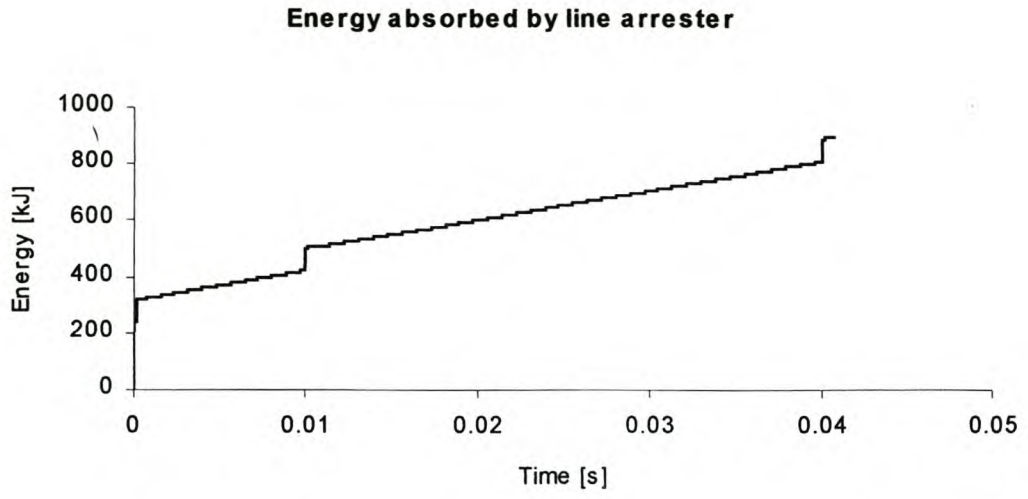

Figure 5.22. The energy absorbed by the W phase line arrester due to a flash consisting of 30 kA, 22 kA and 22 kA strokes and a continuing current of 300 A. The energy exceeds the arrester rating of 79.2 kJ.

The same argument is true for pole-mounted transformers. Figures 5.23a and 5.23b shows the voltage across the pole-mounted transformer without and with line arresters installed respectively. A 22 kV transformer has a BIL of 150 kV, which is far more than 70 kV.

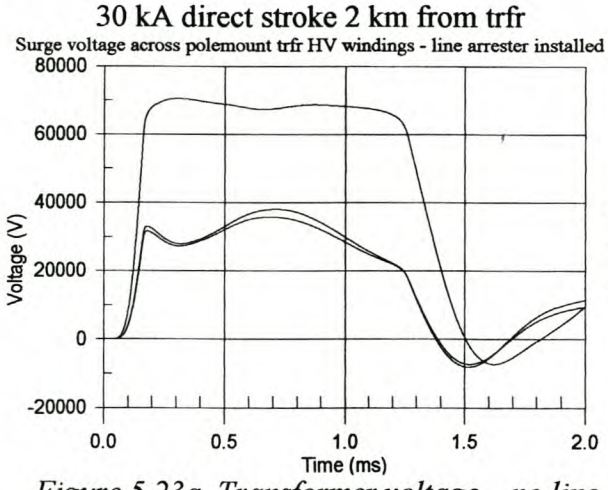

Figure 5.23a. Transformer voltage – no line arresters.

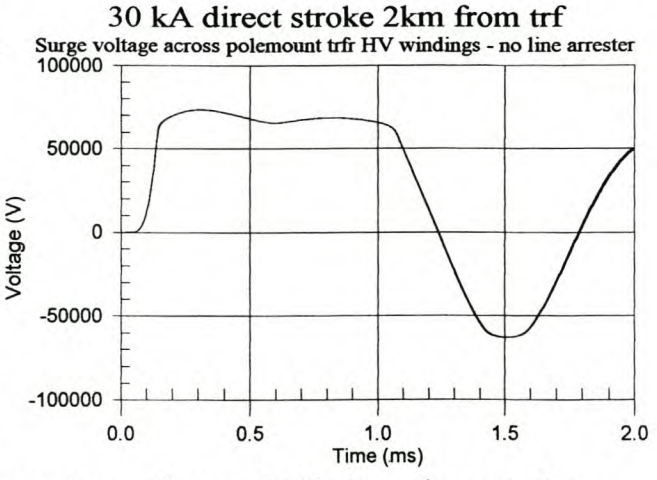

Figure 5.23b. Transformer voltage with line arresters installed.

Practical test were done by Hamel [3] that showed that the transformer starts saturating when the tail of the surge is long (many milliseconds and between 100 A and 300 A) due to the power frequency getting offset. During saturation the transformer impedance become lower than the surge arrester impedance and the surge arrester current gets diverted through the transformer. The tests show that the $I^2 t$ value can then equal the maximum limit of the fuse. This can also contribute to fuse operation. It is also possible that an old transformer can get damaged during this long saturation time.

Stellenbosch University http://scholar.sun.ac.za

5.7. Conclusion of theoretical analysis

Simulations where corona and flashovers were ignored, showed that the surge amplitudes along the line, were high (2 MV). Corona decreases the wavefront steepness and therefore the surge amplitude by 50% within the first spanlength. However, flashovers and surge arresters largely minimize the effect of corona.

The best strategy is to discharge the surge energy as soon as possible, in order to prevent a possible flashover and transformer saturation. The idea is not that the line arrester absorbs the lightning surge completely, but to assures an additional low impedance path to earth for the surge. It was learned that the two most critical places where flashovers can occur, are at pole zero (where the surge is injected) and at the end of the line.

The placement of the line arrester is critical and need to be installed at the point where the surge is injected to be fully utilized. If that pole is unknown and the line surge arrester is installed to the left of the pole with the surge on, the arrester will only protect the equipment to the left of the surge. About no protection will be given to equipment on the right (the side away from the arrester) of the surge. The better the earthing of the line arrester, the more effective the arrester becomes.

Most of the energy within the flash is stored in the continuing current and heats up the arresters. The stroke is responsible for breaking the insulation and initiates the flashover.

5.8. References.

1. R.B. Anderson, A.J. Eriksson, Lightning parameters for engineering applications, Electra no. 69, p. 65 – 102, 1980.
2. A.R. Hileman, Insulation Coordination for Power Systems, Marcel Dekker, Inc. 1999, p. 345 – 346.
3. A. Hamel, G St-Jean, M. Paquette, Nuisance fuse operation on MV transformers during storms, IEEE Transactions on Power Delivery, Vol. 5, No. 4, November 1990, p.1867.
4. H.J. Geldenhuys, C.T. Gaunt, A.C. Britten, Insulation co-ordination of unshielded distribution lines from 1kV to 36kV, SAIEE publication, p. 8.
5. W.H. Hayt Jr., Engineering electromagnetics, Third edition, McGraw-Hill Kogakusha, p 382.

Stellenbosch University http://scholar.sun.ac.za

6. PRACTICAL INSTALLATION OF LINE ARRESTERS AND BUSHING-MOUNTED FUSES

The main objective is to create an additional circuit for the surge to earth. Due to the high construction cost and inconvenience to customers (no supply while work progress) the intention is not to do any alterations to the existing network to improve the lightning performance. On the other hand, if line surge arresters are installed, the maintenance (like changing faulty surge arresters elsewhere) must continue according to normal practice.

6.1. Identifying a problem area

The lightning problem areas must first be identified using the network performance system (NAPI). A list of all the equipment failures during the past year on the line under investigation must be made. The failures must then be correlated with LPATS to ensure that the failures are lightning related. As an example, table 6.1, an extract from NAPI, can be investigated. Using LPATS, the lightning strokes for the particular time frame can be plotted on a geographical layout of the line. If there were lightning strokes during this time period in the vicinity of the line as shown in figure 6.1, there is a good change that the failure was lightning related.

Feeder	Date	Time	Incident description	Weather	Address	MVA hours lost	Customers effected
KMP	980118	21:25	Wire burnt off	storm	KMP100/205/1/1	5.96	43
KMP	980118	21:25	Breaker trip	storm	KMP100/2	0	0
KMP	980119	15:55	Fuse blew	storm	KMP354/102/5	0.05	1
KMP	980119	19:30	Trfr fault	storm	KMP354/102/5	0.55	1
KMP	980118	16:59	Trfr fault	storm	KMP354/49/34	0.87	1

Table 6.1. An extract of NAPI

The date and time in NAPI is reported times which is normally about 10 minutes later than the real incident if the customer is at home at the time of the incident. In the extreme cases where a transformer or fuse fail at a water pumping installation, it can happen that reporting only gets done 2 weeks later when the customer needs his pump again. It is necessary to rely on the initiative and integrity of the field personnel to establish whether the failure was lightning related in such a case.

A supervisory control system in the Network Control room is also a very useful tool for monitoring breaker operations. Many times equipment failures cause the nearest breaker to trip. In this case an accurate time for the incident get logged in the supervisory control database. Again there can be a delay of 1 to 2 seconds and in the extreme case 4 minutes (if there is a communication problem) for the breaker information to reach the Sentinal master station where Global Positioning System (GPS) timestamping gets done. Line two in table 6.1 shows the KMP100/2 breaker (which is on supervisory control) trip time taken from the Sentinel.

Stellenbosch University http://scholar.sun.ac.za

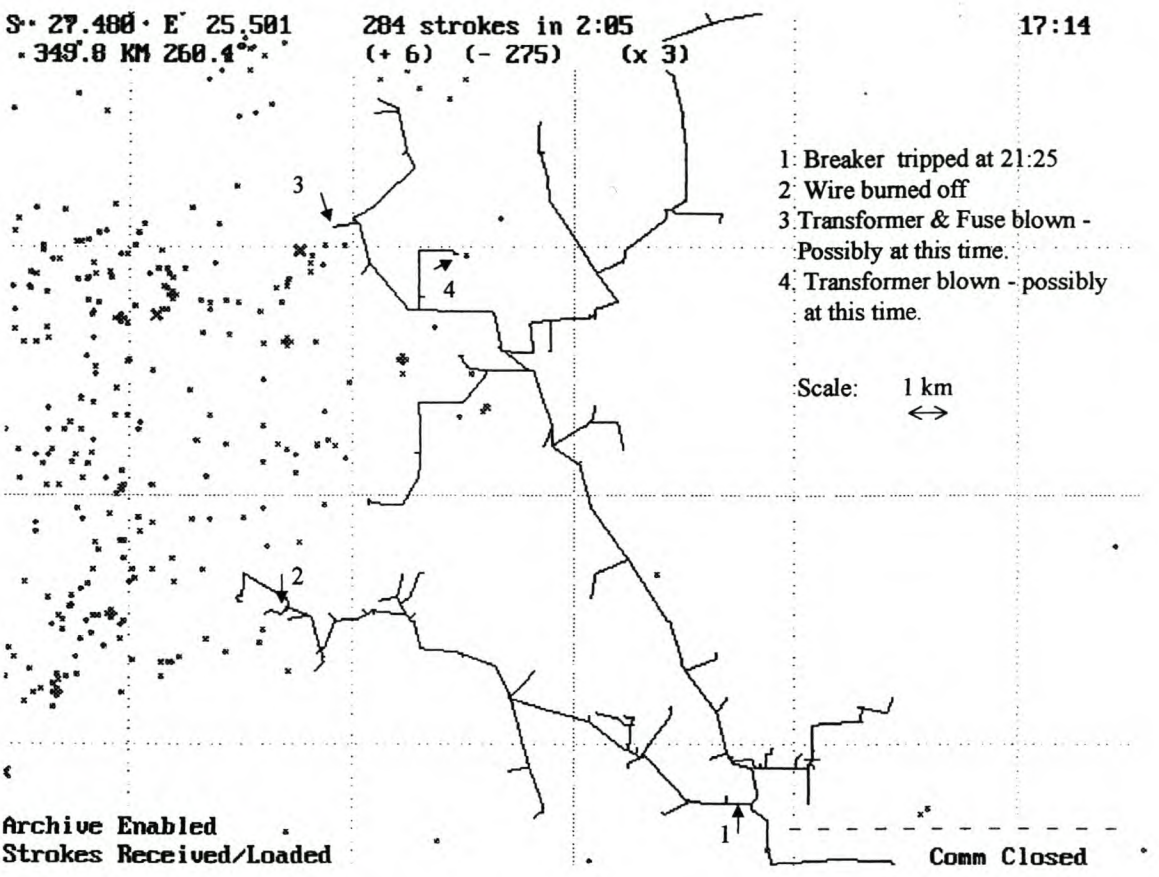

Figure 6.1. Lightning stokes on 18/01/1998 between 20:15 and 22:19 around the KMP line.

As LPATS is only ± 1km accurate on the position of the lightning stroke, the time must be used for comparing the lightning strokes with equipment failure. Approximately 90% of the lightning strokes are captured by LPATS. The other 10 % of the strokes are missed. LPATS also uses GPS time stamping. All the strokes between zero and 4 minutes before the breaker operation time as logged is strongly suspect for causing the damage if it is closer than 1 km from the line or failed equipment. Figure 6.2 is a zoomed in picture of figure 6.1. Five strokes of which one or more is possibly the cause for the damage to the line, resulting in a breaker trip, are shown.

According to NAPI a fuse and a transformer failure on 19/01/98 and another transformer failure on 20/01/98 were reported (see table 6.1). According to LPATS, there was no lightning activity around the KMP line on these two dates. It is therefore possible that these failures occurred on 18/01/98. Figure 6.3 is another zoomed in picture of figure 6.1. Several lightning strokes could be responsible for the one fuse and two transformer failures.

Stellenbosch University http://scholar.sun.ac.za

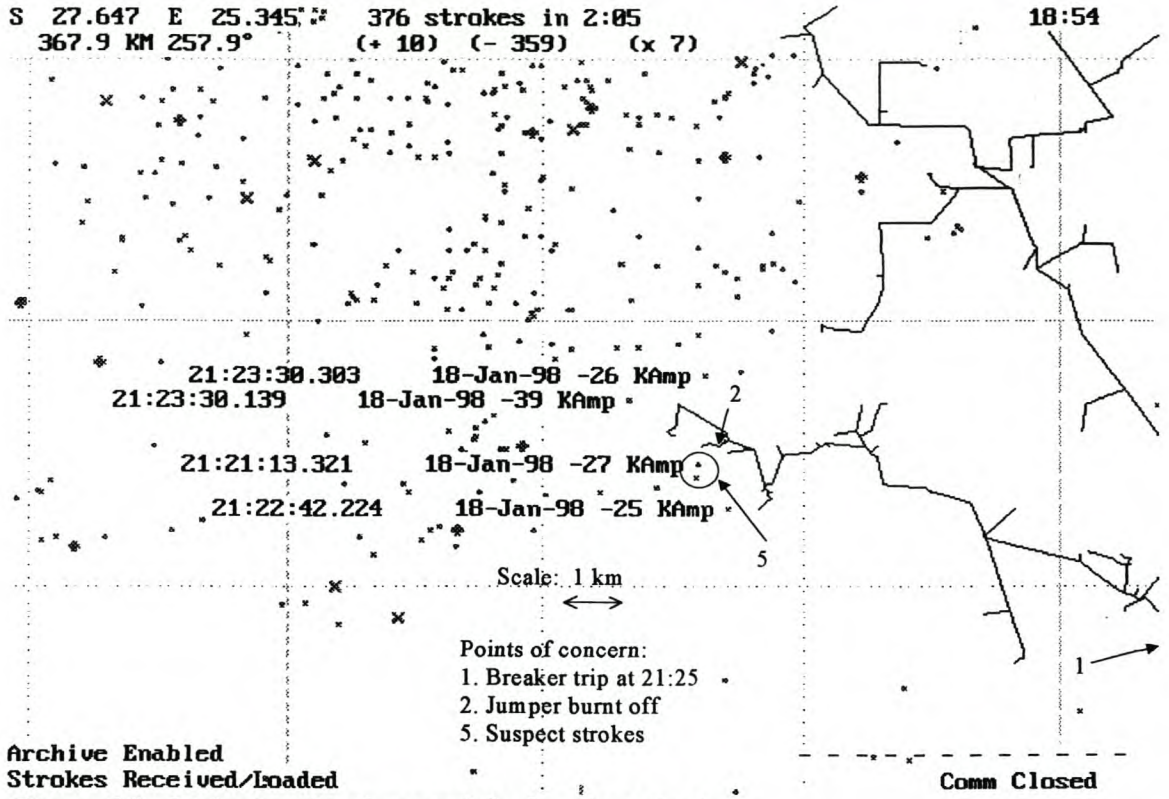

Figure 6.2. Lightning detail around the breaker trip time.

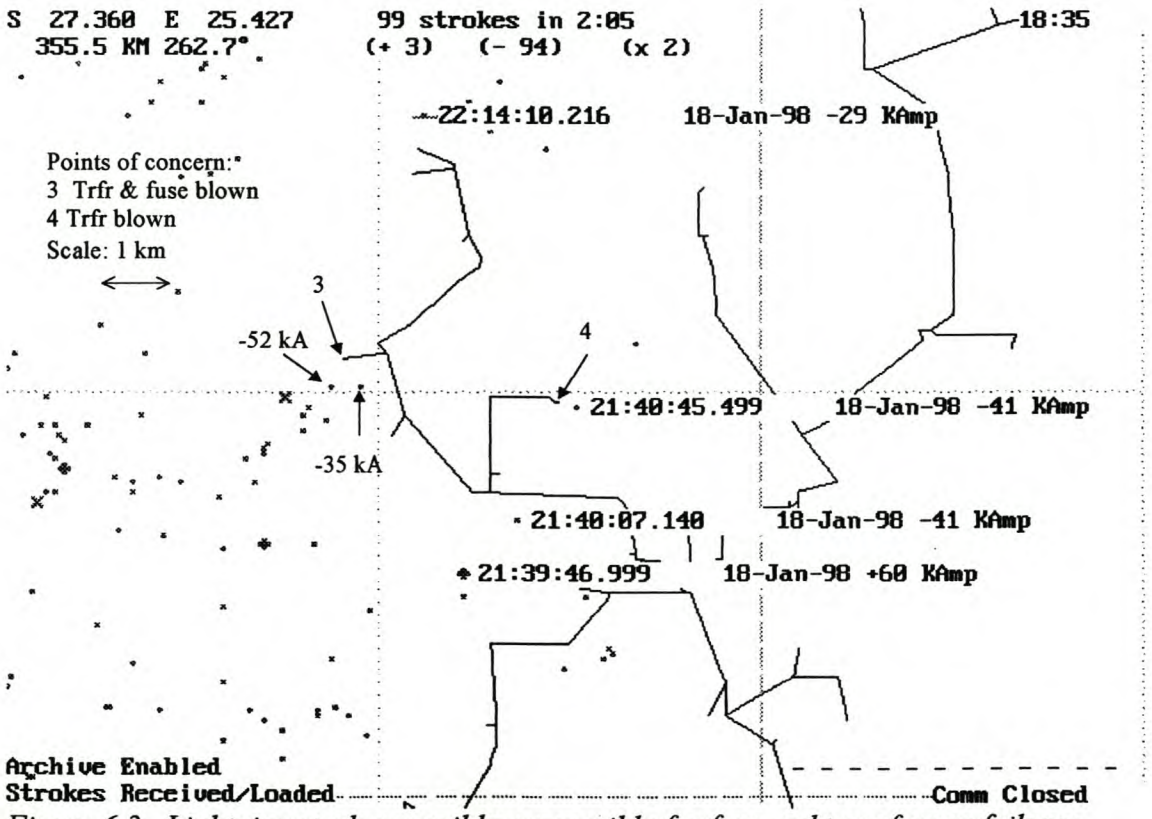

Figure 6.3. Lightning strokes possibly responsible for fuse and transformer failures.

The lightning related failures are then plotted on a geographical layout of the power line as shown in figure 6.4. A more detailed analysis as shown in figure 6.5 is necessary to identify the poorly performing area. As discussed in chapter 5, the

Stellenbosch University http://scholar.sun.ac.za

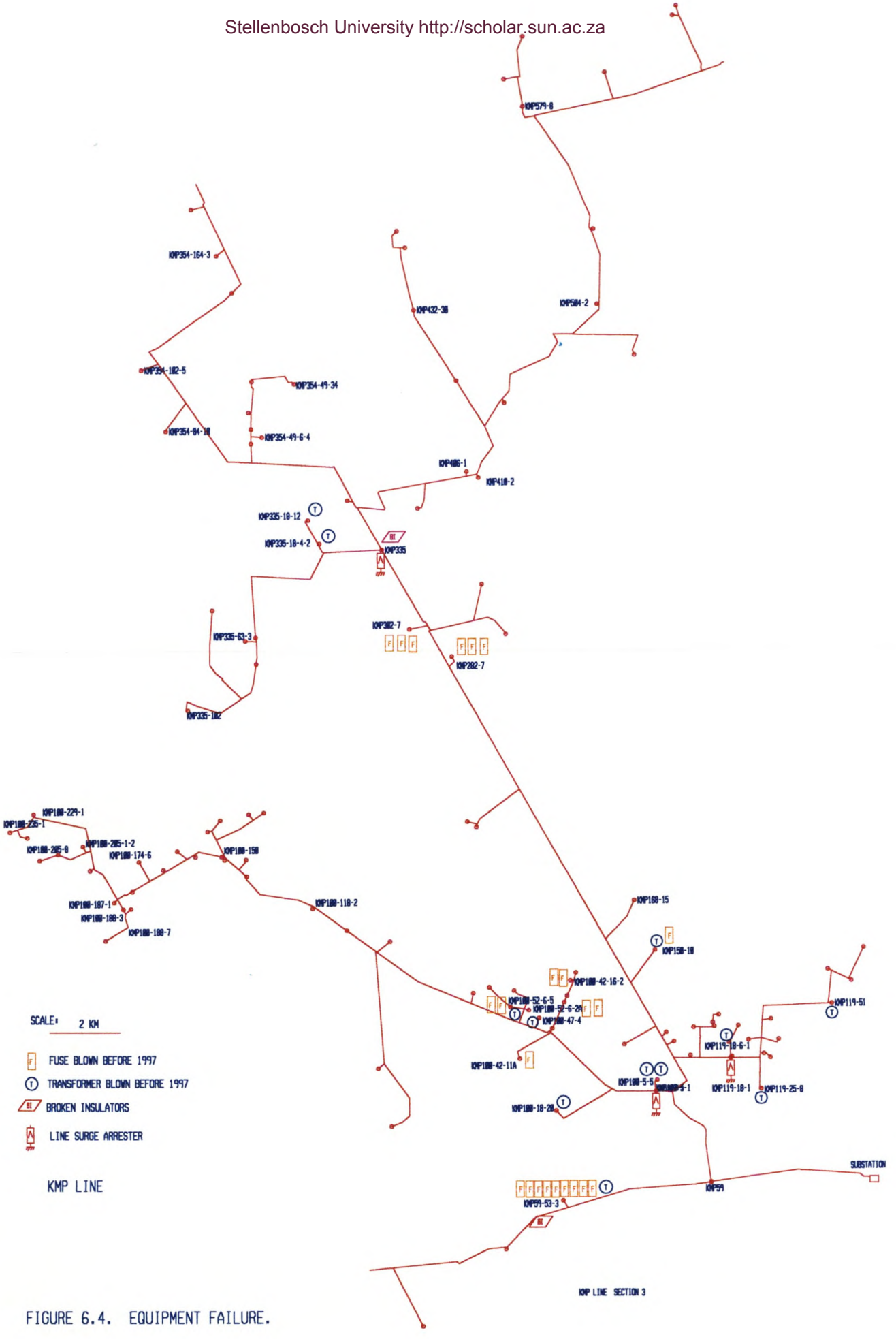

FIGURE 6.4. EQUIPMENT FAILURE.

Stellenbosch University http://scholar.sun.ac.za

line surge arrester must be installed on the pole that is regularly hit by lightning to be effective. It is therefore necessary to get more detail of broken insulators as well as split cross arms and poles. Reporting and or performance logging on this damaged equipment are normally bad and in most cases, a practical investigation in the poorly performing area is necessary.

6.2. Installation of bushing-mounted fuses.

In some cases only one pole-mounted installation has a very high fuse failure rate with no other equipment failure in the same area. Such a case is shown in figure 6.6 where 9 fuses as well as a transformer failed within a year. It was found that pole-mounted installations with excellent earthing (below 5 ohms) tend to lead to nuisance fuse operations if lightning hits the line in close vicinity of the low earth resistance pole. In this case as well as problem pole-mounted installations that is very difficult to reach, bushing-mounted fuses can be installed. The lightning surge is then diverted through the surge arrester to ground before it reaches the fuses.

6.3. The field visit.

A field visit is necessary to visit all the problem installations, checking whether the installation and earthing is up to standard. The line must then be patrolled to look for broken insulators, split poles or any damage caused by lightning. It is also important to verify that insulators are not broken due to vandalism. All the split poles and cross arms as well as new cross arms (that were replaced) must be noted as well. In most cases the field staff has more information on the damaged equipment. The information from the field visit is then used to update the geographical network diagram.

During the field visit, the staff that will assist with the installation of the line surge arresters must be trained how to do the earthing and what the purpose of the line arresters is. It was found that if the field staff knows why new equipment is necessary and what performance improvement is expected, the feedback and reporting improves significantly.

6.4. The necessary documentation.

After the field visit, the geographical network diagram must be finally updated. Places where lightning damage was found on the line, are identified as the points where line surge arresters get installed. In cases where no lightning damage was found, one of two decisions can be made:

a) Where a large number of items of equipment failed due to lightning, a line arrester can be installed in the middle of the poorly performing area. According to the studies done in chapter 5, at least half the equipment will be protected by the line arresters. Figure 6.7 illustrate the principal.

b) In cases where only fuses are lost and it is tolerable for the customers and field staff, no line arresters can be installed (the "do nothing" option) in order not to waste money.

Stellenbosch University http://scholar.sun.ac.za

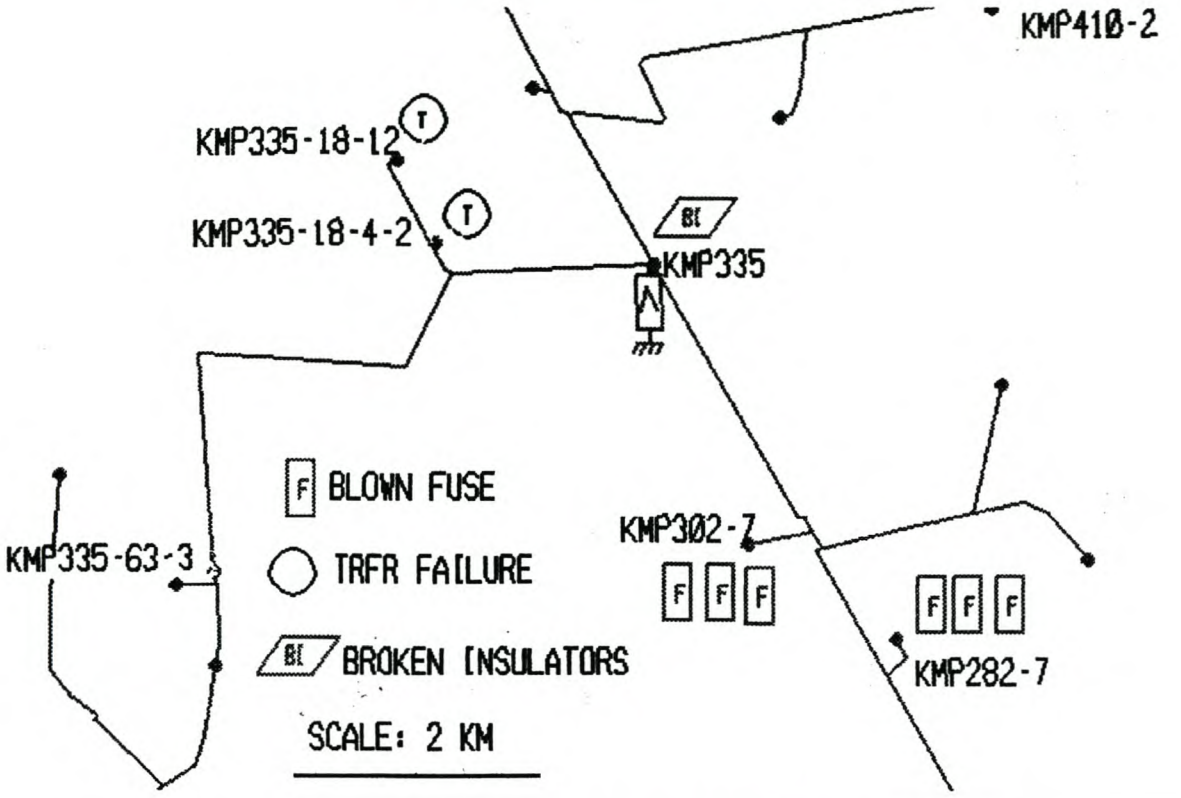

Figure 6.5. A section of the KMP line with a poorly lightning performance.

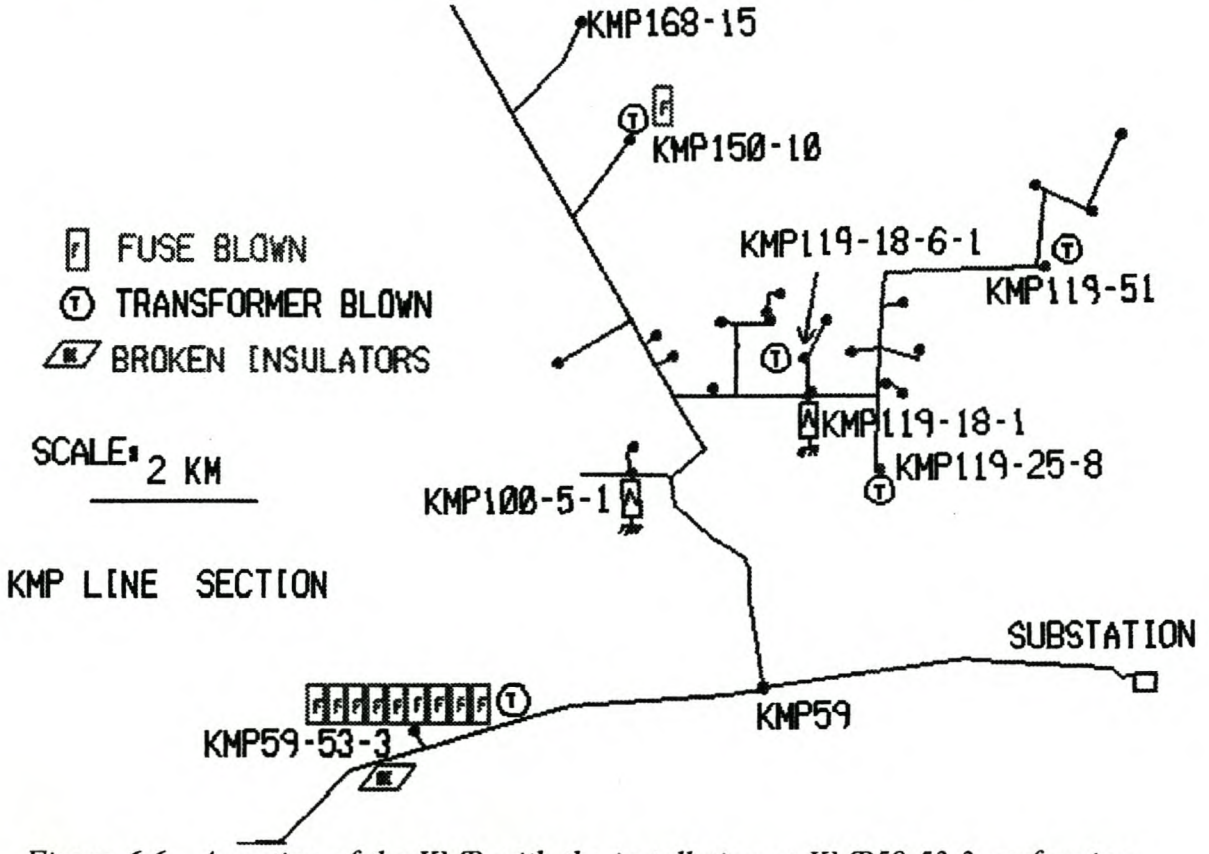

Figure 6.6. A section of the KMP with the installation at KMP59-53-3 performing poorly during lightning activity.

Stellenbosch University http://scholar.sun.ac.za

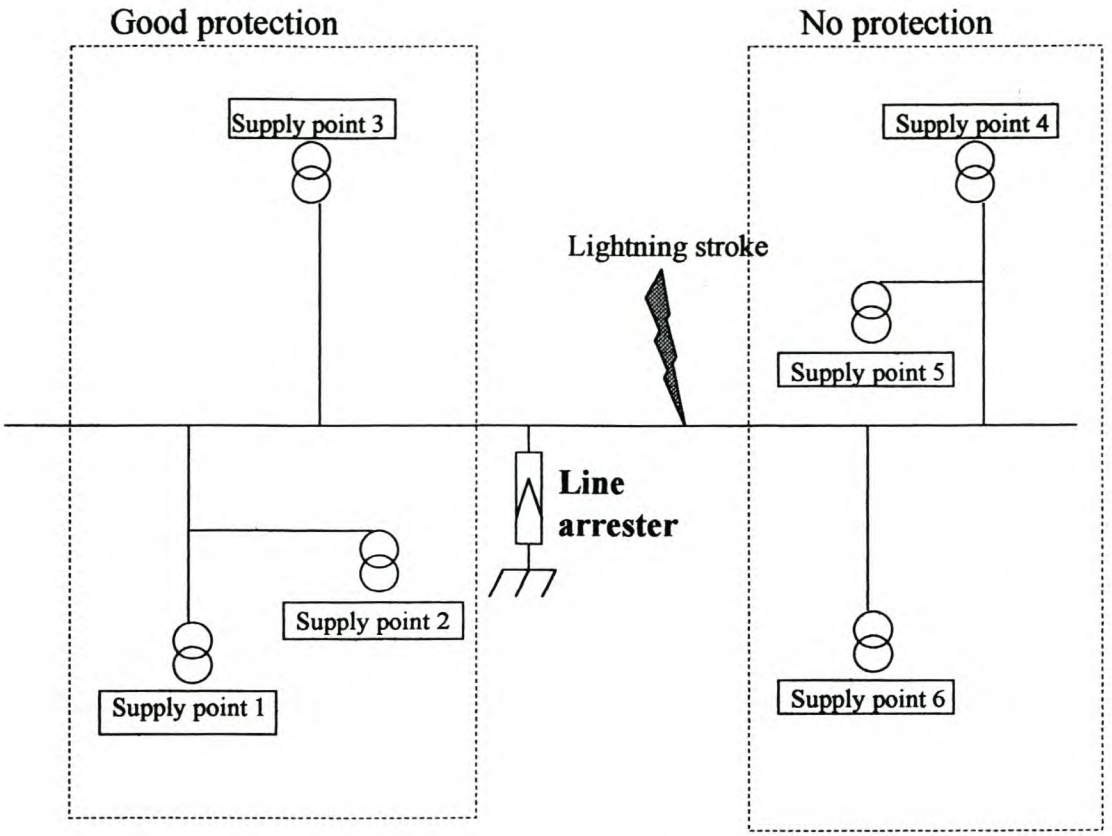

Figure 6.7. If the line arrester is not installed at the point where the lightning strike the line, at least supply points 1, 2, and 3 are well protected. Supply points 4, 5 and 6 will not be protected against the lightning stroke.

After a list of material necessary as well as the labour and transport cost for the project has been made, a financial evaluation must be made to see whether the project is viable. A project proposal needs to be presented to the Technical evaluation and Capital investment committees for authorization. If authorized, the equipment can be ordered.

As the installation of line surge arresters is an unusual project, technical assistance must be given to Project management. Some site visits are also necessary during installation to make sure that the contractor does the installation correctly.

6.5. Performance monitoring after installation

Special attention was given to the fault reports in the area of concern after the line surge arrester projects were commissioned. In order to ensure that all faults are reported and logged in the area of concern, field visits were done once a month. A general view of the field staff on the line performance improvement was also asked.

Stellenbosch University http://scholar.sun.ac.za

6.6. Conclusion

A Geographical diagram (or an electrical diagram) of the feeder need to be updated with all the lightning related equipment failures. The high failure rate areas on the feeder need then to be identified. Poles with signs of lightning damage (broken insulators, burnt-off jumpers and polesplitting) need to be identified during a line inspection in the problem areas. The electrical and earthing configuration at installations where equipment failed must be checked and rectified if necessary during the project.

Line surge arresters must be installed at the points where lightning damage is visible. Bushing-mounted fuses should be install at installations that is remote (more than 5 km) from the nearest problem area.

Stellenbosch University http://scholar.sun.ac.za

7. RESULTS

The failure rate of the equipment in the problem area as well as the line surge arresters were closely monitored. An electrical and financial evaluation was done on the project for the year after installation based on the equipment failure rate before and after installation of line arresters.

7.1 Practical results.

After the line surge arresters were commissioned, a radius of 5 km (along the line) around the point of line arrester installation were monitored for any lightning related failures. Table 7.1 was then updated with the equipment performance after the project was commissioned.

Twenty-seven 3 phase surge arresters were installed on 4 different 22 kV lines to ensure a reliable practical result. The line performance before and after installation of line surge arresters was compared. The distance to the most remote problem point from the line surge arrester in the problem area is also shown in table 7.1. A significant improvement was found. The fact that equipment was "protected" several kilometers away from the line surge arresters can be very misleading. The protection was actually due to the fact that the line arrester was installed on the exact pole where the lightning normally hit the line. It was found that, in most cases, lightning tends to regularly strike a specific pole.

Table 7.1 shows that only two out of the previously 76 transformers failed during lightning. Line 3 in table 7.1 shows that one transformer failed afterwards. On investigation it was found that the line arrester at pole KMP100/5/1 was mechanically damaged by a ladder and was lying on the ground. This was most probably why the transformer at pole KMP100/5/5 failed.

Thirteen pole-mounted transformers were fitted with bushing mounted fuses as shown in figure 7.1. At some places the fuses kept blowing (lines 9 and 10 in table 7.1). After investigation, it was found that the fuses operated correctly. The transformers were faulty and due to the low rating of the bushing-mounted fuses, the transformers did not show any physical damage. After the fuses were replaced for the second time, it was only found that the transformer had a high impedance internal fault.

In some cases where bushing-mounted fuses were installed, the transformer failures also stopped. This is not due to the fuse protecting the transformer better, but just because the earthing at the pole-mounted installation was rectified when the fuses were fitted (see lines 4, 12, 14, 23, 37 in table 7.1). The transformer in line 37 had an intermittent bushing fault.

7.2. Financial analysis.

Two different options of lightning protection were investigated. One was to fit each problem point of supply transformer with a bushing-mounted fuse, which was then within the protection zone of the surge arrester. A second option was to "group" the problem points and protects the group by a single set of three phase line surge arresters (dropout type). Figure 7.1 shows the comparison.

Stellenbosch University http://scholar.sun.ac.za

No	Equipment position (pole number)		Equipment blown/damaged				Distance to
	Line Surge Arrester	Bushing mount fuse	Fuses		Transformers		farest point
			before	after	before	after	[km]
1	KMP335		6	0	3	0	4.2
2	KMP119/18/1		1	0	4	0	5.4
3	KMP100-5-1		7	0	5	1	5.3
4		KMP59-53-3	9	0	1	0	0
5	**Total KMP line**		**23**	**0**	**13**	**1**	
6	LG194/351		2	0	1	0	3.5
7	LG171/83/74		4	0	3	0	4
8	LG171/83/1	LG171-83-31 *	12	0	4	0	3.4
9	LG194/262/19		12	2	5	0	2.2
10	LG194/84		5	2	4	1	2.7
11	LG305/1		6	0	4	0	3.9
12		LG508-2	3	0	1	0	0
13		LG533-37-3	3	0	0	0	0
14		LG194-316	2	0	1	0	0
15		LG390-35	4	0	0	0	0
16		LG390-6-3	2	0	0	0	0
17	**Total LG line**		**55**	**4**	**23**	**1**	
18	LMD129		0	1	3	0	2.2
19	LMD146/11		9	0	3	0	3.9
20	LMD184/201		3	0	3	0	0.8
21	LMD291/42/62/17	LMD291-42-62-60 **	2	0	4	0	3.9
22		LMD165-22	7	0	0	0	0
23		LMD223-29-1	7	0	1	0	0
24		LMD46-292-5	2	0	0	0	0
24		LMD46-349-26	2	0	0	0	0
26	**Total LMD line**		**32**	**1**	**14**	**0**	
27	MAS182		1	0	3	0	4.4
28	MAS381/55		1	0	3	0	1.6
29	MAS381/76	MAS381-73-4 ***	4	0	3	0	5
30	MAS475/14/15		4	1	2	0	8.4
31	MAS475/139		3	0	4	0	5.1
32	MAS475/221		5	0	4	0	5
33	MAS550		1	0	5	0	4.9
34	MAS478/40		4	0	3	0	1.8
35	MAS478/22/72		1	0	3	0	3.4
36	MAS192/213/31		1	0	4	0	2.6
37		MAS265-4	6	6	2	0	0
38	**Total MAS line**		**31**	**7**	**36**	**0**	
39	**Grand total**		**141**	**12**	**86**	**2**	

*3 of the 12 fuses have blown at LG171-83-31
**Both the fuses have blown at LMD291-42-62-60
***All 4 of the fuses blew at LMD381-73-4

Table 7.1. Annual equipment failures before and after the installation of line surge arresters.

If only bushing-mounted fuses are installed (at the problem points), it will also result in a significant lightning performance improvement, but it will cost more than installing it in combination with line surge arresters. On the other hand, if only line surge arresters are installed to protect all the problem points, the return on investment (ROI) will be higher than the bushing-mounted fuse option. The best option will be a combination of the two options. Problem points close to each other can be protected

Stellenbosch University http://scholar.sun.ac.za

with line surge arresters and remote problem points can be fitted with bushing-mounted fuses.

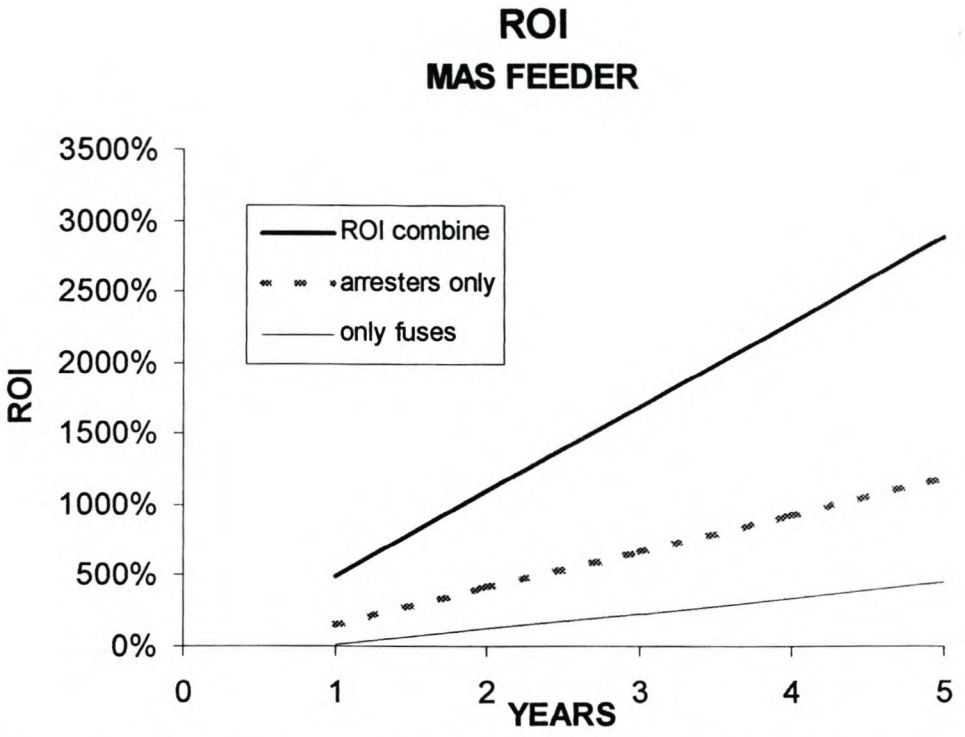

Figure 7.1. ROI comparison between installing line surge arresters, bushing-mounted fuses and a combination of the two options on the MAS feeder.

As long as the problem installations, which were grouped together as a problem area, are in close proximity, the line surge arrester option works nearly as well as the bushing-mounted fuse option. The success of this option depends on the reliability of the assumption that lightning strikes regularly at the same pole. Further work is required to identify these preferred points more accurately. Installing line surge arresters is also more difficult, as correct earthing must be done as well.

The ROI of all 4 the feeders are shown in figure 7.2. The KMP line project had the best ROI (figure 7.2). Within a year, 5 times more money was saved (on equipment, transport and overtime) than was spent on the project.

More financial detail can be found in Appendix C.

Stellenbosch University http://scholar.sun.ac.za

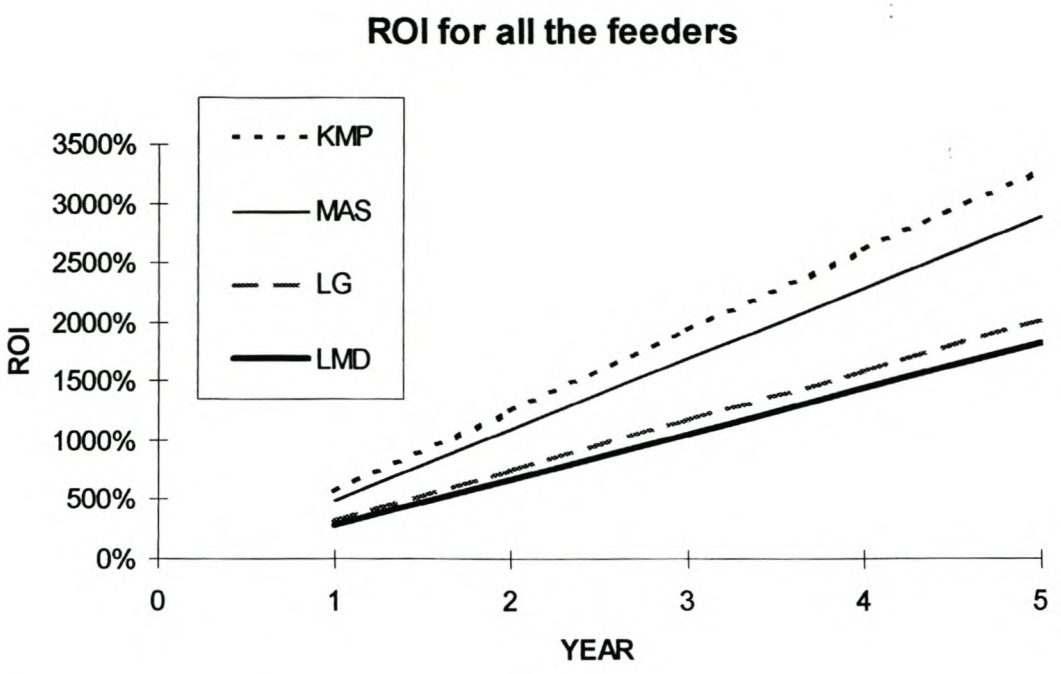

Figure 7.2. The ROI for installing line arresters and bushing-mounted fuses on each of the four feeders.

7.3. Conclusion

The results achieved in table 7.1 proved that line surge arresters installed strategically on the line, reduce the surge stresses on the polemount installations to such an extent that equipment stop failing. This does not only save Eskom time and money, but also reduce the stress level on employees (staff working in the field, call centre, control centre and work management centre).

Although the LMD feeder performed financially the worst, the annual savings due to the LMD project was 250% more than the once off cost of the LMD project. This proved that the project is not only technically a success, but is also an excellent financial investment (savings due to less equipment failures, transport and overtime).

Stellenbosch University http://scholar.sun.ac.za

8. CONCLUSIONS

8.1 Installing line surge arresters.

Installing line surge arresters is not a new concept and has been done worldwide. The objective is usually to improve line performance by preventing flashovers due to lightning. When the line's BIL is low, many line surge arresters have to be installed to achieve some success and to limit flashovers and therefore line trips.

The objective of this study was mainly to create an additional low impedance circuit to earth for the lightning surge energy. A secondary objective was to limit the flashover occurrence due to lightning. Only the first objective was measured and showed a big improvement on equipment failures, compared to the time before line arresters were installed. The success depended on the accurate placement of the line arrester. A detail line inspection was necessary to find the actual places where the lines were struck by lightning. This was done with success.

It was found that the lightning has some preferred locations or poles of striking the line. The investigation depended very much on this finding. In order to ensure that the lightning density did not vary from year to year, the actual lightning density was measured for the area over a four-year period. The LPATS findings as well as feedback from field staff confirm that the lightning density stayed the same. Some other problem points that were not part of the investigation continued to perform badly.

As discussed in paragraph 5.6, the main objective is to get rid of the surge on the line. From a theoretical investigation it would appear as is not necessary to install line surge arresters, as the surge arresters on the pole-mounted installations should be adequate. However, in practice it was found that this is not the case and the same supply points kept on failing. Although the failures could be linked to lightning, it can be that some of the equipment that failed were in a bad condition due to aging or previous surges and just needed a small surge to give enough stress for final failure.

The financial investment does look good. The return on investment is more than a 1000% over a five year period. Three years after the project was commissioned, no arrester failed and are still in good order.

8.2. Installing bushing-mounted fuses.

In the standard configuration as shown in figure 1.3, the lightning surge current flows through the fuse and is dissipated in the surge arrester. It was therefore necessary to give some lightning protection to the fuse. The option that was chosen was to place the fuse between the transformer and the surge arrester, thereby diverting the surge to earth before reaching the fuse. A bushing-mounted fuse as shown in figure 1.5 was developed for this purpose.

A second possible reason for fuse failure as discussed in paragraph 5.6, is transformer saturation due to power frequency offset caused by a long surge tail. This could possibly cause even the bushing-mounted fuse to fail. However, the fuse failure rate dropped drastically as shown in table 7.1. The difference between the standard fuse

Stellenbosch University http://scholar.sun.ac.za

and the bushing-mounted fuse is that all mechanical stress was taken off the fuse element of the bushing-mounted fuse where a tremendous mechanical stress is put on the standard fuse's element (to ensure the dropout action). Secondly, the fuse element of the bushing-mounted fuse is much shorter than those of the standard fuse. However, in cases where transformer failures occurred, the bushing-mounted fuse operated perfectly.

It was also found that those pole-mounted installations with excellent earthing (below 5 ohms) tends to give more nuisance fuse failures as well as surge arrester failures. This implies that these installations are a low impedance path to earth for the lightning surge, which also explain the fuse failures. KMP59/53/3 in figure 6.6 is a case where the lightning use to strike 3 poles from the installation causing on average 9 fuse failures annually.

Although a practical solution that seems to work well was found, the exact theoretical fuse failure reasons still need some clarification.

Stellenbosch University http://scholar.sun.ac.za

9. ATTACHMENTS

Appendix A

The probability of a lightning stroke terminating on a distribution line.

In this thesis only unshielded distribution lines are considered when determining the probability of a stroke terminating on the line. The only possible shielding for the line is the surrounding environment. In this case the environment consist mostly of small bushes and grass which is much lower than the conductors.

As the experimental line has a BIL of 350 kV, an indirect stroke will not cause a flashover as discussed in section 3.1.7. A flashover is caused when a stroke terminates on the line and the injected current I is big enough to cause a surge voltage V which has a higher amplitude than the BIL. For a line with impulse impedance Z = 482 Ω, the minimum current required for a flashover is:

$$I = \frac{2V}{Z} \qquad \text{(A1)}$$

$$= \frac{2 \times 350000}{482}$$

$$= 1452 \text{ A}$$

The approaching lightning leader must come into the striking distance of the line and must be successfully intercepted by an upward-connecting leader from the line before the return stroke will terminate on the line [1]. The interception depends upon the relative positions of the two leaders and their relative velocities of approach [3]. The relation between the striking distance (D) and the return stroke current (I) is [2]:

$$D = kI^n \qquad \text{(A2)}$$

where k and n are constants determined by empirical calibration. Whitehead used values of 8 and 0.65 for k and n respectively [5].

Eriksson developed an analytical model which showed that the point of stroke termination is determined by the progression of the downward leader to within the striking distance of the line as well as the continued approach of the downward leader to within the a capture radius of the line where the two leaders intercept [4]. Figure A1 shows a schematic representation of the leader progression model. He also showed that the expressions for the striking distance and attractive radius varied with structure height and that they are not only functions of the stroke current [1].

Stellenbosch University http://scholar.sun.ac.za

A study on the attractive effects of structures up to 500 m and for stroke current up to 200 kA, produced a generalised expression for the attractive radius R [1]:

$$R = I^{0.64} H^{(0.66+2I\times10^{-4})} \qquad \text{(A3)}$$

where H is the structure height in m and I is the stroke current in kA. Standard atmospheric conditions are assumed and the criterion for the initiation of the upward leader is taken as the attainment of critical electric field strength of 30 kV/cm [4].

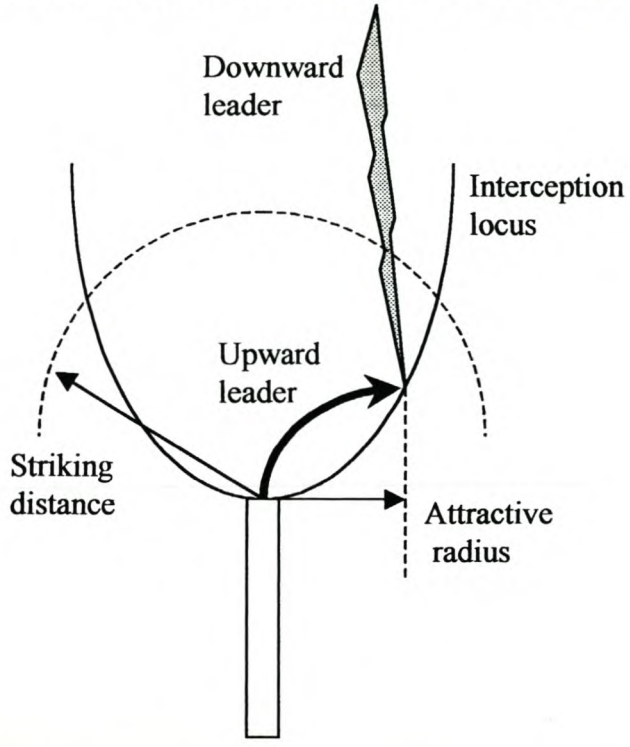

Figure A1. Downward leader intercepted by an upward connecting leader within the attractive radius of the structure [4].

Due to the difference in electric field configuration on horizontal cylindrical geometry involved in the line spans and the rod-plane geometry of a structure, equation A3 must be modified to [3]:

$$R = 0.67 \times I^{0.74} H^{0.6} \qquad \text{(A4)}$$

After general consideration of structure attractiveness and the incidence of lightning strikes to power lines, Eriksson rewrite A4 as [4]:

$$R = 14 H^{0.6} \qquad \text{(A5)}$$

The number of lightning strikes N_s to a line may be estimated from [6]

Stellenbosch University http://scholar.sun.ac.za

$$N_s = N_g(2R + w)L \times 10^{-3} \text{ per km/year} \quad \text{(A6)}$$

where N_g = lightning density in flashes per year per km^2, w = width of the line and L = length of the line in km.

Substituting A5 into A6:

$$N_s = N_g(28H^{0.6} + w)L \times 10^{-3} \quad \text{(A7)}$$

In the case where the line runs through a forest or a high object is close to the line, the number of flashovers on the line due to direct strokes decrease significantly. For example, consider that a fence runs parallel with a single phase line and on the other side of the line is an avenue of trees over a distance of 500 m as shown in figure A2.

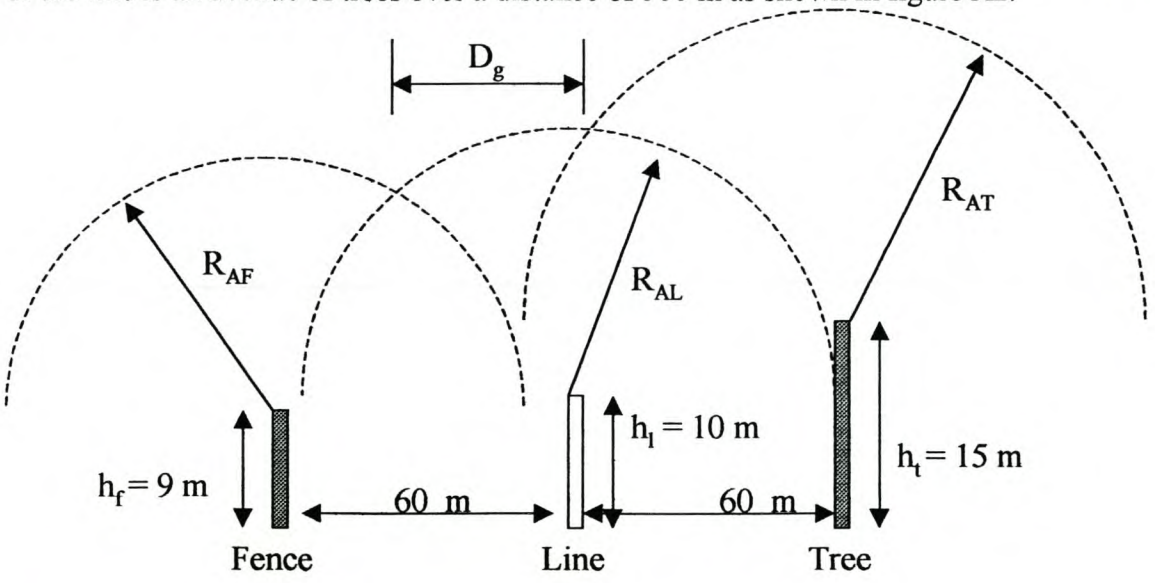

Figure A2. A line running between a fence and a avenue of trees.

Using eq. A5, the attractive radii for the fence (R_{AF}), line (R_{AL}), and tree (R_{AT}) are 52.3 m, 55.7 m and 71.1 m respectively. Geometrical calculations shows that the unprotected distance, D_g = 43.0 m. Using eq. A6:

$$N_s = N_g(2R + w)L \times 10^{-3}$$
$$= N_g(D_g)L \times 10^{-3}$$
$$= 4(43 + 0) \times 0.5 \times 10^{-3}$$
$$= 0.086 \text{ direct strikes per 500 m per year if } N_g \text{ is taken as 4.}$$

If there are no objects close to the line for the next 500 m, the number of direct strikes to that section of line will be:

Stellenbosch University http://scholar.sun.ac.za

$$N_s = N_g(2R + w)L \times 10^{-3}$$

$$= 4(2\times55.7 + 0)\times0.5\times10^{-3}$$

$$= 0.223$$

The section of line with no environment protection will therefore be hit by lightning 2.60 times more often than the section with the trees and fence along the line as shown in figure A2.

In practice it was found that all of the poles and insulators that were damaged by direct lightning strokes, were at sites where there are no or little environmental protection. These sites include high ground, fallow lands, hill tops and are in many cases adjacent to roads. None of the line arresters is close to houses because in most cases there are high trees and fences around the farm houses.

References

1. A.J. Eriksson, The lightning ground flash – an engineering study, Ph.D. University of Natal, CSIR special report, ELEK 189, Pretoria, Dec 1979.
2. F.S. Young, J.M. Clayton, A.R. Hileman, Shielding of transmission lines, AIEE Trans, PAS, Special Supp., Paper no. 63-640, 1963.
3. L. Dellera, A. Pigini, L. Thione, E. Garbagnati, W. Seravelli, Some aspects of the evaluation of the lightning performance of electrical systems, CIGRE paper 33-13, Paris, August 1980.
4. A.J. Eriksson, An improved electrogeometric model for transmission line shielding analysis, IEEE Transactions on Power Delivery, Vol. PWRD-2, no. 3, July 1987, p. 871 – 886.
5. E.R. Whitehead, H.R. Armstrong, Field and analytical studies of transmission line shielding, IEEE Trans., PAS 87, 1961, p 270 – 281.
6. A.J. Eriksson, The incidents of lightning strikes to power lines, Proc SAIEE, Symposium on lightning performance of overhead lines, Pretoria, Feb 1982.

Stellenbosch University http://scholar.sun.ac.za

Appendix B

The JMarti model

Models, which assume constant parameters, cannot accurately simulate the response of the line over the wide range of frequencies that are present in transients. The parameters of lines with ground return are highly dependent on the frequency. Mathematical solutions of the frequency-dependent line equations in the time domain are difficult and numerical approximation techniques are required for practical solutions.

JMarti used methods to overcome or avoid a series of numerical difficulties encountered in previous formulations. The methods are accurate with no stability problems in the frequency range between 0 Hz and 1 MHz [1].

Two important parameters for wave propagation are the characteristic impedance Z_c and the propagation constant γ [3]:

$$Z_c = \sqrt{\frac{R'+j\omega L'}{G'+j\omega C'}} \tag{B1}$$

$$\gamma = \sqrt{(R'+j\omega L')(G'+j\omega C')} \tag{B2}$$

where R' = series resistance, L' = series inductance, G' = shunt conductance and C' = shunt capacitance.

The JMarti model is based on Meyer and Dommel's line model as shown in figure B1 [1]. They defined two nodes, m and k, on each end of a line and a forward travelling function at node k, $f_k(t)$ *as:*

$$f_k(t) = V_k(t) + R_1 i_k(t) \tag{B3}$$

The backward travelling function at node k is given as:

$$b_k(t) = V_k(t) - R_1 i_k(t) \tag{B4}$$

where V_k and I_k is the voltage and current at node k respectively. R_1 is a real constant defined as $R_1 = \lim_{\omega \to \infty} Z_c(\omega)$.

Two weighting factors, $a_1(t)$ and $a_2(t)$, which are related to the voltages at nodes m and k respectively, were also defined. The backward travelling function b_k is obtained by the weighted past history of the currents and voltages at both ends of the line and is given by the convolution integral [1]:

Stellenbosch University http://scholar.sun.ac.za

$$b_k(t) = \int_0^{\infty} [f_m(t-u)a_1(u) + f_k(t-u)a_2(u)]du \qquad \text{(B5)}$$

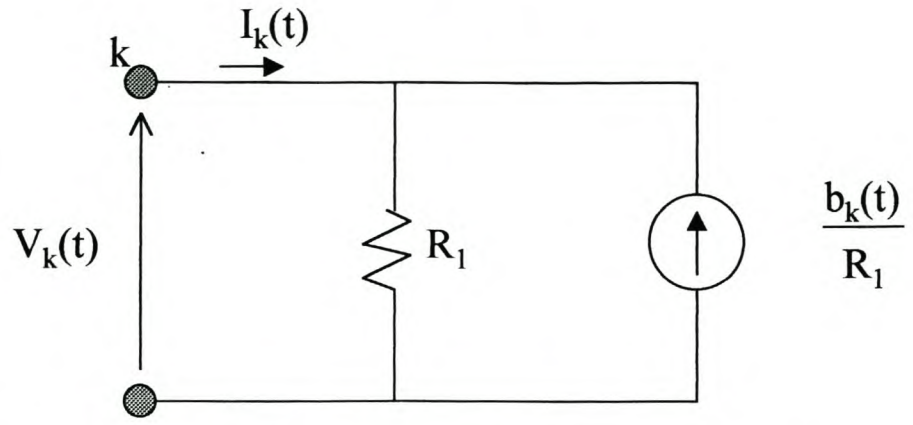

Figure B1. Meyer and Dommel's frequency-dependent line model at node k [1].

JMarti then replaced R_1 by an equivalent network Z_{eq} whose frequency response is the same as the characteristic impedance Z_c of the line. There will then be no reflections at either end of the line and $a_2(t)$ become zero while $a_1(t)$ become more simplified. This overcomes the difficult evaluation of the tail portions of the weighting factors and the accuracy problems at low frequencies.

To represent the line in the EMTP, it is necessary to convert the line parameters into a weighting function and into a R-C network (approximates Z_c) [2]. The network Z_{eq} representing the line characteristics impedance $Z_c(\omega)$ is simulated by a series of Resistance-Capacitance parallel blocks as shown in figure B2. The number of R-C blocks is determined automatically by the approximating subroutine. A subroutine named Line Constants is used to calculate Z_c and γ.

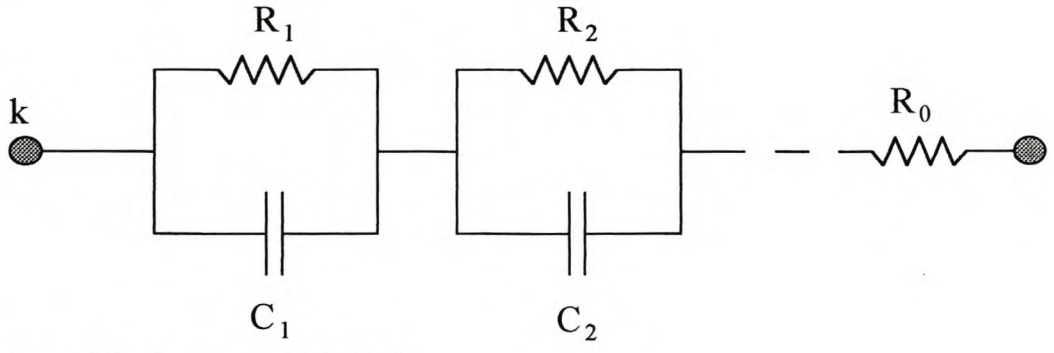

Figure B2. Realization of $Z_c(\omega)$.

Z_c is approximated by a rational function of the form [2]:

Stellenbosch University http://scholar.sun.ac.za

$$Z_c(s) = k_0 \times \frac{(s+z_1)(s+z_2)...(s+z_n)}{(s+p_1)(s+p_2)...(s+p_n)} \tag{B6}$$

where s = jω. All the poles of the function are real, positive and simple. This can be expanded into a series of simple fractions:

$$Z_c(s) = k_0 + \frac{k_1}{s+p_1} + \frac{k_2}{s+p_2} + ... + \frac{k_n}{s+p_n} \tag{B7}$$

from where in figure B2:

$R_0 = k_0$

$$R_i = \frac{k_i}{p_i}$$

$$C_i = \frac{1}{k_i}$$

for i = 1, 2, 3, ... , n

For each R-C block:

$$i = \frac{v_i}{R_i} + C_i \frac{dv_i}{dt} \tag{B8}$$

which have the exact solution:

$$v_i(t) = e^{-\alpha_i \Delta t} \times v_i(t-\Delta t) + \frac{1}{C_i} \int_{t-\Delta t}^{t} e^{-\alpha_i (t-u)} i(u) du \tag{B9}$$

with $\alpha_i = \frac{1}{R_i C_i}$

By using linear interpolation on i, the solution can be written in the format:

$$v_i(t) = R_{equiv-i} \times i(t) + e_i(t-\Delta t) \tag{B10}$$

The impedance R_{equiv} accross all the R-C blocks is the sum of $R_{equiv0.....n}$ where n is the number of blocks. Eq. B10 can then be rewritten as:

$$i(t) = \frac{1}{R_{equiv}} v(t) + hist_{RC} \tag{B11}$$

Stellenbosch University http://scholar.sun.ac.za

In the solution for the entire network with eq. B12, the line (frequency-dependent) is represented by a constant resistance R_{equiv} to ground in parallel with a current source $hist_{RC} + hist_{propagation}$ as shown in figure B3.

$$[G][v(t)] = [i(t)] - [hist] \qquad (B12)$$

where [G] = n×n symmetric nodal conductance matrix
[v(t)] = vector of n node voltages
[i(t)] = vector of n current sources
[hist] = vector of known history terms

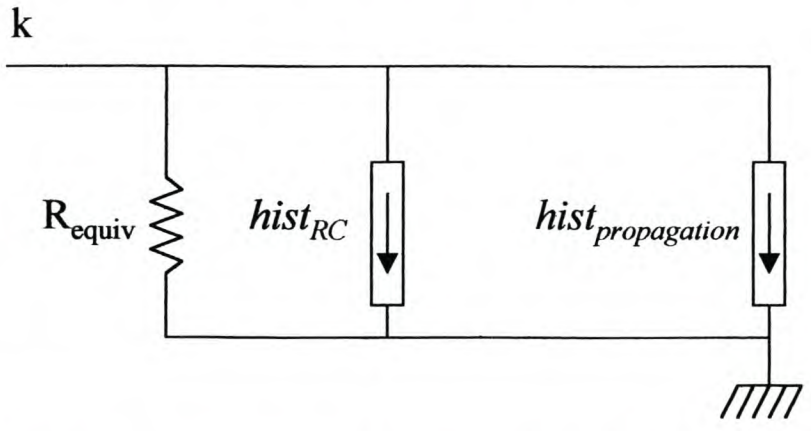

Figure B3. Frequency dependent line reprensentation seen from node k [2].

Jmarti approximates $Z_c(\omega)$ and $A(\omega)$ with Bode's procedure [4]. The basic principal is to approximate the given curve by straight-line segments, which are only asymptotic traces and the actual function becomes a smooth curve without sharp corners.

The magnitude and phase error in the propagation factor is less than 2% and 4% respectively while the error for Z_c is 2% or less for both the magnitude and phase [2]. Care must be taken to ensure that that the time step Δt is small enough.

References

1. J.R. Marti, Accurate modelling of frequency-dependant transmission lines in electromagnetic transient simulations, IEEE Transactions on Power Apparatus and Systems, Vol. PAS-101, No. 1, Jan 1982, p. 147-157.
2. W. Scott Meyer, Tsu-huei Liu, BPA EMTP Theory Book in WP 5.1, July 1995, p. 4-1 - 86.
3. W.H. Hayt Jr., Engineering electromagnetics, Third edition, McGraw-Hill Kogakusha, p 382.
4. J.R. Marti, The problem of frequency dependence in transmission line modeling, Ph. D thesis, The University of British Columbia, Vancouver, Canada, April 1981.

Stellenbosch University http://scholar.sun.ac.za

Appendix C

Financial background and detail

Klerksdorp-Wes **Fuse** incidents :

COSTS

Manhours (overtime) :	(1 x B-upper)	3	hours @	44.76	R/hour =	R 152.89
	and	42	% of incidents are after hours.			
Cost of fuse element :		9	Rand			
Vehicle cost (4x4):		1.33	R/km.			
parts and accesories :		5	rand per incident.			

Klerksdorp-Wes **Transformer** incidents.

COSTS

Manhours	(2 x B-Upper)	4	hours @	44.76	R/hour = R 358.08
	(1 x B- Lower)	4	hours @	34.845	R/hour = R 139.38
	(3 x A band)	4	hours @	27.135	R/hour = R 325.62
Cost of a 50 kVA,11kV trfr. :		5427	rand.		
Vehcile cost:	4X4	1.33	R/km.		
	8 ton crane truck	3.16	R/km.		
			total:	4.49	R/km.
Parts and accessories		15	rand per incident.		

FEEDERS

	Average distance from depot to place of incident [km]	Amount of transformer incidents/YEAR	Transformer Total cost [Rand]	Amount of fuse Incidents/yr	Fuse Total cost [Rand]	Feeder Total cost [Rand](annual)
FAILURES OVER ONE YEAR PERIOD BEFORE INSTALLATION OF LINE SURGE ARRESTERS AND BUSHING MOUNT FUSE						
KMP	105	13	93,703.74	23	10,262.40	103,966.14
MAS	103	36	258,840.72	31	13,667.01	272,507.73
LG	35	23	151,325.74	55	14,299.52	165,625.26
LMD	25	14	90,854.12	32	7,468.52	98,322.64
FAILURES OVER ONE YEAR PERIOD AFTER INSTALLATION OF LINE SURGE ARRESTERS AND BUSHING MOUNT FUSE						
KMP		1	7207.98	0	0.00	7,207.98
MAS		0	0	7	3,086.10	3,086.10
LG		1	6579.38	4	1,039.96	7,619.34
LMD		0	0	1	233.39	233.39

Stellenbosch University http://scholar.sun.ac.za

Financial detail on the Mooiplaas feeder:

Nett present value (NPV) in this context means the present value of a project taking into account the initial implementation cost as well as the annual savings for the next 5 years as a result of the project. It can be formulated as:

$$NPV = \sum_{j=1}^{5} \frac{P_j}{(1+r)^j} - I$$

Where P = annual savings, I = initial investment and r = the inflation rate.

The return on investment (ROI) is given as:

$$ROI = \frac{NPV + I}{I}$$

Stellenbosch University http://scholar.sun.ac.za

Mooiplaas (KMP)Feeder

PRESENT COST	R	**102,191.64**
FUTURE COST	R	7,071.48
SAVINGS	R	**95,120.16**
INFLATION RATE		8.00
INITIAL INVESTMENT	R	**14,054.45**

YEAR	CASH FLOW	NPV	ROI
0	-14,054.45	-14,054.45	
1	102,729.77	R 81,065.70	577%
2	110,948.15	R 176,185.86	1254%
3	119,824.00	R 271,306.02	1930%
4	129,409.92	R 366,426.18	2607%
5	139,762.72	R 461,546.33	3284%

New installations :

SURGE ARRESTORS:

How many new sets?	Labour cost: (1 set)	Material cost: (1 set)	Transport cost (1 set)	Totals:
3	R 494.00	R 2,767.00	R 268.00	R 10,587.00

DOC FUSES

How many new sets?				
1	R 89.52	R 1,227.00	R 268.00	R 1,584.52

		OVH (15%)	IDC (.0047%/month)	TOTAL
TOTAL COST	R 12,171.52	R 1,825.73	R57.21	R **14,054.45**

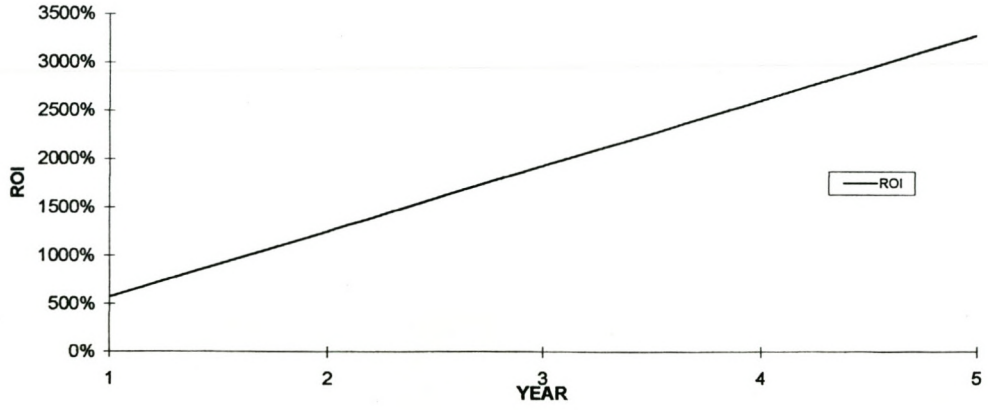

Stellenbosch University http://scholar.sun.ac.za

Financial detail on the Aandster feeder

Aandster (MAS) Feeder

PRESENT COST	R	267,687.33
FUTURE COST	R	3,086.10
SAVINGS	R	264,601.23
INFLATION RATE		8.00
INITIAL INVESTMENT	R	44,408.65

YEAR	CASH FLOW	NPV	ROI
0	-44,408.65	-44,408.65	
1	285,769.33	R 220,192.58	496%
2	308,630.87	R 484,793.80	1092%
3	333,321.34	R 749,395.03	1687%
4	359,987.05	R 1,013,996.26	2283%
5	388,786.01	R 1,278,597.49	2879%

New installations :

SURGE ARRESTORS:

How many new sets?	Labour cost: (1 set)	Material cost: (1 set)	Transport cost (1 set)	Totals:
10	R 494.00	R 2,767.00	R 268.00	R 35,290.00

DOC FUSES

How many new sets?				
2	R 89.52	R 1,227.00	R 268.00	R 3,169.04

		OVH (15%)	IDC (.0047%/month)	TOTAL
TOTAL COST	R 38,459.04	R 5,768.86	R180.76	R 44,408.65

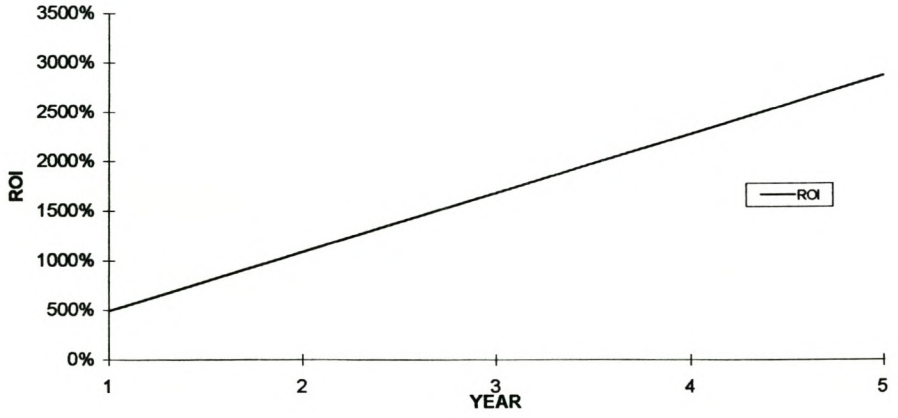

Stellenbosch University http://scholar.sun.ac.za

Financial detail on the Greylingsdrift feeder:

Greylingsdrift (LG) Feeder

PRESENT COST	R	164,578.76
FUTURE COST	R	7,573.84
SAVINGS	R	157,004.91
INFLATION RATE		8.00
INITIAL INVESTMENT	R	37,257.13

YEAR	CASH FLOW	NPV	ROI
0	-37,257.13	-37,257.13	
1	169,565.30	R 119,747.78	321%
2	183,130.53	R 276,752.69	743%
3	197,780.97	R 433,757.60	1164%
4	213,603.45	R 590,762.51	1586%
5	230,691.72	R 747,767.42	2007%

New installations :

SURGE ARRESTORS:

How many new sets?	Labour cost: (1 set)	Material cost: (1 set)	Transport cost (1 set)	Totals:
6	R 494.00	R 2,767.00	R 268.00	R 21,174.00

DOC FUSES

How many new sets?				
7	R 89.52	R 1,227.00	R 268.00	R 11,091.64

		OVH (15%)	IDC (.0047%/month)	TOTAL
TOTAL COST	R 32,265.64	R 4,839.85	R151.65	R 37,257.13

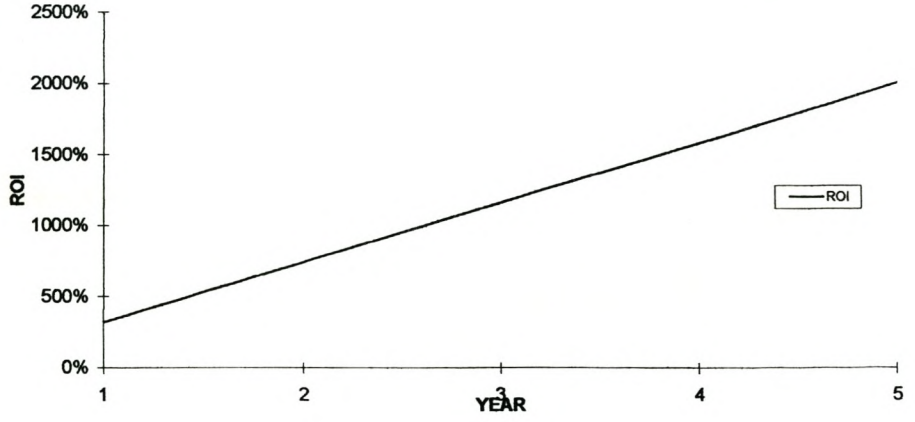

Stellenbosch University http://scholar.sun.ac.za

Financial detail on the Meitjiesdoorn feeder:

Mietjiesdoorn (LMD) Feeder

PRESENT COST	R	97,867.64
FUTURE COST	R	233.39
SAVINGS	R	97,634.25
INFLATION RATE		8.00
INITIAL INVESTMENT	R	25,447.97

YEAR	CASH FLOW	NPV	ROI
0	-25,447.97	-25,447.97	
1	105,444.99	R 72,186.28	284%
2	113,880.59	R 169,820.52	667%
3	122,991.03	R 267,454.77	1051%
4	132,830.32	R 365,089.02	1435%
5	143,456.74	R 462,723.27	1818%

New installations :

SURGE ARRESTORS:

How many new sets?	Labour cost: (1 set)	Material cost: (1 set)	Transport cost (1 set)	Totals:
4	R 494.00	R 2,767.00	R 268.00	R 14,116.00

DOC FUSES

How many new sets?				
5	R 89.52	R 1,227.00	R 268.00	R 7,922.60

		OVH (15%)	IDC (.0047%/month)	TOTAL
TOTAL COST	R 22,038.60	R 3,305.79	R103.58	R 25,447.97

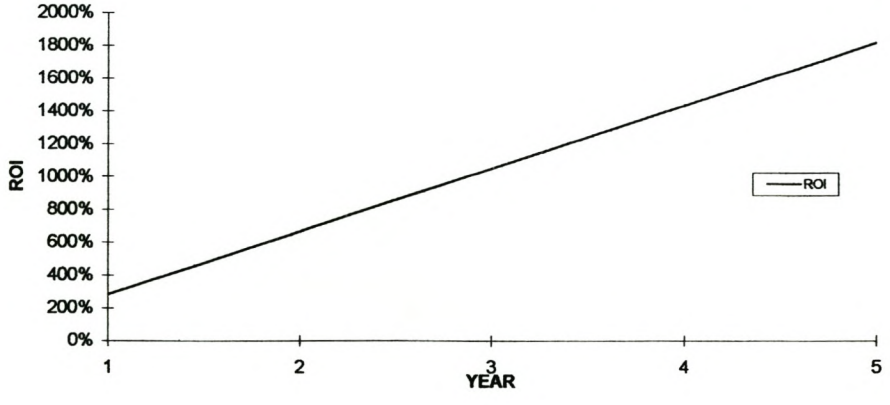

Stellenbosch University http://scholar.sun.ac.za

Financial comparison between feeders:

ROI GRAPH (ALL TOGETHER)		ROI 1	ROI 2	ROI 3	ROI 4
FEEDERS:	YEAR	KMP	MAS	LG	LMD
	0				
	1	577%	496%	321%	284%
	2	1254%	1092%	743%	667%
	3	1930%	1687%	1164%	1051%
	4	2607%	2283%	1586%	1435%
	5	3284%	2879%	2007%	1818%

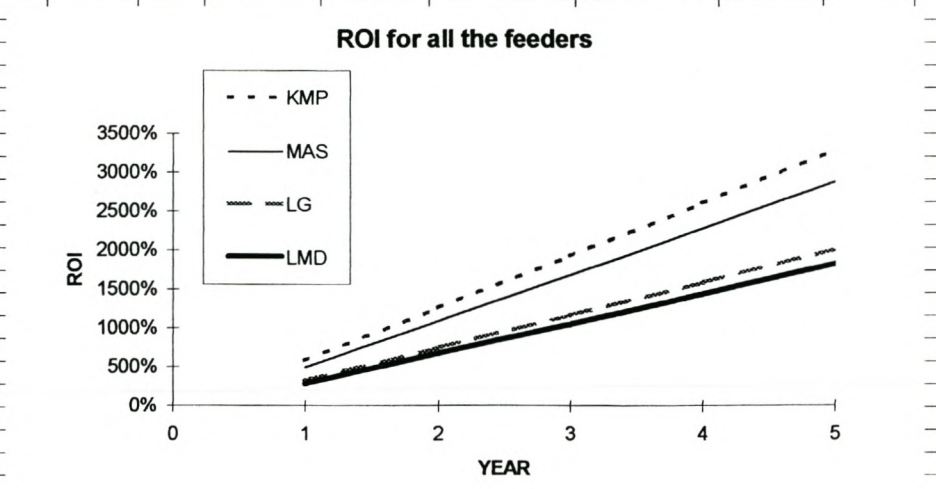

Stellenbosch University http://scholar.sun.ac.za

Financial impact if only fuses are installed:

Aandster Feeder

PRESENT COST	R	97,867.64
FUTURE COST	R	3,086.10
SAVINGS	R	94,781.54
INFLATION RATE		8.00
INITIAL INVESTMENT	R	85,993.33

YEAR	CASH FLOW	ROI	NPV
0	-85,993.33		-85,993.33
1	102,364.06	10%	R 8,788.21
2	110,553.19	120%	R 103,569.75
3	119,397.44	231%	R 198,351.29
4	128,949.24	341%	R 293,132.83
5	139,265.18	451%	R 387,914.37

New installations :

SURGE ARRESTORS:

How many new sets?	Labour cost: (1 set)	Material cost: (1 set)	Transport cost (1 set)	Totals:
0	R 494.00	R 2,767.00	R 268.00	R -

DOC FUSES

How many new sets?				
47	R 89.52	R 1,227.00	R 268.00	R 74,472.44

		OVH (15%)	IDC (.0047%/month)	TOTAL
TOTAL COST	R 74,472.44	R 11,170.87	R350.02	R 85,993.33

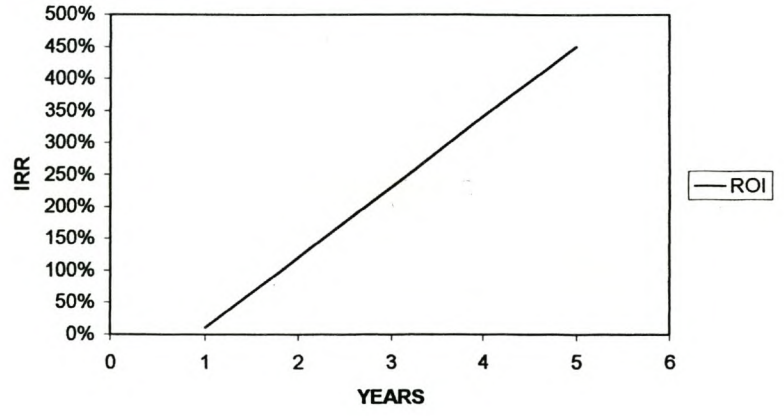

Stellenbosch University http://scholar.sun.ac.za

Financial impact if only line surge arresters are installed

Aanster Feeder

PRESENT COST	R	97,867.64
FUTURE COST	R	3,086.10
SAVINGS	R	94,781.54
INFLATION RATE		8.00
INITIAL INVESTMENT	R	36,674.43

YEAR	CASH FLOW	NPV	ROI
0	-36,674.43	-36,674.43	
1	102,364.06	R 58,107.11	158%
2	110,553.19	R 152,888.65	417%
3	119,397.44	R 247,670.19	675%
4	128,949.24	R 342,451.73	934%
5	139,265.18	R 437,233.27	1192%

New installations :

SURGE ARRESTORS:

How many new sets?	Labour cost: (1 set)	Material cost: (1 set)	Transport cost (1 set)	Totals:
9	R 494.00	R 2,767.00	R 268.00	R 31,761.00

DOC FUSES

How many new sets?				
0	R 89.52	R 1,227.00	R 268.00	R -

		OVH (15%)	IDC (.0047%/month)	TOTAL
TOTAL COST	R 31,761.00	R 4,764.15	R149.28	R 36,674.43

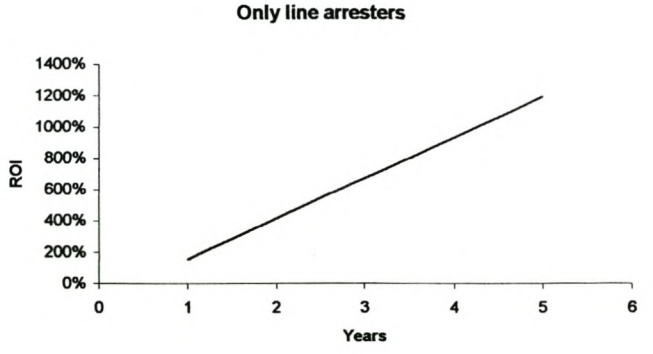

Stellenbosch University http://scholar.sun.ac.za

Financial comparison between different options:

YEAR	only fuses	arresters only	ROI combine
0			
1	10%	158%	496%
2	120%	417%	1092%
3	231%	675%	1687%
4	341%	934%	2283%
5	451%	1192%	2879%

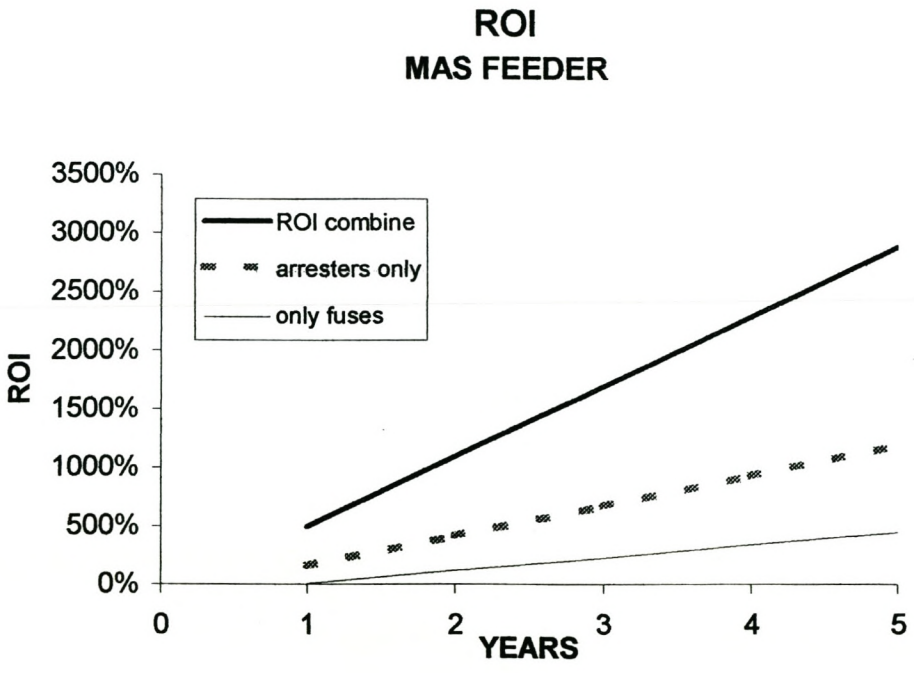

Stellenbosch University http://scholar.sun.ac.za

Appendix D

CSIR fuse tests

Stellenbosch University http://scholar.sun.ac.za

Division of Energy Technology
PO Box 395 Pretoria 0001 South Africa
Telephone : (012) 841-2911
International +27 (12) 841-2911
Telefax : (012) 841-2135
International +27 (12) 841-2135
Telex : 320430 DET SA

Direct Telephone Line : (012) 841-3999

Direct Telefax: (012 841-4038

Our Ref.: 12/7/90/14-4

Energy Technology

CSIR

19 December 1991

Mr W van Schalkwyk
Eskom, Western Transvaal Region
P O Box 1403
JOHANNESBURG
2000

Dear Mr van Schalkwyk

Preliminary results on current impulse testing of fuses

The following tests have been done to date:

1. An 8/20 μs current impulse test - to determine the breakdown currents of the fuses
2. Ten impulses of 50 % peak of 8/20 μs breakdown current for the 5 A and 8 A fuses

The results obtained were as follows:

5 A fuse

Starting with new fuses, the peak 8/20 μs currents leading to breakdown of the fuse for two samples, were

1. 15 kA
2. 14.5 kA

However, if fuses are taken to approximately 15 kA without breakdown, then the breakdown current reduces to

1. 11.8 kA
2. 11.6 kA

NB Only the 5 A fuses showed a step degradation in the breakdown current.

After 10 impulses of 6 kA peak current (8/20 μs), the breakdown currents for three samples were

1. 11.7 kA
2. 11.0 kA
3. 12.2 kA

Stellenbosch University http://scholar.sun.ac.za

8 A fuse

The 8/20 μs breakdown value for two samples of 8 A fuses were

1. 16.5 kA
2. 16.6 kA

After ten impulses of 8 kA peak current, 8/20 μs, the breakdown currents for three samples were

1. 14.9 kA
2. 13.4 kA
3. 14.8 kA

15 A and 20 A fuses

The 8/20 μs impulse breakdown current for two samples of 15 A and two samples of 20 A fuses were

	15 A	20 A
1.	20.9 kA	31.4 kA
2.	25.5 kA	37.8 kA

I trust that you will find these preliminary results to be of interest. We will complete the test programme in January.

Please feel free to contact me if you have any queries.

Yours sincerely

R B Lagesse
Electric Power Programme

Stellenbosch University http://scholar.sun.ac.za

Appendix E

Surge arrester information:

ABB Medium Voltage Surge Arresters

Stellenbosch University http://scholar.sun.ac.za

With **ABB metal-oxide resistors** without spark-gaps

Polim-D..N Technical Data

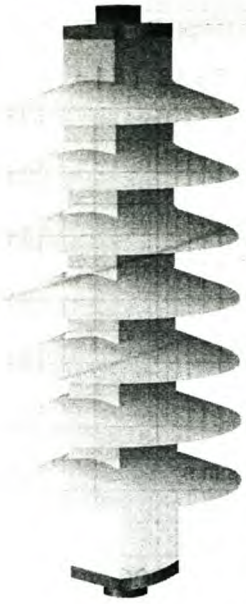

With one line discharge	1.5 kJ / kV_{Uc}
Energy at one high current impulse 100 kA 4/10 µs. (as tested in the operating duty test)	3.6 kJ / kV_{Uc}
Pressure relief up to a fault current of	20 kA / 0.2 s
Explosion and shatter-resistant design as per IEC TC 37/ 199 / CDV	class X

For system voltages up to	36 kV
Rated discharge current 8/20 µs	10 kA
Impulse withstand current 4/10 µs	100 kA
Long duration current impulse	250 A / 2000 µs
For a.c. systems	up to 62 Hz
Line discharge class according to IEC 99-4, 1991	Class 1
Classification as per IEEE (ANSI) C 62.11 - 1993	heavy duty distribution
Cantilever strength	250 Nm
Torsional strength	50 Nm

Application

Protection of medium voltage networks against both atmospheric and switching voltages. Suitable for the protection of distribution transformers and medium voltage cables. For indoor and outdoor installation (also available with an extended creepage distance, Polim-D...L).

Advantages

- Low protection level
- Long protection distance
- High energy input capacity
- Stable characteristic
- Proof against ageing
- Pollution-resistant (silicone housing)
- Housing resistant to rough handling
- Maintenance free
- Stable against shock and vibration
- High cantilever and torsional strength

Guarantee Data

Type	U_R	U_c	Residual voltage in kV at current impulses with (peak value)									
	Rated Voltage r.m.s.	Max. Cont. Oper. Volt. r.m.s	Wave 1/... µs		Wave 8/20 µs					Wave 30/60 µs		
POLIM-D..N	kV	kV	5 kA	10 kA	1 kA	2.5 kA	5 kA	10 kA	20 kA	100 A	250 A	500 A
04	5.0	4.0	14.3	16.0	11.7	12.4	13.1	14.0	15.9	10.4	10.8	11.1
06	7.5	6.0	21.7	24.0	17.5	18.5	19.6	21.0	23.9	15.6	16.1	16.6
08	10.0	8.0	28.9	32.0	23.3	24.7	26.1	28.0	31.8	20.8	21.5	22.2
10	12.5	10.0	36.1	39.9	29.1	30.8	32.6	35.0	39.8	25.9	26.8	27.7
12	15.0	12.0	43.3	47.9	34.9	37.0	39.1	42.0	47.7	31.1	32.2	33.2
14	17.5	14.0	50.5	55.9	40.7	43.2	45.6	49.0	55.7	36.3	37.5	38.8
16	20.0	16.0	57.7	63.9	46.5	49.3	52.1	56.0	63.6	41.5	42.9	44.3
18	22.5	18.0	64.9	71.9	52.3	55.5	58.6	63.0	71.6	46.7	48.2	49.8
20	25.0	20.0	72.1	79.8	58.1	61.6	65.1	70.0	79.5	51.8	53.6	55.3
22	27.5	22.0	79.4	87.7	64.0	67.8	71.7	77.0	87.4	57.0	59.0	60.9
24	30.0	24.0	86.6	95.8	69.8	74.0	78.2	84.0	95.4	62.2	64.3	66.4

Stellenbosch University http://scholar.sun.ac.za

Polim-D..N

Temporary overvoltage withstand strength

Temperature of test sample (preheated) : 60 °C acc. to IEC 99-4

The data refer to an ambient temperature of 45°C. Curve b applies to an arrester which has just received a prestress with an energy as in the operating duty test. No energy input has occured in the case of curve a.

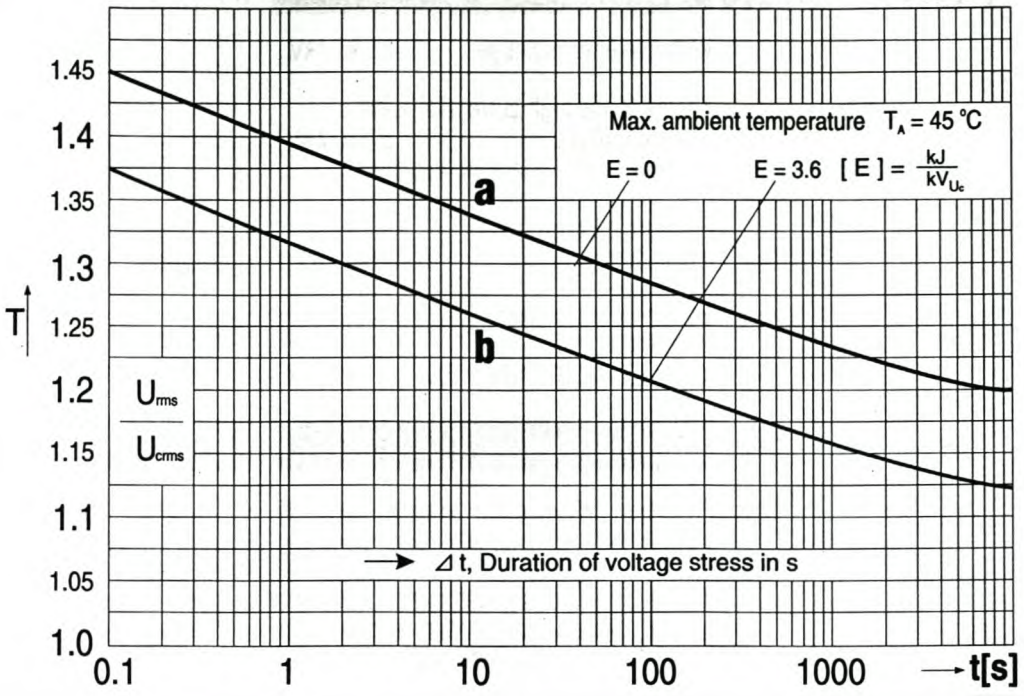

Insulation Data, Dimensions, Weight

Type	Creepage distance	Flashover distance	Minimum clearances		Height H	Weight	Insulation withstand voltage on empty housing BIL 1.2 / 50 µs		50 Hz 60 s wet	
POLIM-D..N	mm	mm	E min mm	F min mm	mm	kg	Min. Values acc. to IEC kV	Gar. Values acc. to tests kV	Min. Values acc. to IEC kV r.m.s.	Gar. Values acc. to tests kV r.m.s.
04	153	121	73	100	144	< 0.8	18.2	78	8.3	20
06	153	121	96	121	144	< 0.8	27.3	78	12.4	20
08	306	170	118	143	191	< 1.2	36.4	110	16.6	28
10	306	170	140	165	191	< 1.2	45.5	110	20.8	28
12	306	170	162	186	191	< 1.2	54.6	110	24.9	28
14	460	217	184	208	239	< 1.6	63.7	140	29.1	38
16	460	217	207	230	239	< 1.6	72.8	140	33.2	38
18	460	217	229	251	239	< 1.6	81.9	140	37.3	38
20	610	264	251	273	286	< 2.2	91.0	170	41.4	50
22	610	264	274	295	286	< 2.2	100.1	170	45.6	50
24	610	264	296	316	286	< 2.2	109.2	170	49.8	50